In vivo overexpression of reprogramming factor Oct4 enhances remyelination in Krabbe disease

Kim, Kyungri

Department of Medical Science

Graduate School

Yonsei University

In vivo overexpression of reprogramming factor Oct4 enhances remyelination in Krabbe disease

Advisor Cho, Sung-Rae

A Dissertation Submitted

to the Department of Medical Science
and the Committee on Graduate School

of Yonsei University in Partial Fulfillment of the

Requirements for the Degree of

Doctor of Philosophy in Medical Science

Kim, Kyungri

June 2025

***In vivo* overexpression of reprogramming factor Oct4 enhances remyelination in Krabbe disease**

This Certifies that the Dissertation of Kim, Kyungri is Approved

Committee Chair	Cho, Sung-Rae
Committee Member	Kim, Hyungbum
Committee Member	Ha, Yoon
Committee Member	Kim, Sung Hoon
Committee Member	Bae, Sangsu

Department of Medical Science

Graduate School

Yonsei University

June 2025

ACKNOWLEDGEMENTS

First, I want to thank my sister and parents who have always supported me. When I was tired and having a hard time, they always encouraged me. Because of their support, I was able to finish my degree successfully.

I also want to thank my advisor, Professor Cho, Sung-Rae. During my degree program, he not only guided my experiments but also showed me how to do research properly. Thanks to his guidance, this thesis was able to be completed. I dedicated my doctoral degree to Professor Cho.

Furthermore, I would like to express my gratitude to Professor Kim, Hyungbum, Professor Ha Yoon, Professor Kim, Sung Hoon, and Professor Bae, Sangsu for their invaluable advice. It is thanks to their guidance that I was able to conduct better research.

I also want to thank everyone at the Avison Biomedical Research Center. To the research support staff who never hesitated to offer their assistance, the veterinarians and cage managers in the animal facility, the MRI staff, the confocal imaging center staff, the histology support staff, the EM staff, and the building maintenance and janitorial staff, I am truly thankful. There are many kind and warm-hearted individuals within the same building who have provided me with tremendous support, even if I may have unintentionally forgotten mentioning them.

I would also like to express my gratitude to my friends and the members of the "Eunpyeong N Gathering" who have provided me with emotional support and maintained a close friendship with me throughout the entirety of my doctoral program. Your willingness to listen to my complaints, help me through tough times, and empathize with me is deeply appreciated. They have broadened my perspective and alleviated my pain.

Lastly, I would like to greet my lab family. Without such warm and wonderful individuals, I would never have been able to withstand my doctoral program. To the senior members who always had my back, the adorable juniors who complemented my flaws, and my colleagues who journeyed with me throughout the degree program, I sincerely thank you. I want to give special thanks to Kim Jin Young.

TABLE OF CONTENTS

LIST OF FIGURES

LIST OF TABLES

ABSTRACT

In vivo overexpression of reprogramming factor Oct4 enhances remyelination in Krabbe disease

Krabbe disease, a rare progressive genetic disorder, is caused by a deficiency of galactocerebrosidase (Galc). Patients with Krabbe disease exhibit characteristics such as deterioration of mental and motor functions, muscle weakness, muscle stiffness, myoclonic seizures, rigidity, fever, blindness, swallowing difficulties, and hearing impairment. Hematopoietic stem cell therapy and Galc enzymatic therapy have been used to alleviate the symptoms of Krabbe disease, but there is currently no cure. Therefore, fundamental therapeutic strategies are needed to cure Krabbe disease.

Oct4, also known as Oct3 or Oct3/4, is a key transcription factor encoded by the Pou5f1 gene. During embryonic development, Oct4 is highly expressed in pluripotent and germline cells, but its expression rapidly decreases upon differentiation. Thus, Oct4 is considered a master regulator for initiating and maintaining pluripotent cells during embryonic development and in adult stem cells. Previous studies have shown that overexpression of Oct4 alone or in combination with other reprogramming factors induces plasticity in cells.

In the twitcher mouse, one of the animal models for Krabbe disease, AAV9-Oct4 was intraventricularly injected within 12 hours after birth. Motor performance was assessed weekly (rotarod, wire-hang, open-field). At post-natal day 37, we analysed brain tissue by qRT-PCR, GALC enzyme assay, diffusion-tensor MRI, Luxol-fast-blue/PAS staining, immunofluorescence and RNA-seq.

Oct4-treated mice retained motor coordination and grip strength up to day 35, whereas untreated and AAV-GFP controls declined. Fractional anisotropy in the corpus callosum increased by 29%, paralleled by preserved myelin basic protein staining and luxol-fast blue/PAS staining. Oct4 up-regulated oligodendrocyte-lineage markers and

down-regulated astroglial GFAP in the striatum. RNA-sequencing in the striatum revealed enrichment of oligodendrocyte-differentiation pathways without changes in cell division or cell cycle pathways.

A single neonatal AAV9-Oct4 dose enhances oligodendrocyte regeneration and myelin integrity, translating into functional benefit and modest survival benefit in twitcher mice-despite persistent GALC deficiency. *In vivo* Oct4-mediated reprogramming therefore represents a promising adjunct or bridge therapy for Krabbe disease and potentially other genetic demyelinating disorders.

Key words: Krabbe disease, galactocerebrosidase, *in vivo* reprogramming, Oct4, oligodendrocyte, myelination

1. Introduction

Krabbe disease is a rare neurodegenerative and progressive genetic disorder caused by a deficiency of galactocerebrosidase (Galc)[1,2]. Patients with Krabbe disease exhibit characteristics such as deterioration of mental and motor functions, muscle weakness, muscle stiffness, seizures, blindness, and hearing impairment[3]. Depending on the onset, Krabbe disease can be classified into early-infantile, late-infantile, juvenile, and adult forms. The majority of Krabbe disease patients, accounting for approximately 85-90%, are early-infantile cases, and most of these patients die before the age of two[4]. Currently, there is no cure for Krabbe disease. The only available method to delay the progression of the disease or alleviate symptoms is through hematopoietic stem cell transplantation (HSCT), which allows the expression of functional Galc[5-8]. However, there are several difficulties in HSCT, emphasizing the need for more fundamental therapeutic strategies.

Galc is an enzyme involved in the metabolism of lipids, specifically responsible for the breakdown of galactosylceramide and galactosylsphingosine (also known as psychosine)[2,9]. When Galc function is genetically impaired, these two substances accumulate within cells. The accumulation of galactosylceramide can also lead to its conversion into psychosine by acid ceramidase[10,11], but it is the lack of functional Galc that primarily results in the buildup of psychosine. This overaccumulation of psychosine can further lead to inflammation[12], apoptosis[13], degeneration of oligodendrocytes[14,15], dysfunction in axonal transport[16], and altering membrane fluidity and compositions[17-19]. The exact correlation between these factors, however, is still not fully understood.

Oct4, also known as Oct3 or Oct3/4, is a key transcription factor encoded by the Pou5f1 gene. Initially identified in mice, Oct4 is specific to embryonic stem cells (ESCs) and germline cells. During embryonic development, Oct4 is highly expressed in pluripotent and germline cells, but its expression rapidly decreases upon differentiation[20]. Without Oct4, embryos fail to implant due to a lack of pluripotent inner cell mass. Thus, Oct4 is considered a master regulator for initiating and maintaining pluripotent cells during embryonic development. The level of Oct4 expression critically determines the fate of ESCs. The pluripotent potential can only be sustained when Oct4 expression is within a normal range[21,22].

Oct4, when overexpressed either alone or in combination with other reprogramming factors, has exhibited the capacity to initiate reprogramming or aid in the conversion of cellular lineages. In their research, Kim et al. observed the generation of induced OPCs through the overexpression of Oct4 in mouse fibroblasts[23]. Similarly, Yun et al. provided evidence that the Oct4-induced transformation of human fibroblasts into oligodendrocytes effectively prompted reprogramming in rats with experimental autoimmune encephalomyelitis[24]. Moreover, through the administration of lentivirus carrying Oct4 into the ventricles along with valproic acid, there was an accelerated myelin repair observed in mice with degenerated optic chiasm[25]. Thus, the potential of Oct4 to induce oligodendrocyte lineage commitment and neural regeneration presents a promising avenue for addressing the demyelination observed in Krabbe disease. In this study, Oct4 overexpression was suggested as a therapeutic strategy in a mouse model of Krabbe disease.

2. Materials and methods

2.1. Animals and housing conditions

The twitcher mice (C57BL/6, Galc-twi), which were heterozygous for the galactocerebrosidase (Galc) gene mutation at codon 355 resulting in a G to A nucleotide change and substitution of tryptophan with a stop codon (p.W355*), were acquired from Jackson Laboratory and bred on a C57BL/6 background. The onset of the disease in twitcher mice typically occurs around 20 days of age, manifesting in symptoms such as head tremors, reduced body weight, and decreased activity. Twitcher mice exhibit a deficiency in functional Galc, leading to a truncated form of the enzyme. As a result of this deficiency, these mice have a significantly shortened lifespan, typically reaching only about 40 days of age. The heterozygous twitcher mice were housed in standard cages (27 × 22.5 × 14 cm^3) in the Association for Assessment and Accreditation of Laboratory Animal Care (AAALAC) accredited animal facility. All animals were kept on a 12-hour light/12-hour dark schedule in accordance with animal-welfare guidelines. Experimental protocols received approval from the Yonsei University College of Medicine Institutional Animal Care and Use Committee (IACUC #2020-0047).

2.2. AAV9 viral vectors containing the Oct4 gene

The AAV9 vectors (VectoBuilder, Chicago, USA) containing the Oct4 gene (mPou5f1; NCBI reference sequence: NM_013633.3) were expressed using the CMV promoter (Figure 1).

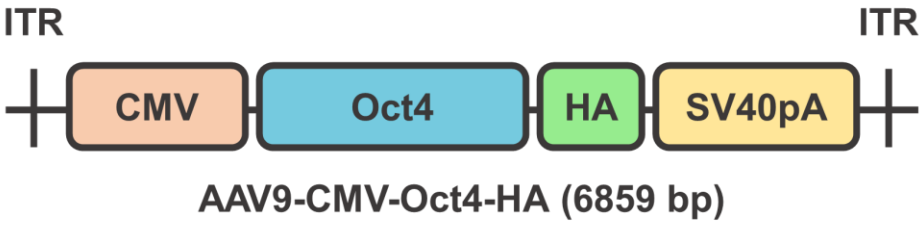

Figure 1. Structure of the AAV9-CMV-Oct4-HA vector. The vector includes CMV promoter, Oct4 gene with HA tag, SV40 polyadenylation signal, and flanking ITRs.

2.3. Intracerebroventricular (ICV) injection of AAV9-Oct4 on postnatal day 1

The intracerebroventricular (ICV) injection of AAV9-Oct4 was carried out on postnatal day 1 (P1; within 24 hours) in the twitcher mice. Following anesthesia by placing the pup on ice for 5 minutes, a 1μL volume of virus (1 × 10^{10} vg/μL) was injected into both lateral ventricles over a period of 1 minute, using a 30-gauge Hamilton syringe. The stereotaxic coordinates were AP +1.5mm, ML

±0.8mm from the lambda, and DV -1.5mm from the dura mater (Figure 2). After each virus infusion, the needle was held in position for 1 minute to prevent any backward flow. After completion of all surgeries, the pups were observed to regain consciousness on a heating pad and then placed back into the cage with their dam. 5-bromo-2'-deoxyuridine (BrdU) was administered to the injection group at a dosage of 250 mg/kg from postnatal day 5 to 7. The experimental scheme is illustrated in Figure 3.

To verify the accuracy of the injection site, 0.4% trypan blue was injected and confirmed that the brain showed blue staining along the ventricles (Figure 4). To verify the expression of the AAV9 virus, AAV9-GFP was used, which was expressed in the septal area (Figure 5).

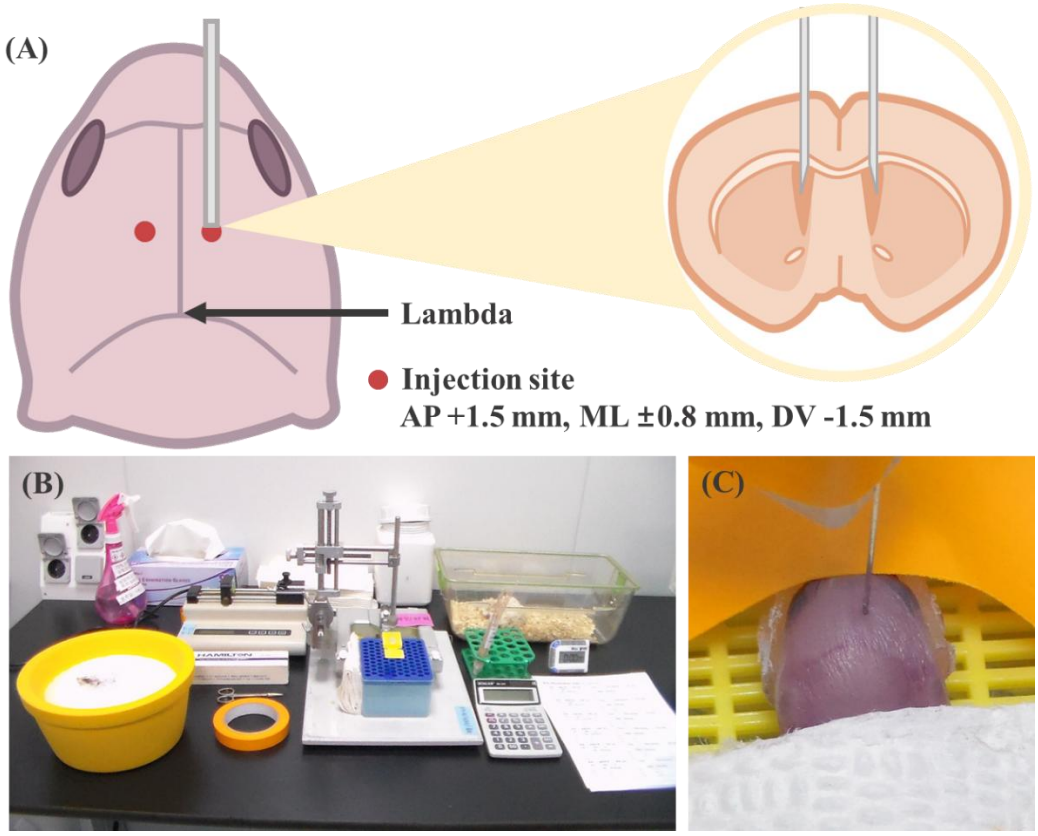

Figure 2. Intracerebroventricular (ICV) injection of AAV9-Oct4 on postnatal day 1. AAV9-Oct4 was injected into the lateral ventricles of twitcher mice on postnatal day 1 (P1). (A) Schematic illustration of the stereotaxic injection coordinates: AP +1.5 mm, ML ±0.8 mm, DV -1.5 mm from lambda. (B) Experimental setup for ICV injection on P1. (C) ICV injection being performed on a P1 twitcher mouse.

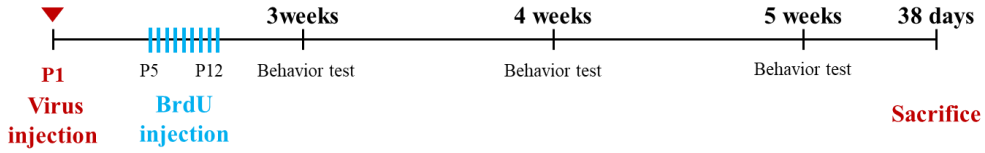

Figure 3. The experimental scheme. AAV9-Oct4 was injected on P1, and animals were sacrificed on postnatal day 38. Behavioral tests were performed weekly from weeks 3-5. 5-bromo-2'-deoxyuridine (BrdU) injections were administered from P5-P12 (250 mg/kg).

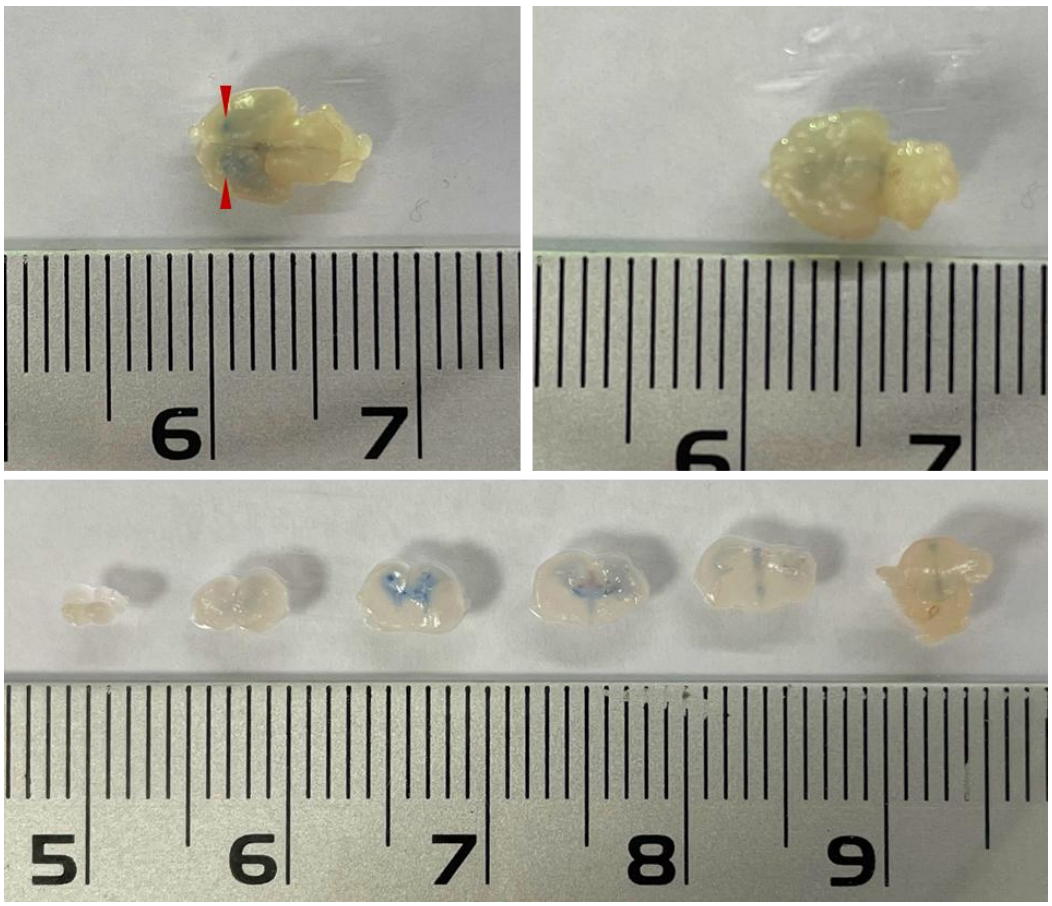

Figure 4. Verification of injection site using trypan blue. (A) Dorsal view of P1 mouse brain showing bilateral injection sites (red arrowheads). (B) Ventral view of the brain base. (C) Coronal brain sections (0.2 mm thickness) demonstrating blue staining along the ventricular system following 0.4% trypan blue injection, confirming accurate targeting of the lateral ventricles.

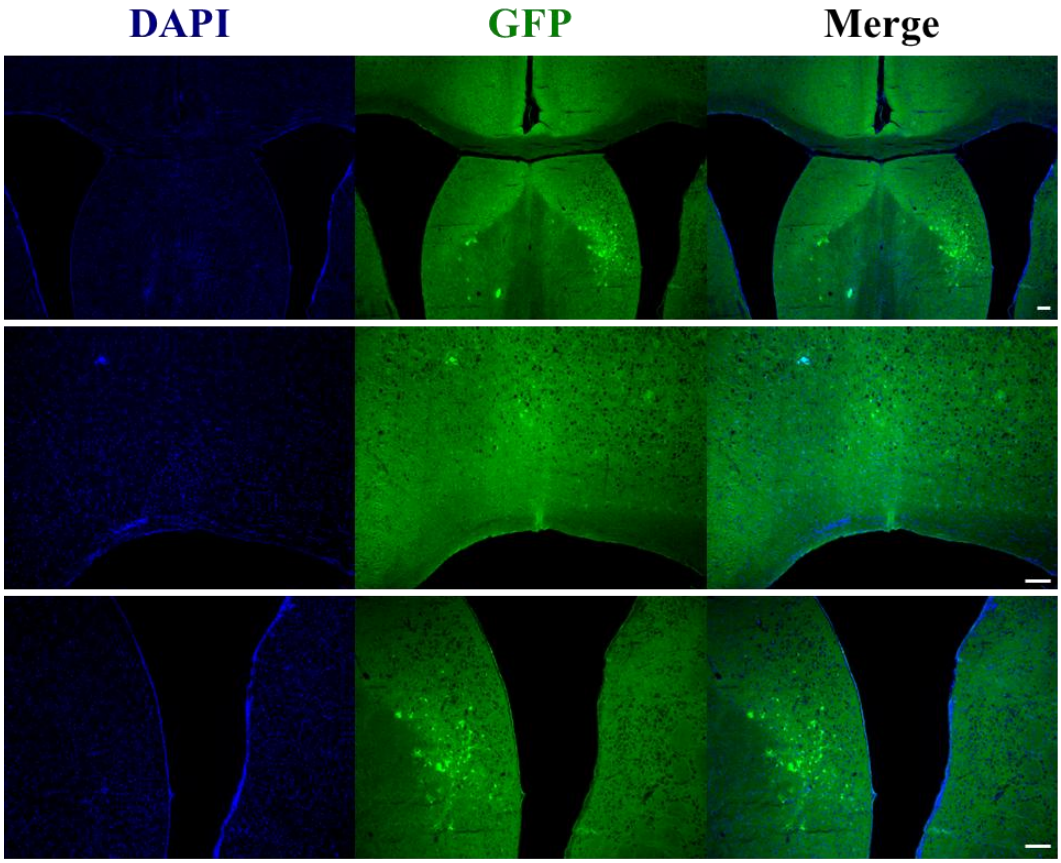

Figure 5. Confirmation of AAV9-GFP Expression. Top, GFP expression in the lateral ventricles and surrounding subventricular zone (SVZ). Middle, GFP expression in the septal area showing successful viral transduction. Bottom, higher magnification view of GFP-positive cells in the septal region. 4',6-diamidino-2-phenylindole (DAPI; blue) shows cell nuclei, GFP (green) indicates viral expression. Scale bar = 100 μm.

2.4. Behavioral assessments

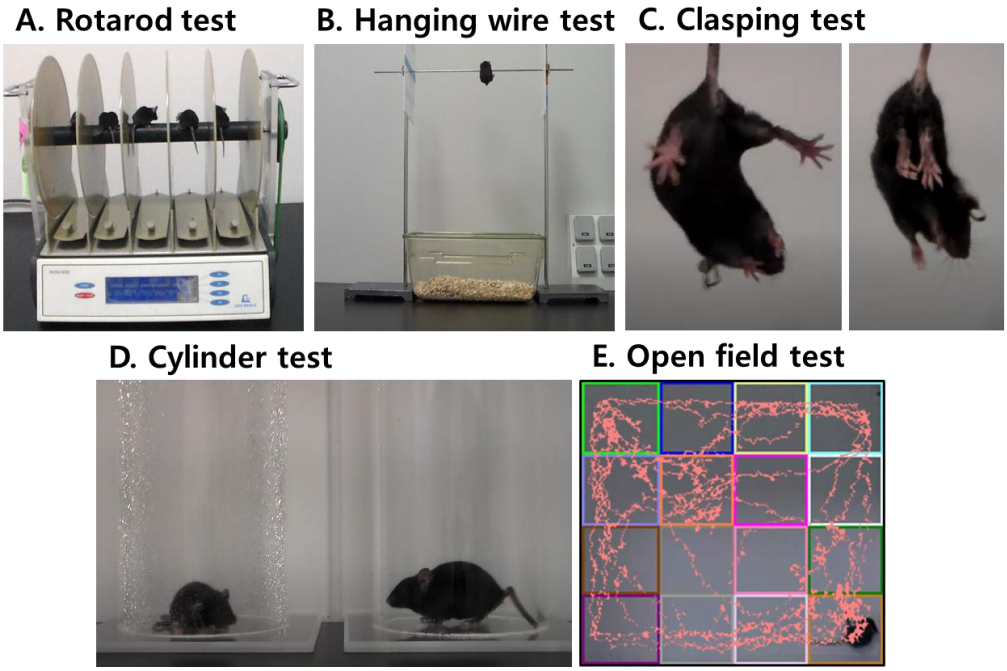

Figure 6. List of behavioral assessments conducted in the mouse model of Krabbe disease. (A) Rotarod test for motor coordination and balance. (B) Hanging wire test for grip strength assessment. (C) Clasping test for neurological dysfunction. (D) Cylinder test for hindlimb usage. (E) Open field test for locomotor activity and anxiety-like behavior.

2.4.1. Rotarod test

The rotarod test was used to assess motor coordination and locomotor function, where mice were placed on a rotarod treadmill (Ugo Basile, Gemonio, Italy) and the latency to fall was recorded, with testing performed at 3, 4, and 5 weeks of age using both constant speeds (4 and 12 rpm) and accelerating speed (4 to 40 rpm), and each test was repeated twice with a maximum duration of 300 seconds per trial.

2.4.2. Hanging wire test

The hanging wire test was utilized to measure the muscle strength of the mice. Each mouse was positioned on a 4 mm thick metallic wire that was firmly fastened to two vertical stands, ensuring stability. The wire was enclosed by plastic boards on both ends to prevent escaping. To prevent injury from falling, the wire was set 35 cm above a cage filled with wood shavings. The test consisted of recording the duration, up to a maximum of 300 seconds, each mouse could maintain its grip on the wire. Each mouse was subjected to three trials, with a 10-minute rest period in between each.

2.4.3. Clasping test

Hindlimb clasping, often observed in several mouse models of neurodegeneration, including twitcher mice, was assessed. Each mouse was raised by grasping the base of its tail, ensuring it was clear of any surrounding objects, and its hindlimb position was observed over a 10-second suspension period. Scores were assigned based on the position of the hindlimbs during this period: a score of 0 was given if the hindlimbs were consistently splayed outward, a score of 1 if one hindlimb was retracted toward the abdomen for 1 to 5 seconds, a score of 2 if both hindlimbs were partially retracted for 5 to 9 seconds, and a score of 3 if both hindlimbs were entirely retracted and in contact with the abdomen for the entire 10 seconds, after which each mouse was returned to its cage and the corresponding clasping score was recorded.

2.4.4. Cylinder test

Mice were placed in a transparent plexiglass cylinder (Jeung Do B&P, Seoul, Korea) measuring 8 cm in diameter and 18 cm in height and video-recorded for subsequent analysis, with the number of mice that stood upright and fully supported their weight on their hind legs counted over a 5-minute period to assess motor function and muscle strength.

2.4.5. Open field test

The open field test is commonly employed to assess locomotor activity and psychological behaviors in a novel environment, where mice were individually placed in a square arena measuring 30 × 30.5 × 31 cm^3 that was divided into 16 sectors with 4 inner sectors forming the central region and 12 outer sectors forming the periphery, and allowed to freely explore for 25 minutes while being video monitored, with the total time spent in the periphery recorded as an index of anxiety and data analysis performed using the Smart Vision 2.5.21 video tracking system (Panlab, Barcelona, Spain) to evaluate both motor function and anxiety-related behaviors.

2.5. RNA isolation and Quantitative reverse transcription polymerase chain reaction

Quantitative RT-PCR assays were carried out in triplicate on a LightCycler 480 instrument (Roche, Mannheim, Germany) with the LightCycler 480 SYBR Green Master Mix from the same supplier, using a thermoprofile that began with a 10-minute denaturation at 95 °C followed by 40 amplification cycles of 95 °C for 10 seconds, 60 °C for 30 seconds, and 72 °C for 10 seconds, after which a melt-curve analysis was performed (95 °C for 5 seconds, then 60 °C for 1 minute) to confirm single-product amplification, with glyceraldehyde-3-phosphate dehydrogenase (GAPDH) serving as the endogenous reference and relative transcript abundance calculated using the 2^-ΔΔCt method, and primer sequences provided in Table 1.

2.6. RNA sequencing data processing and analysis

Paired-end libraries were sequenced on an Illumina NovaSeq X platform, with raw reads processed using Trimmomatic v0.38 to remove adapters and low-quality bases, then filtered reads were aligned to the Mus musculus reference genome (mm10) using HISAT2 v2.1.0 with genome FASTA and RefSeq annotation (GTF) files downloaded from NCBI, after which alignment files were sorted and indexed with SAMtools v1.9, and transcript assembly and quantification were performed using StringTie v2.1.3b to generate gene- and isoform-level counts expressed as raw read counts, FPKM, and TPM.

2.7. Differential Gene Expression Analysis

Statistical analyses of differential gene expression were performed using edgeR v3.26.8 with raw counts as input, where genes with non-zero counts in at least one sample were selected during the QC step, PCA (Principal component analysis) and MDS (Multidimensional scaling) plots were generated to confirm the similarity of expression between samples, and the filtered dataset was normalized using TMM normalization to correct for variation in library sizes among samples, after which statistical significance of differentially expressed genes was determined using edgeR exactTest with fold changes and P-values extracted from the exactTest results, all P-values adjusted using the Benjamini-Hochberg algorithm to control false discovery rate (FDR), and genes displaying an absolute |fold-change| $\geq$ 1.2 together with an unadjusted $P < 0.05$ designated as significant, with rlog-transformed counts for these transcripts subjected to hierarchical clustering (Euclidean distance, complete linkage) and functional enrichment of the significant gene set performed using gProfiler (https://biit.cs.ut.ee/gprofiler/orth) against the Gene Ontology (GO) database, where adjusted P-values reported from gProfiler results were derived using one-sided hypergeometric test corrected by the Benjamini-Hochberg method, and all differential-expression analyses and visualizations generated in R 4.2.2 (www.r-project.org).

2.8. Galc enzyme activity test with 6-Hexadecanoylamino-4-methylumbelliferyl b-D-galactopyranoside (HMU-β-Gal)

2.8.1. Materials preparation

All materials used in this experiment were obtained from the following sources: sodium phosphate dibasic (CAS No. 7558-79-4, 1065860), citric acid (CAS No. 77-92-9, 791725), sodium azide (CAS No. 26628-22-8, S2002), oleic acid (CAS No. 112-80-1, O1008), n-hexane (CAS No. 110-54-3, 1.04367), taurocholic acid sodium salt hydrate (CAS No. 345909-26-4, T4009), sodium bicarbonate (CAS No. 144-55-8, 792519), sodium carbonate (CAS No. 497-19-8, 222321), 4-methylumbelliferone sodium salt (MU, CAS No. 5980-33-6, M1508), Triton X-100 (CAS No. 9036-19-5, T8787), and chloroform (CAS No. 67-66-3, C2432) from Sigma-Aldrich (St. Louis, MO, USA), 6-hexadecanoylamino-4-methylumbelliferyl β-D-galactopyranoside (HMU-βGal, CAS No.

94452-17-2, EH05989) from BioSynth (Berkshire, UK), clear flat-bottom 96-well assay plates with lids from Corning (Corning, NY, USA), bovine serum albumin, hydrogen chloride (4097-3700), and sodium hydroxide (7572-3700) from DAEJUNG (Siheung-si, Korea), and methanol (CAS No. 67-56-1, 1.06009) from Merck (Rahway, NJ, USA).

2.8.2. Reagent preparation

A substrate buffer was prepared using McIlvaine buffer containing 0.2 M sodium phosphate dibasic, 0.1 M citric acid, and 0.02% (w/v) sodium azide dissolved in distilled water, with the pH adjusted to 5.2 using hydrogen chloride solution. For BSA-0.2% solution, 1g of BSA was dissolved in 20 ml of distilled water to make a 5% solution and incubated overnight at 4 °C to inactivate lysosomal enzymes. The pH was then raised to 10.0 using sodium hydroxide, and the solution was incubated at 50 °C for 4 hours in a water bath. After that, the pH was brought to 7.0 using 1 M hydrogen chloride solution, and the solution was centrifuged at 3000 rpm for 10 minutes. The supernatant was collected and diluted 25-fold with 0.02% sodium azide solution, aliquoted into 1 ml portions, and stored at –20 °C. The stop buffer was prepared by dissolving 0.5 M sodium bicarbonate, 0.5 M sodium carbonate, and 0.25% Triton X-100 in distilled water.

2.8.3. Preparation of HMU-β-Gal substrate film

To prepare the HMU-βGal substrate film, 10 mg of HMU-βGal (from two 5mg vials) was dissolved by adding 1 ml of chloroform/methanol mixture (2:1, v/v) to each vial, transferring the dissolved solution to a 50 ml glass flask, then washing each vial two additional times with 1 ml of the same solvent mixture to recover any remaining substrate and transferring to the flask. After adding 15.8 ml of chloroform/methanol to achieve a final volume of 18.8 ml, the solution was mixed until clear, with incubation at 37 °C applied if necessary for complete clarification. This HMU-βGal solution was then immediately combined with 6.3 ml of oleic acid solution (0.6% w/v in n-hexane) and 4.24 ml of taurocholate solution (3% w/v sodium taurocholate in chloroform/methanol) for a total volume of 29.34 ml. The final mixture was aliquoted into 462 µL portions in Eppendorf tubes, dried under nitrogen using an evaporator until organic solvents were completely removed, and the resulting substrate films were sealed with parafilm and stored at –80 °C for up to one year.

2.9. Immunofluorescence staining

Mice treated with BrdU received daily intraperitoneal injections of 5-bromo-2'-deoxyuridine (BrdU; 250 µg/mouse, Sigma-Aldrich, St. Louis, MO, USA) for eight days, starting from postnatal day 5 through day 12, and at 37 days of age, both BrdU-treated and untreated twitcher mice were euthanized via transcardial perfusion with cold 1X PBS followed by 4% paraformaldehyde (PFA, BPP-9004, Tech & Innovation, Chuncheon-si, Korea).

The harvested brain tissues were embedded in paraffin and sectioned along the coronal plane at 4µm thickness, then deparaffinized and hydrated through immersion in xylene and ethanol, after which sections were treated with a standard solution composed of 1% normal goat serum (NGS) and

0.01% saponin (S7900, Sigma-Aldrich, St. Louis, MO, USA) in 1X PBS for blocking, permeabilized for 15 minutes with a solution containing 1% NGS and 0.1% saponin in 1X PBS, treated with a blocking solution consisting of 5% NGS and 0.01% saponin, and incubated overnight at 4 °C with primary antibodies. The sections were subsequently washed with the standard solution three times for 10 minutes each, treated with the blocking solution for one hour at room temperature, stained with secondary antibodies for one hour at room temperature, washed again with the standard solution three times for 10 minutes each, and mounted with DAPI mounting solution (H-1200, Vector Laboratories, Inc., Newark, CA, USA).

The stained sections were observed by confocal microscopy (LSM780, Zeiss, Gottingen, Germany) and analyzed using ZEN black and blue edition (Zeiss, Gottingen, Germany), with each staining performed on four sections per mouse and all primary and secondary antibodies diluted using the standard solution, with specific antibodies listed in Table 2.

2.10. Magnetic resonance imaging

At 37 days of age, twitcher mice were anesthetized using 3-3.5% isoflurane, and the isoflurane concentration was adjusted to 1.5-2% to maintain anesthesia. MRI experiments were conducted on a 9.4T BioSpec scanner (Bruker BioSpin GmbH, Ettlingen, Germany) equipped with ParaVision 5.1 software. A mouse brain surface coil with an 86mm transmit (Tx) coil was used. Anatomical images were acquired using the rapid acquisition with relaxation enhancement (RARE) protocol, followed by diffusion experiments using the diffusion tensor imaging (DTI) echo planar imaging (DTI-EPI) protocol. The DTI imaging parameters were as follows: slice thickness, 0.32 mm; number of slices, 20; matrix size, 128 × 128; matrix resolution, 0.156 mm/pixel × 0.156 mm/pixel; TE/TR = 23.5/5000 ms; 30 directions with b = 670 s/mm²; and $\delta/\Delta = 4/10$ ms. The acquired diffusion images were processed using DSI studio software (http://dsi-studio.labsolver.org). The processed data were then further analyzed using MATLAB (Mathworks, Natick, MA, USA) to obtain fractional anisotropy and diffusivity measurements. For T_2 imaging, the following parameters were used: slice thickness, 0.16 mm; number of slices, 30; matrix size, 128 × 128; matrix resolution, 0.125 mm/pixel × 0.125 mm/pixel; and TE/TR = 20/2100 ms. Image reconstruction and processing were carried out in ParaVision 5.1.

2.11. Luxol fast blue Periodic acid-Schiff staining

To assess the myelin sheaths and globoid cell count in twitcher mice, luxol fast blue (LFB) and periodic acid-Schiff staining (PAS) techniques were performed. The LFB-PAS double stain facilitated accurate differentiation of distinct structures, including myelin sheaths (stained blue) and activated glial cell bodies (stained red). These procedures were conducted following previously established methods.

Briefly, transcardial perfusion of twitcher mice was performed using 1X PBS and 10% paraformaldehyde, followed by extraction and dehydration of the brain in 30% sucrose (CAS No. 57-50-1, S5390, Sigma-Aldrich, St. Louis, MO, USA) until it sank. The brain tissue was

subsequently embedded in paraffin and cut into 4 μm-thick sections. The sections were deparaffinized by immersing them in xylene twice for 10 minutes each time, and xylene was subsequently removed with two 10-minute washes in 100% ethanol. The sections were then hydrated with 95% ethanol for 5 minutes and stained overnight with a 10% luxol fast blue solution (Solvent Blue 38, CAS No. 1328-51-4, S3382, Sigma-Aldrich, St. Louis, MO, USA) in ethanol. After staining, the sections were rinsed in 95% ethanol for 1 minute and washed in tap water for 10 minutes. Neutralization was achieved by exposing the stained sections to 0.05% lithium carbonate (CAS No. 554-13-2, 431559, Sigma-Aldrich, St. Louis, MO, USA) in distilled water for 20 seconds, followed by differentiation in 70% ethanol until a distinct contrast between bluish white matter and opaque gray matter was observed.

After the LFB staining process, the tissue sections underwent a PAS staining procedure. This began with the acidification of the stained sections using a 0.05% periodic acid solution in 1N hydrogen chloride. The sections were then carefully washed three times using distilled water. Following this, the tissue was treated with the Schiff reagent for 15 minutes to promote further staining. This was followed by two 2-minute rinses using a sulfurous rinse solution. After rinsing, the sections were thoroughly washed with tap water for 10 minutes. Mayer's hematoxylin solution was then used for 1 minute to stain the nuclei. Subsequently, the sections were rinsed using 1X Tris-buffered saline (TBS), and then washed again with tap water for another 10 minutes. Finally, the stained sections were gradually dehydrated with ethanol and xylene. Lastly, the dehydrated sections were mounted using a water-resistant mounting solution. The tissue sections underwent microscopic analysis, and myelin fibers and globoid cells were quantified using ImageJ software.

2.12. Statistical Analysis

Data are presented as mean ± standard error of the mean (SEM). Each experiment was repeated at least four times, with four animals per group (n = 4 per group). Analyses were carried out using IBM SPSS Statistics for Windows, version 25.0 (IBM Corp., Armonk, NY, USA). Between-group differences were evaluated using the appropriate statistical test: paired Student's t-test for paired comparisons, one-way ANOVA for single-factor comparisons, or two-way ANOVA for multiple-factor comparisons. When ANOVA indicated significant differences, Bonferroni's post-hoc test was performed for multiple comparisons. Survival curves were compared using the Gehan–Breslow–Wilcoxon test. Results were considered statistically significant at $P < 0.05$.

Gene	Primer sequence
Oct4	Forward: 5'- AGA CCA CCA TCT GTC GCT TC-3' Reverse: 5'- CTC CAC CTC ACA CGG TTC TC-3'
Galc	Forward: 5'- GTG TTG CGG TGC CCT TAT TG3' Reverse: 5'- AGA ACG ATA GGG CTC TGG GTA-3'
GAPDH	Forward: 5'- GTG GAG CCA AAA GGG TCA TCA-3' Reverse: 5'- CCC TTC CAC AAT GCC AAA GTT-3'

Table 1. Primers sequences for PCR.

Target	Company	Catalog number	Dilution factor
Nestin	R&D Systems	MAB2736	1:400
Olig2	Sigma	AB9610	1:400
GFAP	Neuromics	RA22101	1:400
Tuj1	BioLegend	801201	1:400
BrdU	Abcam	ab6326	1:200
MBP	Abcam	ab7349	1:400
GALC	ABclonal	A3873	1:400

Table 2. Antibodies for immunofluorescence staining.

3. Results

3.1. Overexpression of Oct4 in twitcher mice preserved motor function in the behavioral assessments

To estimate the effect of Oct4 overexpression in twitcher mice, AAV9-Oct4 virus was injected intracerebroventricularly within 24 hours after birth. To verify the precise injection site in the brain, trypan blue, a blue dye, was injected at the site and the brain was immediately dissected after injection (Figure 4). Additionally, to confirm viral transduction efficiency, GFP expression was confirmed through immunofluorescence staining (Figure 5). Using qRT-PCR, the relative mRNA level of Oct4 was measured in different regions of the brain and spinal cord (Figure 7). The Oct4-treated group exhibited significantly higher mRNA expression than the other groups in the brain, but not in the spinal cord.

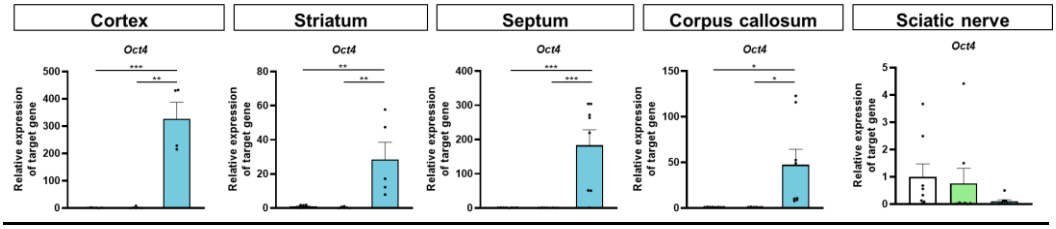

Region	Group1	vs	Group2	Mean		SEM	vs	Mean		SEM	N	Summary	P-value
Cortex	Untreated	vs	GFP	1.000	±	0.266	vs	1.744	±	1.288	3:3	ns	>0.9999
	Untreated	vs	Oct4	1.000	±	0.266	vs	326.909	±	60.634	3:3	***	<0.0001
	GFP	vs	Oct4	1.744	±	1.288	vs	326.909	±	60.634	3:3	***	<0.0001
Striatum	Untreated	vs	GFP	1.000	±	0.323	vs	0.369	±	0.170	3:3	ns	>0.9999
	Untreated	vs	Oct4	1.000	±	0.323	vs	28.490	±	10.078	3:3	**	0.006
	GFP	vs	Oct4	0.369	±	0.170	vs	28.490	±	10.078	3:3	**	0.005
Septum	Untreated	vs	GFP	1.000	±	0.133	vs	0.695	±	0.088	3:3	ns	>0.9999
	Untreated	vs	Oct4	1.000	±	0.133	vs	183.487	±	44.963	3:3	***	0.000
	GFP	vs	Oct4	0.695	±	0.088	vs	183.487	±	44.963	3:3	***	0.000
Corpus callosum	Untreated	vs	GFP	1.000	±	0.056	vs	0.961	±	0.095	3:3	ns	>0.9999
	Untreated	vs	Oct4	1.000	±	0.056	vs	47.280	±	17.010	3:3	*	0.015
	GFP	vs	Oct4	0.961	±	0.095	vs	47.280	±	17.010	3:3	*	0.025
Sciatic nerve	Untreated	vs	GFP	1.000	±	0.475	vs	0.759	±	0.554	3:3	ns	>0.9999
	Untreated	vs	Oct4	1.000	±	0.475	vs	0.101	±	0.060	3:3	ns	0.443
	GFP	vs	Oct4	0.759	±	0.554	vs	0.101	±	0.060	3:3	ns	0.852

Figure 7. The mRNA expression of Oct4 by the brain regions after ICV injection of AAV9-Oct4. The graph represents Oct4 mRNA expression in different regions of the brain in twitcher mice. To compare groups at each time point, one-way ANOVA was conducted. Results are reported as mean ± SEM. Statistical significance is denoted as *P < 0.05, **P < 0.01, and ***P < 0.001.

Behavioral assessments were performed to evaluate the effects of Oct4 overexpression in twitcher mice. The following tests were performed: rotarod test, hanging wire test, clasping test, cylinder test, and open field test.

For the rotarod test, three different speed protocols were conducted weekly on twitcher mice from 3 to 5 weeks of age (Figure 8). At a constant speed of 4 rpm, the Oct4 group maintained their latency time, while the other groups showed deteriorating performance at 5 weeks. At a constant speed of 12 rpm, however, no significant difference was observed between the untreated group and the Oct4 group at 5 weeks. When tested with an accelerating speed from 4 to 40 rpm, the Oct4 group maintained locomotor activity until 5 weeks of age, while the other groups did not. Two-way ANOVA analysis revealed significant effects of time and treatment group at 4 rpm and 4-40 rpm protocols, but not at the 12 rpm protocol.

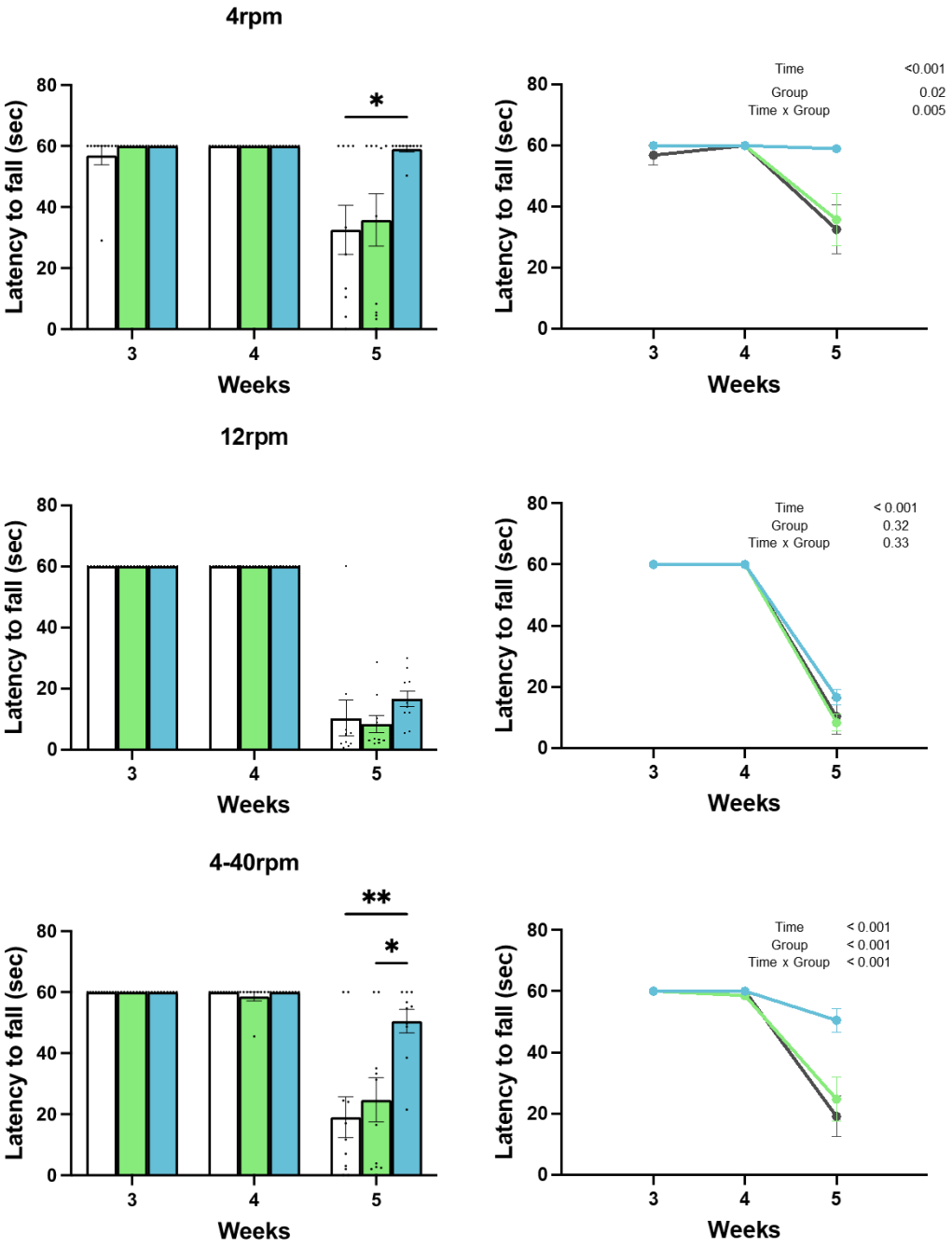

Experiment	Weeks	Group1	vs	Group2	Mean	±	SEM	vs	Mean	±	SEM	N	Summary	P-value
4rpm	3	Untreated	vs	GFP	56.900	±	3.100	vs	60.000	±	0.000	10:10	ns	>0.9999
		Untreated	vs	Oct4	56.900	±	3.100	vs	60.000	±	0.000	10:10	ns	>0.9999
		GFP	vs	Oct4	60.000	±	0.000	vs	60.000	±	0.000	10:10	ns	NA
	4	Untreated	vs	GFP	60.000	±	0.000	vs	60.000	±	0.000	10:10	ns	NA
		Untreated	vs	Oct4	60.000	±	0.000	vs	60.000	±	0.000	10:10	ns	NA
		GFP	vs	Oct4	60.000	±	0.000	vs	60.000	±	0.000	10:10	ns	NA
	5	Untreated	vs	GFP	32.560	±	8.035	vs	35.780	±	8.572	10:10	ns	>0.9999
		Untreated	vs	Oct4	32.560	±	8.035	vs	59.030	±	0.970	10:10	*	0.028
		GFP	vs	Oct4	35.780	±	8.572	vs	59.030	±	0.970	10:10	ns	0.072
12rpm	3	Untreated	vs	GFP	60.000	±	0.000	vs	60.000	±	0.000	10:10	ns	NA
		Untreated	vs	Oct4	60.000	±	0.000	vs	60.000	±	0.000	10:10	ns	NA
		GFP	vs	Oct4	60.000	±	0.000	vs	60.000	±	0.000	10:10	ns	NA
	4	Untreated	vs	GFP	60.000	±	0.000	vs	60.000	±	0.000	10:10	ns	NA
		Untreated	vs	Oct4	60.000	±	0.000	vs	60.000	±	0.000	10:10	ns	NA
		GFP	vs	Oct4	60.000	±	0.000	vs	60.000	±	0.000	10:10	ns	NA
	5	Untreated	vs	GFP	10.330	±	5.755	vs	8.310	±	2.778	10:10	ns	>0.9999
		Untreated	vs	Oct4	10.330	±	5.755	vs	16.580	±	2.645	10:10	ns	>0.9999
		GFP	vs	Oct4	8.310	±	2.778	vs	16.580	±	2.645	10:10	ns	0.135
4-40rpm	3	Untreated	vs	GFP	60.000	±	0.000	vs	60.000	±	0.000	10:10	ns	NA
		Untreated	vs	Oct4	60.000	±	0.000	vs	60.000	±	0.000	10:10	ns	NA
		GFP	vs	Oct4	60.000	±	0.000	vs	60.000	±	0.000	10:10	ns	NA
	4	Untreated	vs	GFP	60.000	±	0.000	vs	58.550	±	1.450	10:10	ns	>0.9999
		Untreated	vs	Oct4	60.000	±	0.000	vs	60.000	±	0.000	10:10	ns	NA
		GFP	vs	Oct4	58.550	±	1.450	vs	60.000	±	0.000	10:10	ns	>0.9999
	5	Untreated	vs	GFP	19.018	±	6.664	vs	24.710	±	7.236	10:10	ns	>0.9999
		Untreated	vs	Oct4	19.018	±	6.664	vs	50.510	±	3.857	10:10	**	0.003
		GFP	vs	Oct4	24.710	±	7.236	vs	50.510	±	3.857	10:10	*	0.022

Figure 8. Rotarod test showed that overexpression of Oct4 preserves locomotor function in the twitcher mice. Three different speed protocols were performed weekly on twitcher mice from 3 to 5 weeks of age (4 rpm, 12 rpm, and 4-40 rpm). Time × group interaction effects from two-way ANOVA analysis are presented at the top of each panel. One-way ANOVA was also performed for group comparisons at each time point. Values are reported as mean ± SEM. Statistical significance is denoted as *P < 0.05, **P < 0.01, and ***P < 0.001.

The hanging wire test was performed to confirm the presence of neuromuscular dysfunction in twitcher mice (Figure 9). The Oct4 group maintained grip strength until 5 weeks of age, while the other groups did not. Two-way ANOVA analysis revealed significant main effects of time and group, but no significant time × group interaction.

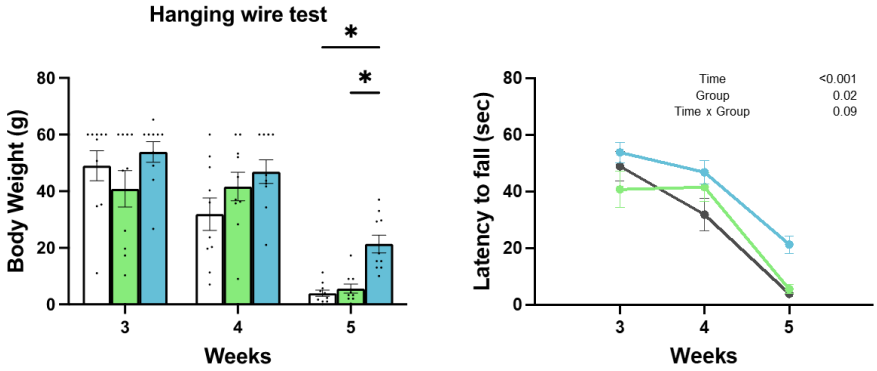

Weeks	Group1	vs	Group2	Mean		SEM	vs	Mean		SEM	N	Summary	P-value
3	Untreated	vs	GFP	49.000	±	5.303	vs	40.860	±	6.425	10:10	ns	>0.9999
	Untreated	vs	Oct4	49.000	±	5.303	vs	53.870	±	3.618	10:10	ns	>0.9999
	GFP	vs	Oct4	40.860	±	6.425	vs	53.870	±	3.618	10:10	ns	0.298
4	Untreated	vs	GFP	31.910	±	5.738	vs	41.660	±	5.008	10:10	ns	0.651
	Untreated	vs	Oct4	31.910	±	5.738	vs	46.910	±	4.180	10:10	ns	0.151
	GFP	vs	Oct4	41.660	±	5.008	vs	46.910	±	4.180	10:10	ns	>0.9999
5	Untreated	vs	GFP	3.940	±	1.118	vs	5.580	±	1.586	10:10	ns	>0.9999
	Untreated	vs	Oct4	3.940	±	1.118	vs	21.360	±	3.102	10:10	***	0.001
	GFP	vs	Oct4	5.580	±	1.586	vs	21.360	±	3.102	10:10	**	0.002

Figure 9. The hanging wire test showed that overexpression of Oct4 preserves grip strength in twitcher mice. The hanging wire test was performed weekly on twitcher mice from 3 to 5 weeks of age. Time × group interaction effects from two-way ANOVA analysis are presented at the top of the panel. One-way ANOVA was also performed for group comparisons at each time point. Values are reported as mean ± SEM. Statistical significance is denoted as *P < 0.05, **P < 0.01, and ***P < 0.001.

The clasping test, a scoring system used to assess neurodegenerative phenotypes, indicated no significant difference between the groups (Figure 10). In the cylinder test, no significant difference was observed between the groups (Figure 11).

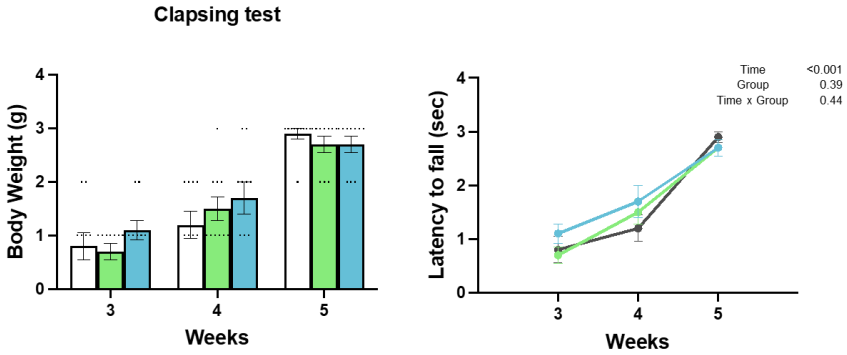

Weeks	Group1	vs	Group2	Mean		SEM	vs	Mean		SEM	N	Summary	P-value
3	Untreated	vs	GFP	0.800	±	0.249	vs	0.700	±	0.153	10:10	ns	>0.9999
	Untreated	vs	Oct4	0.800	±	0.249	vs	1.100	±	0.180	10:10	ns	>0.9999
	GFP	vs	Oct4	0.700	±	0.153	vs	1.100	±	0.180	10:10	ns	0.322
4	Untreated	vs	GFP	1.200	±	0.249	vs	1.500	±	0.224	10:10	ns	>0.9999
	Untreated	vs	Oct4	1.200	±	0.249	vs	1.700	±	0.300	10:10	ns	0.650
	GFP	vs	Oct4	1.500	±	0.224	vs	1.700	±	0.300	10:10	ns	>0.9999
5	Untreated	vs	GFP	2.900	±	0.100	vs	2.700	±	0.153	10:10	ns	0.870
	Untreated	vs	Oct4	2.900	±	0.100	vs	2.700	±	0.153	10:10	ns	0.870
	GFP	vs	Oct4	2.700	±	0.153	vs	2.700	±	0.153	10:10	ns	>0.9999

Figure 10. Clasping-test scores, used to evaluate cerebellar ataxia, did not differ significantly between the Oct4 group and controls. The clasping test is a scoring system used to assess neurodegenerative phenotypes. Time × group interaction effects from two-way ANOVA analysis are presented at the top of the panel. One-way ANOVA was also performed for group comparisons at each time point. Values are reported as mean ± SEM. Statistical significance is denoted as *P < 0.05, **P < 0.01, and ***P < 0.001.

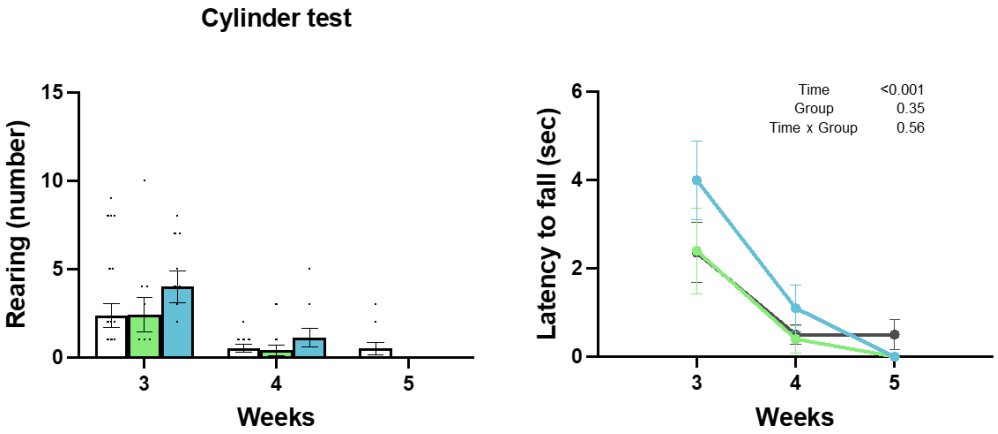

Weeks	Group1	vs	Group2	Mean		SEM	vs	Mean		SEM	N	Summary	P-value
3	Untreated	vs	GFP	2.900	±	1.038	vs	2.400	±	0.980	10:10	ns	>0.9999
	Untreated	vs	Oct4	2.900	±	1.038	vs	4.000	±	0.894	10:10	ns	>0.9999
	GFP	vs	Oct4	2.400	±	0.980	vs	4.000	±	0.894	10:10	ns	0.731
4	Untreated	vs	GFP	0.500	±	0.224	vs	0.400	±	0.306	10:10	ns	>0.9999
	Untreated	vs	Oct4	0.500	±	0.224	vs	1.100	±	0.526	10:10	ns	0.943
	GFP	vs	Oct4	0.400	±	0.306	vs	1.100	±	0.526	10:10	ns	0.806
5	Untreated	vs	GFP	0.500	±	0.342	vs	0.000	±	0.000	10:10	ns	0.532
	Untreated	vs	Oct4	0.500	±	0.342	vs	0.000	±	0.000	10:10	ns	0.532
	GFP	vs	Oct4	0.000	±	0.000	vs	0.000	±	0.000	10:10	ns	NA

Figure 11. The overexpression of Oct4 had no effect on hindlimb strength as assessed by the cylinder test in the twitcher mice. The cylinder test was conducted weekly on twitcher mice from 3 to 5 weeks of age. Time × group interaction effects from two-way ANOVA analysis are presented at the top of the panel. One-way ANOVA was also performed for group comparisons at each time point. Values are reported as mean ± SEM. Statistical significance is denoted as *P < 0.05, **P < 0.01, and ***P < 0.001.

The general activity level in twitcher mice was assessed using an open field test. The travel distance was recorded for 25 minutes, with the first 5 minutes excluded to account for an adaptation phase. The total distance traveled, which indicates the general activity level, was found to be lower in the untreated and GFP groups compared to the Oct4-treated group (Figure 12). These results suggest that overexpression of Oct4 preserved motor function in twitcher mice.

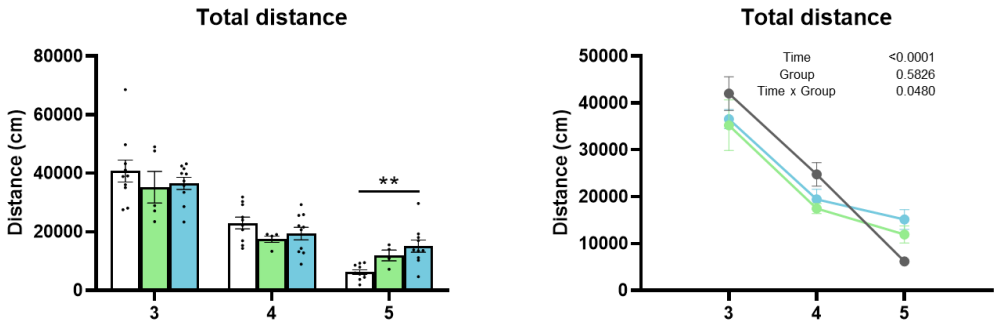

Weeks	Group1	vs	Group2	Mean		SEM	vs	Mean		SEM	N	Summary	P-value
3	Untreated	vs	GFP	40765.950	±	3734.773	vs	35249.154	±	5410.351	10:5	ns	>0.9999
	Untreated	vs	Oct4	40765.950	±	3734.773	vs	36569.670	±	2037.492	10:10	ns	>0.9999
	GFP	vs	Oct4	35249.154	±	5410.351	vs	36569.670	±	2037.492	5:10	ns	>0.9999
4	Untreated	vs	GFP	23026.173	±	1985.486	vs	17486.732	±	1080.624	10:5	ns	0.089
	Untreated	vs	Oct4	23026.173	±	1985.486	vs	19457.400	±	2129.525	10:10	ns	0.709
	GFP	vs	Oct4	17486.732	±	1080.624	vs	19457.400	±	2129.525	5:10	ns	>0.9999
5	Untreated	vs	GFP	6260.455	±	800.279	vs	13015.906	±	1790.803	10:5	*	0.045
	Untreated	vs	Oct4	6260.455	±	800.279	vs	15136.835	±	2098.328	10:10	**	0.006
	GFP	vs	Oct4	13015.906	±	1790.803	vs	15136.835	±	2098.328	5:10	ns	>0.9999

Figure 12. The general locomotor activities were preserved in the Oct4 group during the open field test. The open field test was conducted to assess general locomotor activity levels in twitcher mice. Time × group interaction effects from two-way ANOVA analysis are presented at the top of the panel. One-way ANOVA was also performed for group comparisons at each time point. Values are reported as mean ± SEM. Statistical significance is denoted as *P < 0.05, **P < 0.01, and ***P < 0.001.

To confirm whether there are any effects of AAV9 on twitcher mice, body and brain weights were measured (Figure 13). Body weight was recorded every week from 3 to 5 weeks of age, and no significant changes were observed among the groups. Brain weight was measured after dissection, and the brain was further divided into cerebrum and cerebellum. Total brain weight, as well as the weights of cerebrum and cerebellum, were measured for each group. There were no significant differences observed between the groups. Two-way ANOVA revealed a main effect of age on body weight ($P < 0.001$)—reflecting normal growth—but no main effect of treatment and no age × treatment interaction ($P > 0.05$ for both). Thus, neonatal AAV9-Oct4 did not alter body weight or brain weight trajectories in twitcher mice.

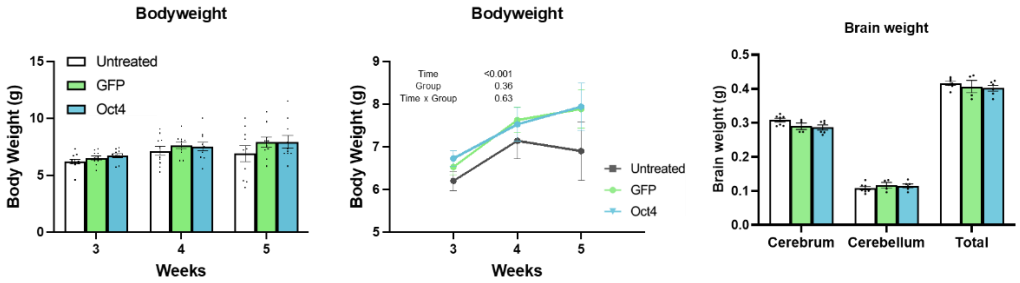

Experiment	Weeks	Group1	vs	Group2	Mean	±	SEM	vs	Mean	±	SEM	N	Summary	P-value
Body weight	3	Untreated	vs	GFP	60.000	±	0.000	vs	60.000	±	0.000	10:10	ns	NA
		Untreated	vs	Oct4	60.000	±	0.000	vs	60.000	±	0.000	10:10	ns	NA
		GFP	vs	Oct4	60.000	±	0.000	vs	60.000	±	0.000	10:10	ns	NA
	4	Untreated	vs	GFP	60.000	±	0.000	vs	60.000	±	0.000	10:10	ns	NA
		Untreated	vs	Oct4	60.000	±	0.000	vs	60.000	±	0.000	10:10	ns	NA
		GFP	vs	Oct4	60.000	±	0.000	vs	60.000	±	0.000	10:10	ns	NA
	5	Untreated	vs	GFP	10.330	±	5.755	vs	8.310	±	2.778	10:10	ns	>0.9999
		Untreated	vs	Oct4	10.330	±	5.755	vs	16.580	±	2.645	10:10	ns	>0.9999
		GFP	vs	Oct4	8.310	±	2.778	vs	16.580	±	2.645	10:10	ns	0.135
Brain weight	Cerebrum	Untreated	vs	GFP	0.308	±	0.006	vs	0.290	±	0.010	7:4	ns	0.493
		Untreated	vs	Oct4	0.308	±	0.006	vs	0.286	±	0.007	7:6	ns	0.133
		GFP	vs	Oct4	0.290	±	0.010	vs	0.286	±	0.007	4:6	ns	1.000
	Cerebellum	Untreated	vs	GFP	0.108	±	0.005	vs	0.117	±	0.009	7:4	ns	1.000
		Untreated	vs	Oct4	0.108	±	0.005	vs	0.115	±	0.005	7:6	ns	1.000
		GFP	vs	Oct4	0.117	±	0.009	vs	0.115	±	0.005	4:6	ns	1.000
	Total	Untreated	vs	GFP	0.416	±	0.006	vs	0.407	±	0.018	7:4	ns	1.000
		Untreated	vs	Oct4	0.416	±	0.006	vs	0.402	±	0.008	7:6	ns	0.568
		GFP	vs	Oct4	0.407	±	0.018	vs	0.402	±	0.008	4:6	ns	1.000

Figure 13. The bodyweight and brain weight were not changed between the control group and Oct4 group. Body weights of twitcher mice were measured weekly from 3 to 5 weeks of age, and brain weight was measured after dissecting the cerebrum and cerebellum. Two-way ANOVA revealed a main effect of age on body weight reflecting normal growth, but no main effect of treatment and no age × treatment interaction. Time × group interaction effects from two-way ANOVA analysis are presented at the top of the panel. One-way ANOVA was also performed for group comparisons at each time point. Values are reported as mean ± SEM. Statistical significance is denoted as *P < 0.05, **P < 0.01, and ***P < 0.001.

The life span and survival rate of twitcher mice were monitored daily. While the median life span did not differ significantly between groups (Figure 14), survival curve analysis revealed notable distinctions. The Gehan–Breslow–Wilcoxon test revealed a significant difference in survival between the groups (P = 0.04), with the Oct4 group showing improved survival rates in the early stages before experiencing a sharp decline. Additionally, Pearson's chi-square test demonstrated significant differences in survival rates between days 34 to 40, indicating that the Oct4 group maintained higher survival rates during this critical period before rapid mortality occurred.

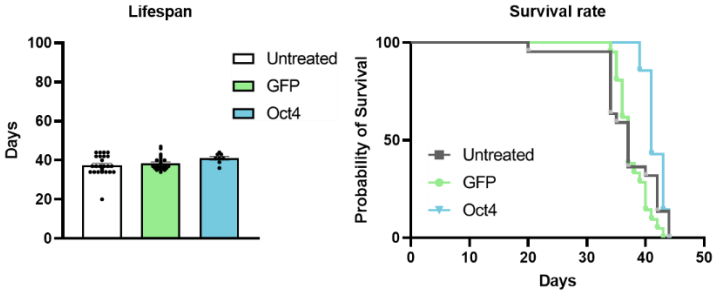

	Untreated	GFP	Oct4	Chi squre	p value
0 days	100%	100%	100%	-	-
20 days	95%	100%	100%	1.000	0.607
34 days	64%	95%	100%	9.445	0.009
35 days	59%	81%	100%	8.355	0.015
36 days	59%	62%	100%	6.481	0.039
37 days	36%	38%	100%	10.018	0.007
38 days	36%	33%	100%	9.628	0.008
39 days	36%	29%	86%	7.111	0.029
40 days	32%	14%	86%	8.144	0.017
41 days	32%	10%	43%	3.823	0.148
42 days	14%	5%	43%	5.948	0.051
43 days	14%	0%	14%	4.511	0.105
44 days	0%	0%	0%	4.511	0.105

Group1	vs	Group2	Mean		SEM	vs	Mean		SEM	N	Summary	P-value
Untreated	vs	GFP	37.400	±	1.047	vs	38.435	±	0.727	25:23	ns	>0.9999
Untreated	vs	Oct4	37.400	±	1.047	vs	41.000	±	0.906	25:8	ns	0.130
GFP	vs	Oct4	38.435	±	0.727	vs	41.000	±	0.906	23:8	ns	0.451

Figure 14. Lifespan and survival rate in the twitcher mice. Lifespan (A) and Kaplan-Meier survival curves (B) of all groups. (C) The chart depicts the survival distribution of all groups using Gehan-Breslow-Wilcoxon test and chi-square statistics. Values are reported as mean ± SEM. Statistical significance is denoted as *P < 0.05, **P < 0.01, and ***P < 0.001.

3.2. Overexpression of Oct4 in twitcher mice preserved myelin structure and MBP level.

To identify the changes that contributed to improved behaviors in twitcher mice, the mRNA expression and enzyme activity of Galc were analyzed (Figures 15 and 16). There were no significant changes between the Oct4 group and the other groups. These results suggest that the improvement in motor function is unlikely to be attributed to the restoration of Galc activity, but rather to alternative mechanisms such as enhanced myelination or neurogenesis.

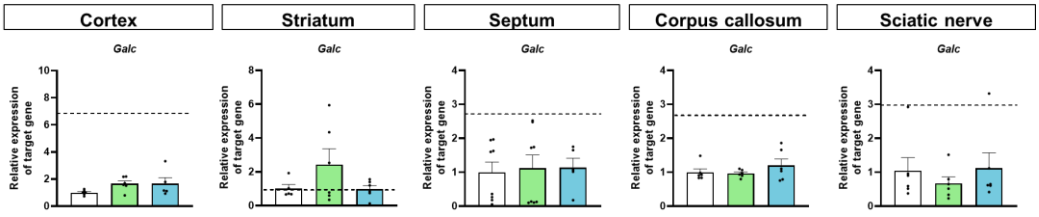

Region	Group1	vs	Group2	Mean		SEM	vs	Mean		SEM	N	Summary	P-value
Cortex	Untreated	vs	GFP	1.000	±	0.076	vs	1.656	±	0.209	3:3	ns	0.263
	Untreated	vs	Oct4	1.000	±	0.076	vs	1.663	±	0.440	3:3	ns	0.295
	GFP	vs	Oct4	1.656	±	0.209	vs	1.663	±	0.440	3:3	ns	>0.9999
Striatum	Untreated	vs	GFP	1.000	±	0.241	vs	2.422	±	0.939	3:3	ns	0.374
	Untreated	vs	Oct4	1.000	±	0.241	vs	0.974	±	0.213	3:3	ns	>0.9999
	GFP	vs	Oct4	2.422	±	0.939	vs	0.974	±	0.213	3:3	ns	0.309
Septum	Untreated	vs	GFP	1.000	±	0.302	vs	1.117	±	0.392	3:3	ns	>0.9999
	Untreated	vs	Oct4	1.000	±	0.302	vs	1.132	±	0.281	3:3	ns	>0.9999
	GFP	vs	Oct4	1.117	±	0.392	vs	1.132	±	0.281	3:3	ns	>0.9999
Corpus callosum	Untreated	vs	GFP	1.000	±	0.101	vs	0.962	±	0.045	3:3	ns	>0.9999
	Untreated	vs	Oct4	1.000	±	0.101	vs	1.200	±	0.187	3:3	ns	0.831
	GFP	vs	Oct4	0.962	±	0.045	vs	1.200	±	0.187	3:3	ns	0.598
Sciatic nerve	Untreated	vs	GFP	1.000	±	0.371	vs	0.673	±	0.188	3:3	ns	>0.9999
	Untreated	vs	Oct4	1.000	±	0.371	vs	1.121	±	0.450	3:3	ns	>0.9999
	GFP	vs	Oct4	0.673	±	0.188	vs	1.121	±	0.450	3:3	ns	>0.9999

Figure 15. Galc mRNA expression across different brain regions in all groups. The mRNA expression of Galc in various brain regions was measured using qRT-PCR. The dotted lines on the graphs represent the values of wild-type mice. One-way ANOVA was performed for group comparisons at each time point. Values are reported as mean ± SEM. Statistical significance is denoted as follows: * $P < 0.05$; ** $P < 0.01$; *** $P < 0.001$.

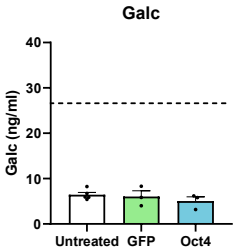

Group1	vs	Group2	Mean		SEM	vs	Mean		SEM	N	Summary	P-value
Untreated	vs	GFP	6.443	±	0.494	vs	6.059	±	1.244	5:3	ns	>0.9999
Untreated	vs	Oct4	6.443	±	0.494	vs	5.052	±	0.944	5:3	ns	0.772
GFP	vs	Oct4	6.059	±	1.244	vs	5.052	±	0.944	3:3	ns	>0.9999

Figure 16. Galc enzyme activity in different brain regions across groups. The enzyme activity of Galc in plasma was compared among groups across brain regions. The dotted lines on the graphs represent the values of wild-type mice. One-way ANOVA was performed for group comparisons at each time point. Values are reported as mean ± SEM. Statistical significance is denoted as follows: * $P < 0.05$; ** $P < 0.01$; *** $P < 0.001$.

To further investigate the underlying mechanisms, the level of myelination was assessed using magnetic resonance imaging (MRI) with diffusion tensor imaging (DTI) in twitcher mice. DTI allows for the measurement of brain microstructure based on diffusivity values (λ1, λ2, λ3). These diffusivity values, known as DTI scalars, were further categorized into fractional anisotropy (FA), axial diffusivity (AD), mean diffusivity (MD), and radial diffusivity (RD). An in-depth DTI analysis was conducted to investigate alterations in the microstructure of both white and gray matter in twitcher mice (Figure 17).

The results revealed that the indicators of demyelination and brain damage, MD and RD, were increased in both the untreated group and the GFP group, indicating demyelination and brain damage in twitcher mice. In contrast, the MD and RD values were significantly preserved in the Oct4 group. However, the indicator of axonal integrity, represented by axial diffusivity (AD), remained unchanged across all experimental groups.

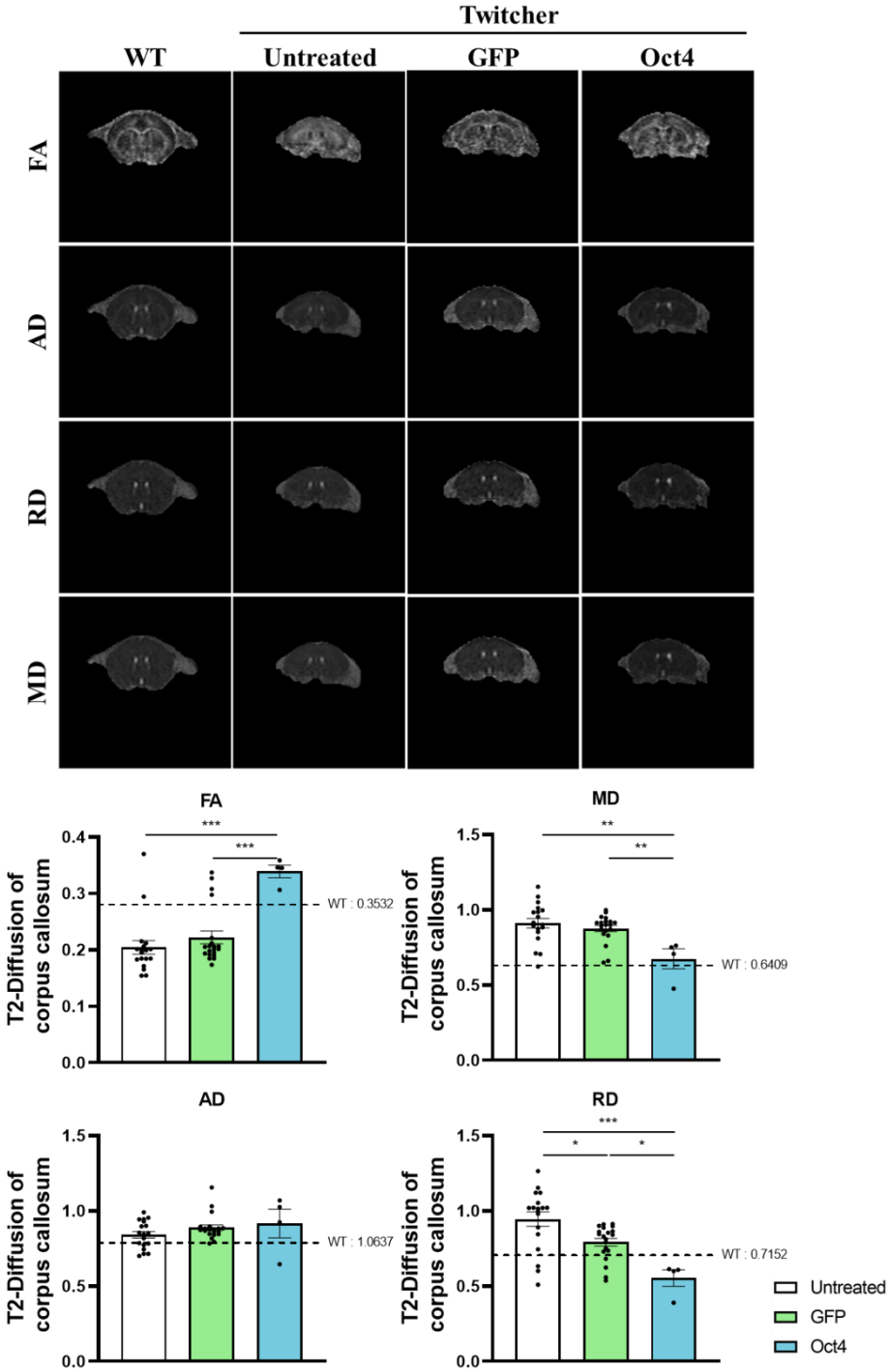

DTI scalars	Group1	vs	Group2	Mean		SEM	vs	Mean		SEM	N	Summary	P-value
FA	Untreated	vs	GFP	0.204	±	0.012	vs	0.222	±	0.011	18:20	ns	0.824
	Untreated	vs	Oct4	0.204	±	0.012	vs	0.339	±	0.011	18:4	***	<0.0001
	GFP	vs	Oct4	0.222	±	0.011	vs	0.339	±	0.011	20:4	***	0.000
MD	Untreated	vs	GFP	0.912	±	0.032	vs	0.876	±	0.021	18:20	ns	>0.9999
	Untreated	vs	Oct4	0.912	±	0.032	vs	0.675	±	0.067	18:4	**	0.002
	GFP	vs	Oct4	0.876	±	0.021	vs	0.675	±	0.067	20:4	**	0.010
AD	Untreated	vs	GFP	0.842	±	0.022	vs	0.890	±	0.019	18:20	ns	0.456
	Untreated	vs	Oct4	0.842	±	0.022	vs	0.917	±	0.095	18:4	ns	0.547
	GFP	vs	Oct4	0.890	±	0.019	vs	0.917	±	0.095	20:4	ns	>0.9999
RD	Untreated	vs	GFP	0.946	±	0.048	vs	0.793	±	0.026	18:20	*	0.016
	Untreated	vs	Oct4	0.946	±	0.048	vs	0.554	±	0.054	18:4	***	0.000
	GFP	vs	Oct4	0.793	±	0.026	vs	0.554	±	0.054	20:4	*	0.029

Figure 17. Diffusion tensor imaging (DTI) in the twitcher mice. (A) Representative images of DTI measured by MRI in all the groups were presented. Fractional anisotropy (FA) (B), mean diffusivity (MD) (C), axial diffusivity (AD) (D), and radial diffusivity (RD) (E) were presented. The dotted lines on the graphs represent the values of wild-type mice. To compare groups at each time point, a one-way ANOVA was conducted. Results are reported as mean ± SEM. Significance thresholds are denoted as *P < 0.05, **P < 0.01, and ***P < 0.001.

T2-weighted imaging, another MRI analysis, was also performed (Figure 18). In wild-type mice, the structures of the corpus callosum and ventricles are clearly visible. However, in twitcher mice and GFP-treated twitcher mice, the corpus callosum structure appears thin and poorly defined. In contrast, Oct4-overexpressed twitcher mice show preserved structure in the corpus callosum and ventricular areas.

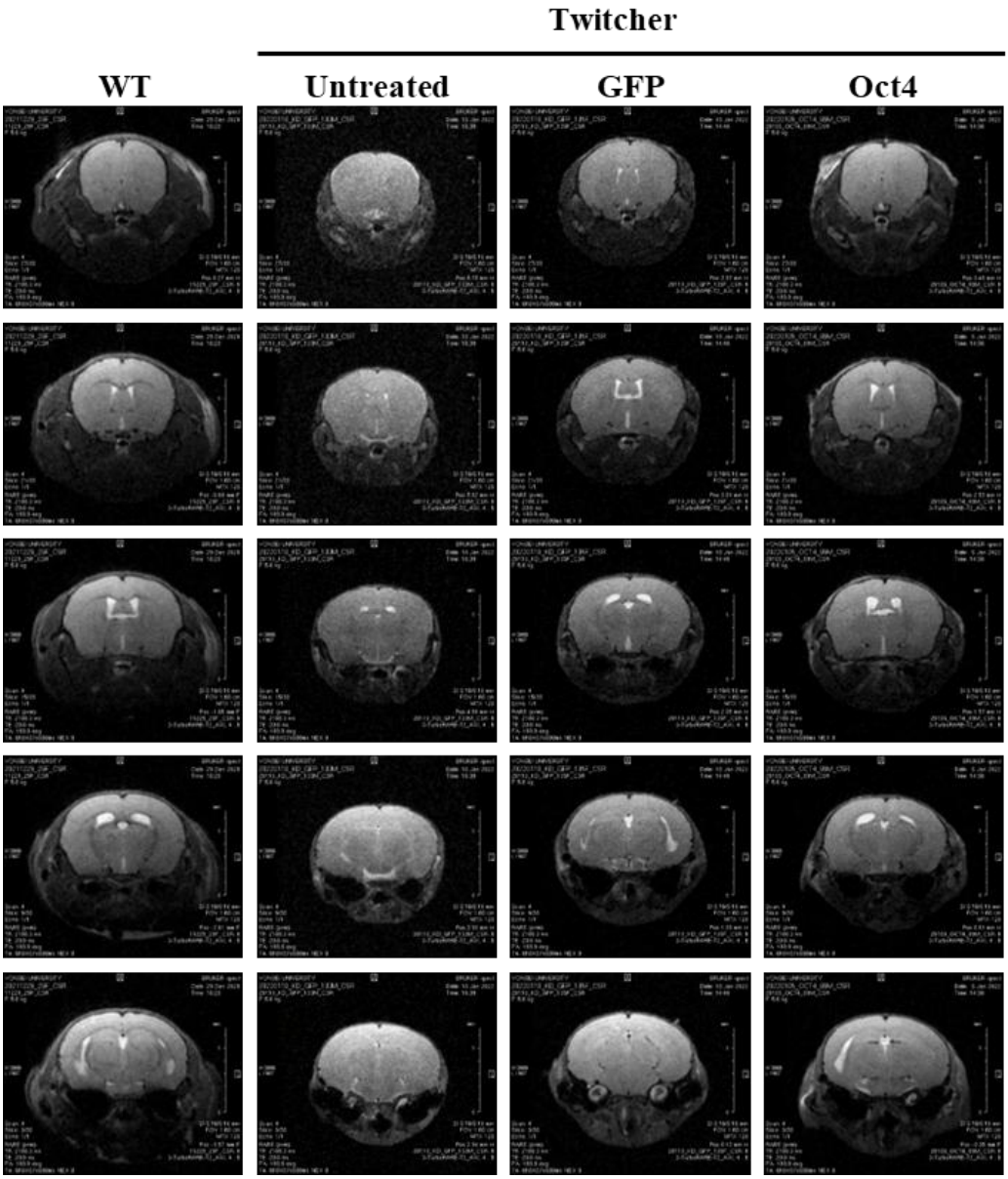

Figure 18. T2-weighted MRI images of twitcher mice. T2-weighted MRI images obtained from all experimental groups are shown. In these images, the bright areas correspond to regions with high water content, such as cerebrospinal fluid in ventricles, while the darker areas indicate regions with lower water content, such as white matter structures.

The density of myelin basic protein (MBP), which serves as a representative marker of mature oligodendrocytes, exhibited similar results (Figure 19). Immunofluorescent staining of MBP in the corpus callosum revealed a noticeable decrease in twitcher mice compared to wild-type mice. However, in Oct4-overexpressed twitcher mice, the MBP density was significantly preserved. Consequently, these findings suggest that Oct4 overexpression plays a crucial role in preserving myelination. By maintaining MBP density, Oct4 may contribute to the maintenance of healthy oligodendrocyte function and the overall integrity of the nervous system in twitcher mice.

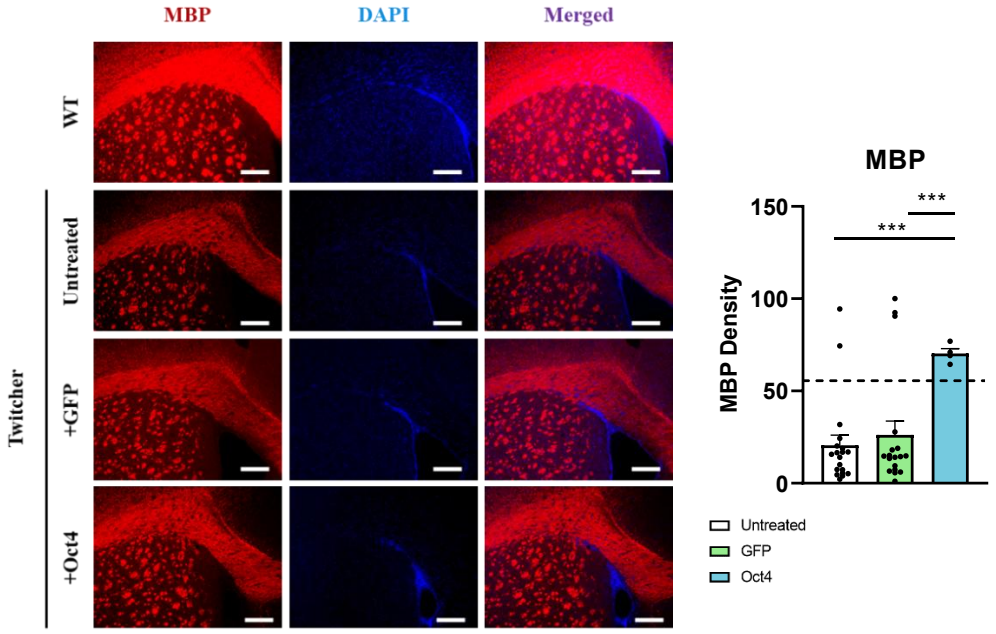

Group1	vs	Group2	Mean		SEM		Mean		SEM	N	Summary	P-value
Untreated	vs	GFP	20.538	±	5.518	vs	26.140	±	7.546	5:4	ns	>0.9999
Untreated	vs	Oct4	20.538	±	5.518	vs	70.373	±	2.582	4:4	***	0.006
GFP	vs	Oct4	26.14	±	7.546	vs	70.373	±	2.582	4:4	***	0.016

Figure 19. The density of myelin basic protein (MBP) was maintained in the Oct4 group. Immunofluorescent staining of myelin basic protein (MBP) shows preservation of MBP density in the Oct4 group. The dotted lines on the graphs represent the values for wild-type mice. Scale bar = 100 μm. One-way ANOVA was performed for group comparisons at each time point. Values are reported as mean ± SEM. Statistical significance is denoted as follows: * $P < 0.05$; ** $P < 0.01$; *** $P < 0.001$.

Luxol-fast-blue / periodic acid-Schiff (PAS) staining, used to assess myelination density, demonstrated a significant reduction of myelination in the corpus callosum of twitcher mice compared to wild-type controls. In contrast, Oct4-overexpressed twitcher mice exhibited significantly preserved myelination. These results indicate that Oct4 overexpression plays a critical role in protecting myelination, potentially supporting oligodendrocyte function and preserving the structural integrity of the nervous system in twitcher mice.

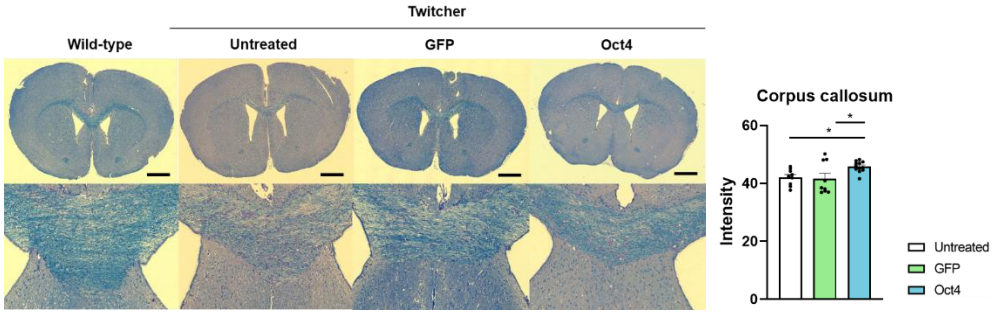

Group1	vs	Group2	Mean		SEM		Mean		SEM	N	Summary	P-value
Untreated	vs	GFP	42.109	±	0.943	vs	41.698	±	1.837	3:3	ns	>0.9999
Untreated	vs	Oct4	42.109	±	0.943	vs	46.347	±	0.404	3:4	*	0.049
GFP	vs	Oct4	41.698	±	1.837	vs	46.347	±	0.404	3:4	*	0.028

Figure 20. Myelination density was preserved in the Oct4-overexpressing group. Luxol-fast-blue/PAS staining revealed maintained myelination in the Oct4 group compared to untreated and GFP control groups. Scale bar = 100 μm. One-way ANOVA was performed for group comparisons at each time point. Values are reported as mean ± SEM. Statistical significance is denoted as follows: * $P < 0.05$; ** $P < 0.01$; *** $P < 0.001$.

3.3. Oct4 overexpression significantly alters the population of Olig2, Nestin, GFAP, and Tuj1-expressing cells in twitcher mice.

To evaluate the regional and cellular specificity of virus transduction, we quantified GFP^+ cell density and marker colocalization in four representative brain regions (Figure 21). The striatum exhibited the highest overall GFP expression and strong transduction of $Tuj1^+$ neurons and $Galc^+$ cells. The corpus callosum showed preferential targeting of $GFAP^+$ astrocytes. The subventricular zone demonstrated broad distribution across progenitor and lineage markers, including $Nestin^+$, $Olig2^+$, $GFAP^+$, and $Tuj1^+$ cells. The cortex displayed relatively sparse viral uptake, with limited transduction of neural progenitor markers.

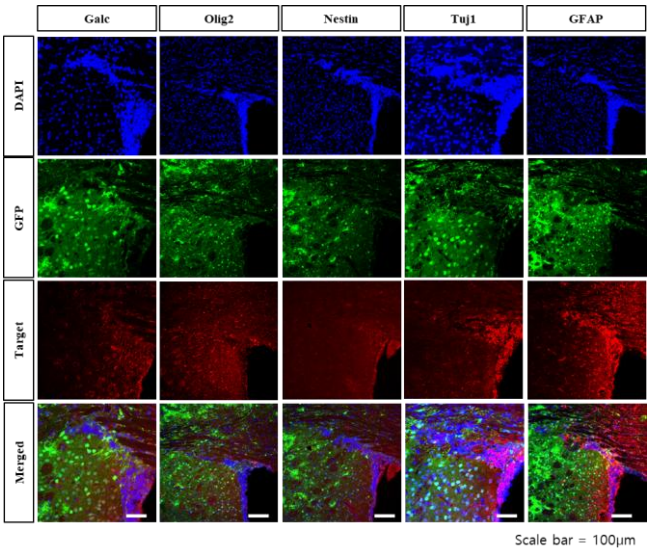

Region	GFP$^+$ Cells	Total volume ($x10^{-3}/mm^3$)	Galc$^+$ cells	Nestin$^+$ cells	Olig2$^+$ cells	GFAP$^+$ cells	Tuj1$^+$ cells
CTX	2.981 ± 0.372	194.664 ± 90.253	2.469 ± 0.642	nan ± nan	0.927 ± 0.162	2.513 ± 0.586	6.930 ± 2.358
STR	4.930 ± 0.828	144.413 ± 79.897	4.403 ± 0.541	2.174 ± 0.628	3.453 ± 2.447	6.894 ± 0.690	10.231 ± 0.537
CC	2.358 ± 0.804	75.725 ± 41.099	2.970 ± 0.972	3.150 ± 0.192	1.765 ± 0.349	13.630 ± 4.690	0.078 ± 0.078
SVZ	2.234 ± 0.312	36.588 ± 20.624	8.567 ± 1.148	18.487 ± 0.600	5.880 ± 0.753	19.325 ± 3.928	17.632 ± 3.628

Region	GFP$^+$ Galc$^+$ cells	GFP$^+$ Nestin$^+$ cells	GFP$^+$ Olig2$^+$ cells	GFP$^+$ GFAP$^+$ cells	GFP$^+$ Tuj1$^+$ cells
CTX	0.388 ± 0.127	0.124 ± 0.013	0.057 ± 0.029	0.504 ± 0.117	1.196 ± 0.498
STR	1.506 ± 0.477	0.105 ± 0.053	0.029 ± 0.029	0.634 ± 0.171	5.731 ± 1.754
CC	0.157 ± 0.060	0.114 ± 0.033	0.038 ± 0.023	0.712 ± 0.282	0.000 ± 0.000
SVZ	0.416 ± 0.152	0.136 ± 0.136	0.214 ± 0.075	0.510 ± 0.113	1.562 ± 1.006

Figure 21. Regional and cellular distribution of virus transduction in the twitcher brain. Representative images and quantitative analysis summarizing the relative abundance of GFP$^+$ cells and their colocalization with specific lineage markers in four brain regions following ICV injection of AAV9-CMV-GFP at P1. Values are normalized to total regional volume and presented as mean ± SEM. Scale bar = 100 μm.

Overexpression of Oct4 significantly altered the populations of cells expressing Olig2, Nestin, GFAP, and Tuj1 in twitcher mice, suggesting a broad impact on glial and neuronal lineage commitment. Detailed quantifications for all markers across brain regions are summarized in Tables 3 and 4.

Olig2-positive cells, which represent oligodendrocyte lineage cells, were markedly decreased in the corpus callosum and striatum of twitcher mice. However, Oct4 overexpression restored this reduction, leading to recovery of Olig2-positive cell numbers to near-normal levels. Furthermore, the number of newly generated cells, identified by BrdU incorporation, was significantly increased after Oct4 overexpression (Figure 22, Tables 3 and 4).

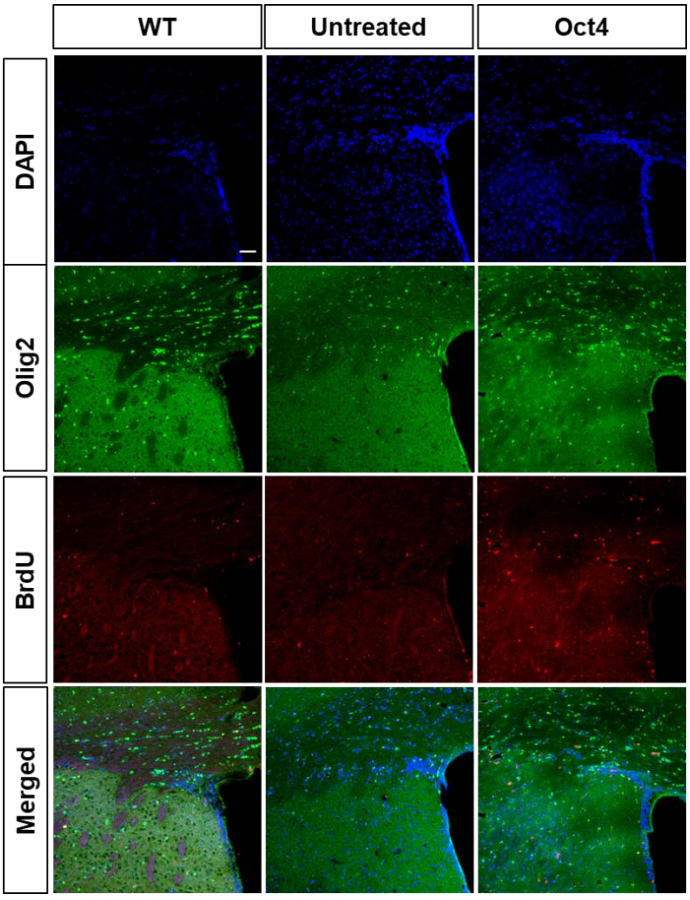

Figure 22. Restoration of Olig2-positive cells after Oct4 overexpression. Immunofluorescent staining for Olig2 revealed an increase in the number of Olig2-positive cells in the Oct4-overexpressed group compared to untreated and GFP control groups. Scale bar = 100 μm. One-way ANOVA was performed for group comparisons. Values are reported as mean ± SEM. Statistical significance is denoted as follows: * $P < 0.05$; ** $P < 0.01$; *** $P < 0.001$.

Similarly, Nestin-positive cells, which are markers of neural stem/progenitor cells, were reduced in the subventricular zone of twitcher mice. Oct4 overexpression significantly increased the number of Nestin-positive cells, indicating a potential enhancement of neural progenitor cell pools. BrdU-positive cell numbers were also increased in this region following Oct4 overexpression (Figure 23, Tables 3 and 4).

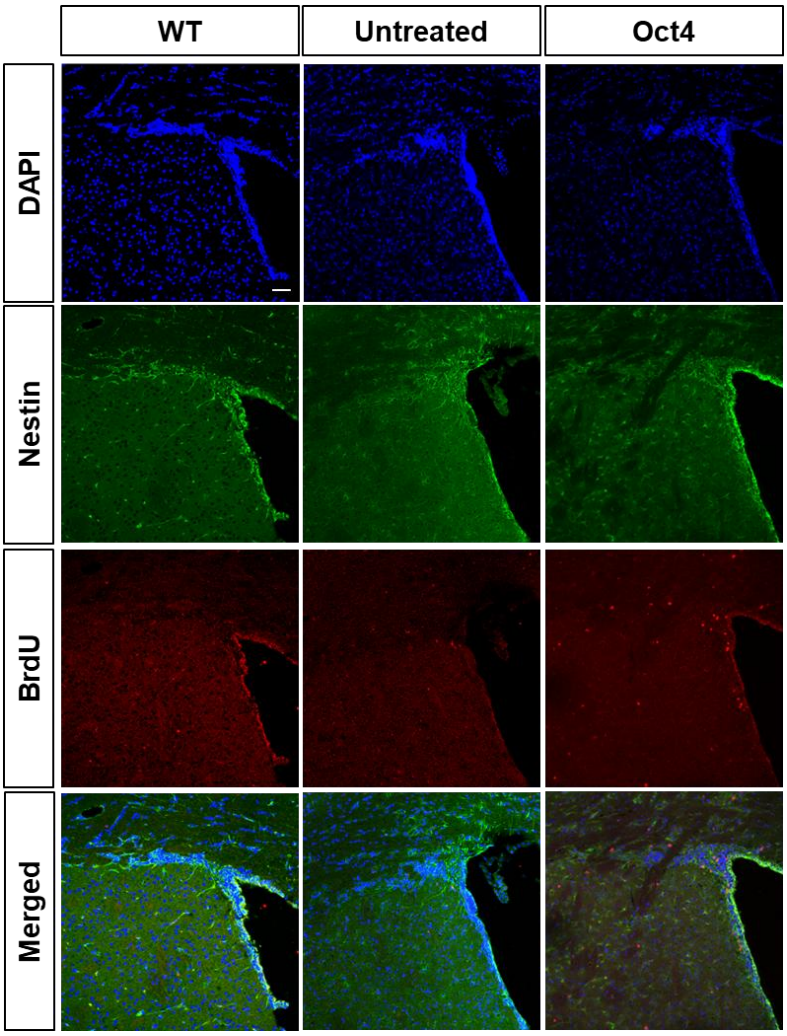

Figure 23. Increased Nestin-positive cells following Oct4 overexpression. Immunofluorescent staining for Nestin showed a significant increase in Nestin-positive cell populations in the SVZ after Oct4 overexpression compared to untreated and GFP control groups. Scale bar = 100 μm. One-way ANOVA was performed for group comparisons. Values are reported as mean ± SEM. Statistical significance is denoted as follows: * $P < 0.05$; ** $P < 0.01$; *** $P < 0.001$.

In the striatum, the number of Tuj1-positive cells, which are an early neuronal marker, was also reduced in twitcher mice. Oct4 overexpression reversed this reduction, leading to increased generation of immature neurons. Consistent with these changes, BrdU-positive cells were also elevated (Figure 24, Tables 3 and 4).

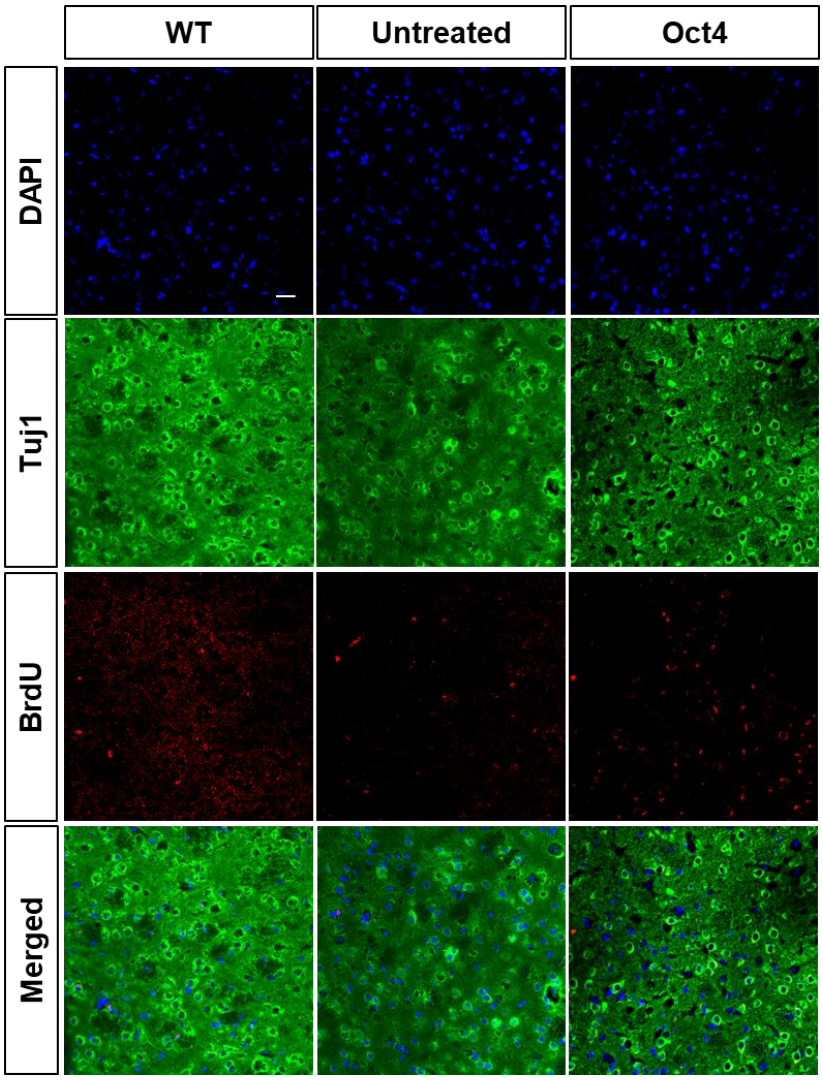

Figure 24. Tuj1-positive cells were increased following Oct4 overexpression. Immunofluorescent staining of Tuj1 demonstrated a higher number of early-stage neuronal cells in the Oct4-overexpressed group compared to untreated and GFP control groups. Scale bar = 100 μm. One-way ANOVA was performed for group comparisons. Values are reported as mean ± SEM. Statistical significance is denoted as follows: * $P < 0.05$; ** $P < 0.01$; *** $P < 0.001$.

In contrast, GFAP-positive cells, which are markers of reactive astrocytes, were significantly elevated across multiple brain regions in twitcher mice. Interestingly, Oct4 overexpression attenuated the number of GFAP-positive cells, suggesting suppression of reactive astrocytosis. Newly generated BrdU-positive cells were also increased following Oct4 overexpression (Figure 25, Tables 3 and 4).

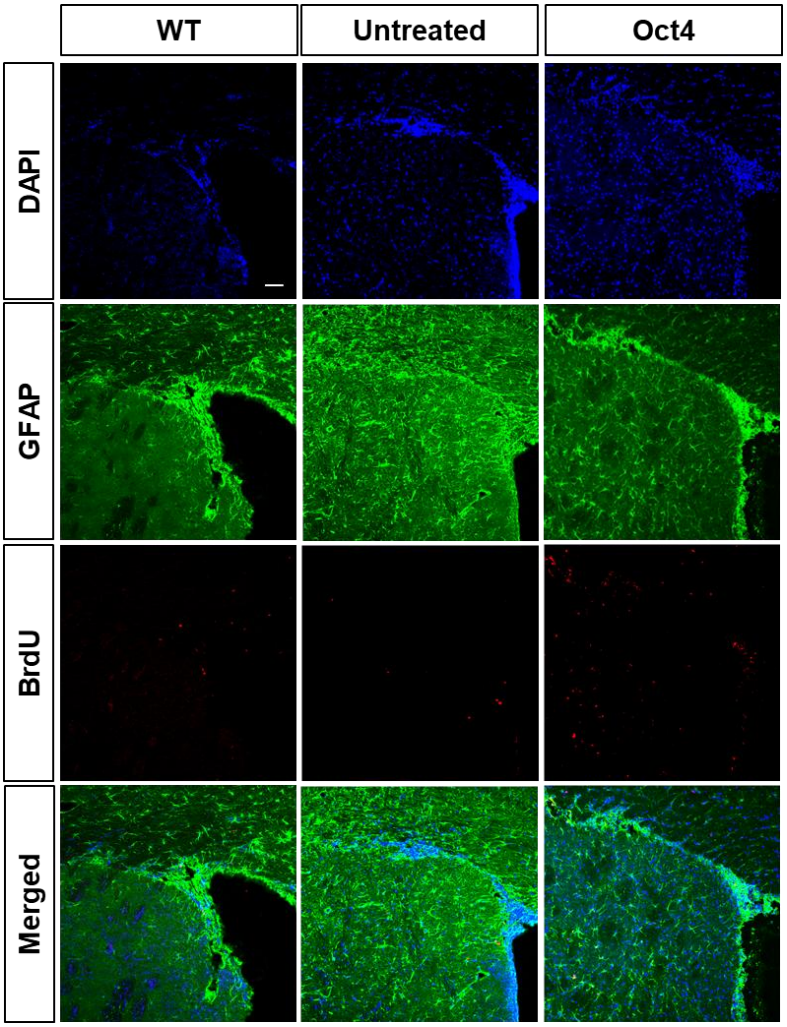

Figure 25. Reduction of GFAP-positive cells after Oct4 overexpression. Immunofluorescent staining for GFAP showed fewer astrocytes in the Oct4-overexpressed group compared to untreated and GFP control groups, indicating possible mitigation of reactive gliosis. Scale bar = 100 μm. One-way ANOVA was performed for group comparisons. Values are reported as mean ± SEM. Statistical significance is denoted as follows: * $P < 0.05$; ** $P < 0.01$; *** $P < 0.001$.

Collectively, these findings demonstrate that Oct4 overexpression promotes oligodendrogenesis and neurogenesis while attenuating reactive astrogliosis, thereby contributing to the restoration of neural integrity in twitcher mice. To better illustrate these effects in a region- and marker-specific manner, quantitative analyses of marker expression levels were conducted and are summarized in Tables 3 and 4.

In the cortex, Tuj1-positive cells were significantly decreased in both the untreated and Oct4 groups compared to wild-type controls. However, BrdU-positive/Nestin-positive and BrdU-positive/Tuj1-positive cells were significantly increased in the Oct4 group compared to both wild-type and untreated groups. BrdU-positive/Olig2-positive cells were also significantly increased in the Oct4 group compared to the untreated group.

In the striatum, Olig2-positive cells were significantly increased in the Oct4 group compared to wild-type and untreated groups. BrdU-positive/Olig2-positive cells were also significantly elevated in the Oct4 group compared to the untreated group.

In the corpus callosum, GFAP-positive cells were significantly increased in the untreated group compared to wild-type controls and subsequently decreased in the Oct4 group compared to the untreated group. BrdU-positive/Olig2-positive and BrdU-positive/GFAP-positive cells were significantly increased in the Oct4 and untreated groups, respectively.

In the subventricular zone, Nestin-positive cells were significantly increased in wild-type controls compared to the untreated group, while BrdU-positive/Nestin-positive cells were significantly decreased in wild-type controls compared to the untreated group. GFAP-positive cells were significantly increased in the untreated group compared to wild-type controls and decreased again in the Oct4 group.

Region	Group	Total volume (x10-3/mm3)	BrdU cells	Nestin$^+$ cells	Olig2$^+$ cells	GFAP$^+$ cells	Tuj1$^+$ cells	BrdU$^+$ Nestin$^+$ Cells	BrdU$^+$ Olig2$^+$ Cells	BrdU$^+$ GFAP$^+$ Cells	BrdU$^+$ Tuj1$^+$ Cells
Cortex	WT	4.187 ± 0.496	3.030 ± 0.504	0.098 ± 0.026	0.610 ± 0.139	10.332 ± 1.336	0.381 ± 0.071	0.182 ± 0.016	1.717 ± 0.391	0.181 ± 0.012	2.217 ± 0.346
	Untreated	4.419 ± 0.513	3.311 ± 0.652	0.083 ± 0.021	0.801 ± 0.038	7.282 ± 0.712	0.286 ± 0.073	0.227 ± 0.006	3.891 ± 0.712	0.102 ± 0.012	2.956 ± 0.485
	Oct4	3.990 ± 0.477	6.210 ± 0.896	0.093 ± 0.015	1.411 ± 0.130	9.341 ± 0.647	0.801 ± 0.143	0.187 ± 0.013	3.434 ± 1.032	0.126 ± 0.011	5.260 ± 0.665
Striatum	WT	2.795 ± 0.160	5.303 ± 0.444	0.033 ± 0.015	1.530 ± 0.115	18.073 ± 0.988	2.525 ± 0.322	0.051 ± 0.006	1.562 ± 0.252	0.146 ± 0.022	3.135 ± 0.605
	Untreated	3.053 ± 0.175	6.764 ± 0.671	0.057 ± 0.008	2.018 ± 0.287	13.357 ± 1.631	1.928 ± 0.247	0.110 ± 0.007	2.348 ± 0.439	0.100 ± 0.010	4.180 ± 0.450
	Oct4	2.962 ± 0.158	7.682 ± 0.683	0.050 ± 0.006	1.932 ± 0.270	27.303 ± 1.893	4.037 ± 0.487	0.059 ± 0.008	2.701 ± 0.505	0.121 ± 0.017	5.933 ± 0.612
Corpus	WT	1.991 ± 0.160	6.893 ± 0.611	0.050 ± 0.011	2.695 ± 0.649	58.426 ± 3.513	3.508 ± 0.210	0.048 ± 0.006	2.292 ± 0.243	0.056 ± 0.012	6.482 ± 1.856
callosum	Untreated	1.838 ± 0.138	8.544 ± 1.055	0.056 ± 0.010	3.401 ± 0.549	51.872 ± 6.157	1.654 ± 0.288	0.112 ± 0.008	5.945 ± 1.012	0.053 ± 0.008	6.663 ± 1.130
	Oct4	1.781 ± 0.169	11.440 ± 1.463	0.062 ± 0.007	3.059 ± 0.623	76.839 ± 10.357	5.910 ± 1.107	0.064 ± 0.010	4.558 ± 0.745	0.055 ± 0.005	11.799 ± 3.074
Subventricular	WT	0.305 ± 0.024	30.432 ± 2.816	0.382 ± 0.067	23.043 ± 3.942	26.354 ± 3.167	12.738 ± 1.736	0.274 ± 0.024	12.305 ± 0.915	0.214 ± 0.028	22.032 ± 2.800
Zone	Untreated	0.311 ± 0.020	23.476 ± 1.491	0.140 ± 0.013	10.378 ± 0.958	25.275 ± 3.520	7.176 ± 1.676	0.438 ± 0.031	16.292 ± 1.489	0.204 ± 0.033	21.932 ± 3.266
	Oct4	0.358 ± 0.018	24.880 ± 1.673	0.293 ± 0.042	13.249 ± 1.403	34.015 ± 4.472	8.265 ± 1.684	0.330 ± 0.022	14.531 ± 2.407	0.223 ± 0.017	17.259 ± 2.577

Table 3. The population of Olig2, Nestin, GFAP, Tuj1, and BrdU-expressing cells by brain regions. Data are presented as mean ± SEM. One-way ANOVA followed by Bonferroni post hoc correction was applied. Statistical significance is denoted as *P < 0.05, **P < 0.01, ***P < 0.001.

Region	Marker	WT	Untreated	Oct4	N	P-value (WT vs Untreated)	P-value (WT vs Oct4)	P-value (Untreated vs Oct4)
Cortex	Total volume	4.187 ± 0.496	4.419 ± 0.513	3.990 ± 0.477	3:3:3	1.000	1.000	1.000
	BrdU cells	3.030 ± 0.504	3.311 ± 0.652	6.210 ± 0.896	3:3:3	1.000	0.011*	0.036*
	$Nestin^+$ cells	0.098 ± 0.026	0.083 ± 0.021	0.093 ± 0.015	3:3:3	1.000	1.000	1.000
	$Olig2^+$ cells	10.332 ± 1.336	7.282 ± 0.712	9.341 ± 0.647	3:3:3	0.209	1.000	0.152
	$Gfap^+$ cells	0.182 ± 0.016	0.227 ± 0.006	0.187 ± 0.013	3:3:3	0.197	1.000	0.161
	$Tuj1^+$ cells	0.181 ± 0.012	0.102 ± 0.012	0.126 ± 0.011	3:3:3	0.002*	0.012*	0.501
	$BrdU^+$ $Nestin^+$ Cells	0.610 ± 0.139	0.801 ± 0.038	1.411 ± 0.130	3:3:3	0.802	0.017*	0.044*
	$BrdU^+$ $Olig2^+$ Cells	0.381 ± 0.071	0.286 ± 0.073	0.801 ± 0.143	3:3:3	1.000	0.075	0.027*
	$BrdU^+$ $Gfap^+$ Cells	1.717 ± 0.391	3.891 ± 0.712	3.434 ± 1.032	3:3:3	0.142	0.593	1.000
	$BrdU^+$ $Tuj1^+$ Cells	2.217 ± 0.346	2.956 ± 0.485	5.260 ± 0.665	3:3:3	0.731	0.004*	0.043*
Striatum	Total volume	2.795 ± 0.160	3.053 ± 0.175	2.962 ± 0.158	3:3:3	0.844	1.000	1.000
	BrdU cells	5.303 ± 0.444	6.764 ± 0.671	7.682 ± 0.683	3:3:3	0.222	0.014*	1.000
	$Nestin^+$ cells	0.033 ± 0.015	0.057 ± 0.008	0.050 ± 0.006	3:3:3	0.605	1.000	1.000
	$Olig2^+$ cells	18.073 ± 0.988	13.357 ± 1.631	27.303 ± 1.893	3:3:3	0.073	0.002*	0.000***
	$Gfap^+$ cells	0.051 ± 0.006	0.110 ± 0.007	0.059 ± 0.008	3:3:3	0.000***	1.000	0.000**
	$Tuj1^+$ cells	0.146 ± 0.022	0.100 ± 0.010	0.121 ± 0.017	3:3:3	0.268	1.000	0.903
	$BrdU^+$ $Nestin^+$ Cells	1.530 ± 0.115	2.018 ± 0.287	1.932 ± 0.270	3:3:3	0.463	0.581	1.000
	$BrdU^+$ $Olig2^+$ Cells	2.525 ± 0.322	1.928 ± 0.247	4.037 ± 0.487	3:3:3	0.469	0.059	0.006*
	$BrdU^+$ $Gfap^+$ Cells	1.562 ± 0.252	2.348 ± 0.439	2.701 ± 0.505	3:3:3	0.416	0.182	1.000
	$BrdU^+$ $Tuj1^+$ Cells	3.135 ± 0.605	4.180 ± 0.450	5.933 ± 0.612	3:3:3	0.568	0.015*	0.105
Corpus Callosum	Total volume	1.991 ± 0.160	1.838 ± 0.138	1.781 ± 0.169	3:3:3	1.000	1.000	1.000
	BrdU cells	6.893 ± 0.611	8.544 ± 1.055	11.440 ± 1.463	3:3:3	0.542	0.018*	0.340
	$Nestin^+$ cells	0.050 ± 0.011	0.056 ± 0.010	0.062 ± 0.007	3:3:3	1.000	1.000	1.000
	$Olig2^+$ cells	58.426 ± 3.513	51.872 ± 6.157	76.839 ± 10.357	3:3:3	1.000	0.340	0.156
	$Gfap^+$ cells	0.048 ± 0.006	0.112 ± 0.008	0.064 ± 0.010	3:3:3	0.000***	0.549	0.006*
	$Tuj1^+$ cells	0.056 ± 0.012	0.053 ± 0.008	0.055 ± 0.005	3:3:3	1.000	1.000	1.000
	$BrdU^+$ $Nestin^+$ Cells	2.695 ± 0.649	3.401 ± 0.549	3.059 ± 0.623	3:3:3	1.000	1.000	1.000
	$BrdU^+$ $Olig2^+$ Cells	3.508 ± 0.210	1.654 ± 0.288	5.910 ± 1.107	3:3:3	0.000**	0.159	0.007*
	$BrdU^+$ $Gfap^+$ Cells	2.292 ± 0.243	5.945 ± 1.012	4.558 ± 0.745	3:3:3	0.012*	0.056	0.852
	$BrdU^+$ $Tuj1^+$ Cells	6.482 ± 1.856	6.663 ± 1.130	11.799 ± 3.074	3:3:3	1.000	0.560	0.532
Subventricular zone	Total volume	0.305 ± 0.024	0.311 ± 0.020	0.358 ± 0.018	3:3:3	1.000	0.252	0.268
	BrdU cells	30.432 ± 2.816	23.476 ± 1.491	24.880 ± 1.673	3:3:3	0.100	0.286	1.000
	$Nestin^+$ cells	0.382 ± 0.067	0.140 ± 0.013	0.293 ± 0.042	3:3:3	0.025*	0.855	0.011*
	$Olig2^+$ cells	26.354 ± 3.167	25.275 ± 3.520	34.015 ± 4.472	3:3:3	1.000	0.540	0.427
	$Gfap^+$ cells	0.274 ± 0.024	0.438 ± 0.031	0.330 ± 0.022	3:3:3	0.001*	0.290	0.031*
	$Tuj1^+$ cells	0.214 ± 0.028	0.204 ± 0.033	0.223 ± 0.017	3:3:3	1.000	1.000	1.000
	$BrdU^+$ $Nestin^+$ Cells	23.043 ± 3.942	10.378 ± 0.958	13.249 ± 1.403	3:3:3	0.044*	0.134	0.321
	$BrdU^+$ $Olig2^+$ Cells	12.738 ± 1.736	7.176 ± 1.676	8.265 ± 1.684	3:3:3	0.105	0.243	1.000
	$BrdU^+$ $Gfap^+$ Cells	12.305 ± 0.915	16.292 ± 1.489	14.531 ± 2.407	3:3:3	0.104	1.000	1.000
	$BrdU^+$ $Tuj1^+$ Cells	22.032 ± 2.800	21.932 ± 3.266	17.259 ± 2.577	3:3:3	1.000	0.688	0.858

Table 4. Regional and marker-specific quantification of proliferation and differentiation. Total volume, BrdU+ cells per volume, Olig2+, Nestin+, Tuj1+, GFAP+ cells, and BrdU+ double-positive cells were quantified in each brain region. Data are presented as mean ± SEM. One-way ANOVA followed by Bonferroni post hoc correction was applied. Statistical significance is denoted as *P < 0.05, **P < 0.01, ***P < 0.001.

To evaluate potential morphological changes associated with Oct4 overexpression, hematoxylin-eosin (H&E) staining was performed. Histological examination revealed no notable morphological abnormalities, cellular atypia, or evidence of dysplasia across all experimental groups, indicating that Oct4 overexpression did not induce overt pathological changes (Figure 26).

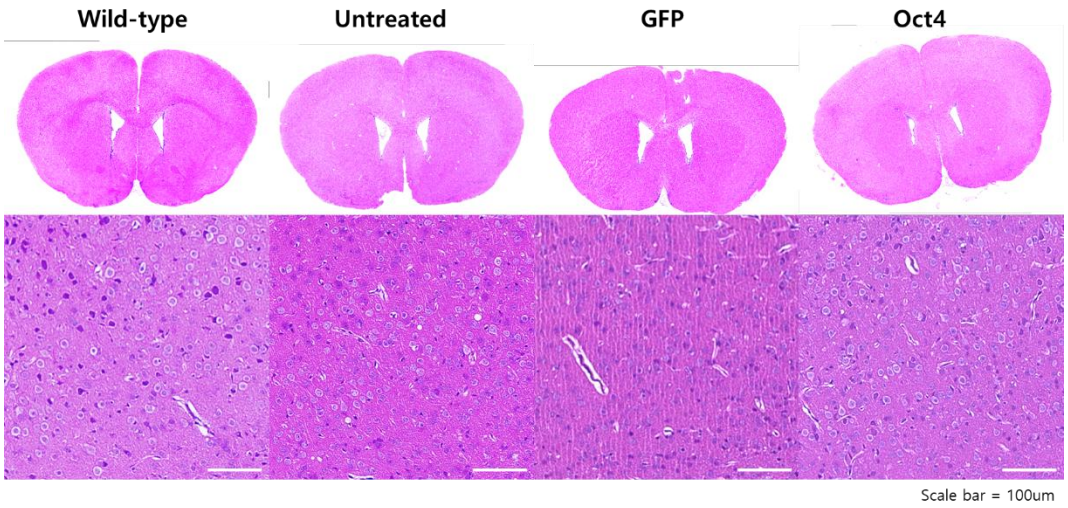

Figure 26. Hematoxylin and eosin (H&E) staining of brain tissue sections. No significant morphological abnormalities or dysplasia were observed in any experimental group. Scale bar = 100 μm.

3.4. Effects of Oct4 overexpression on gene expression related to oligodendrocyte differentiation, cell division, and cell cycle

RNA sequencing was performed on the striatum to identify genes altered by Oct4 overexpression among the Untreated, GFP, and Oct4 groups. Initially, we utilized UniProt Keywords in combination with DAVID (Database for Annotation, Visualization, and Integrated Discovery) to identify differences between the Oct4 and untreated groups (Figure 27). This comparison revealed no genes directly associated with oligodendrocytes or specifically implicated in Krabbe disease pathology.

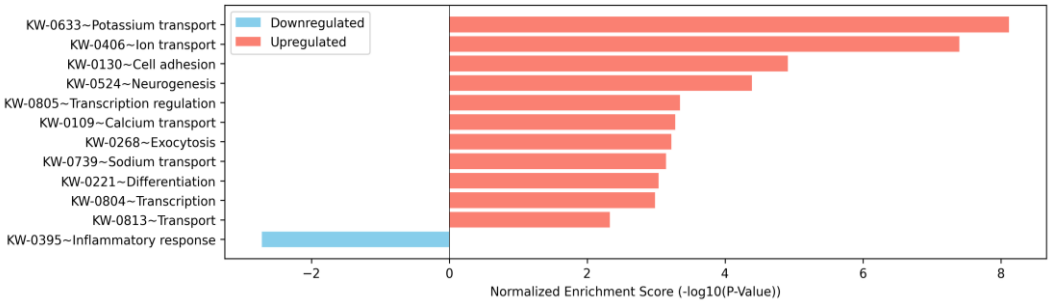

Figure 27. Enrichment analysis of UniProt Keywords comparing untreated and Oct4 groups performed with DAVID. The enrichment analysis highlights differences between the Oct4 and Untreated groups (Oct4/Untreated). UniProt Keywords analysis was conducted using DAVID with the following criteria: Fold Change (FC) $\geq \pm 1.2$, P-value < 0.05, FDR < 1.5, and Benjamini < 1.5, focusing on Biological Processes.

To further investigate the specific effects of Oct4 overexpression, Gene Ontology (GO) analysis using DAVID was performed to examine the differences between the Oct4 and GFP groups (Figure 28). Interestingly, when compared to the GFP control group, genes associated with GO:0048709 ~ Oligodendrocyte differentiation were found to be upregulated in the Oct4 group.

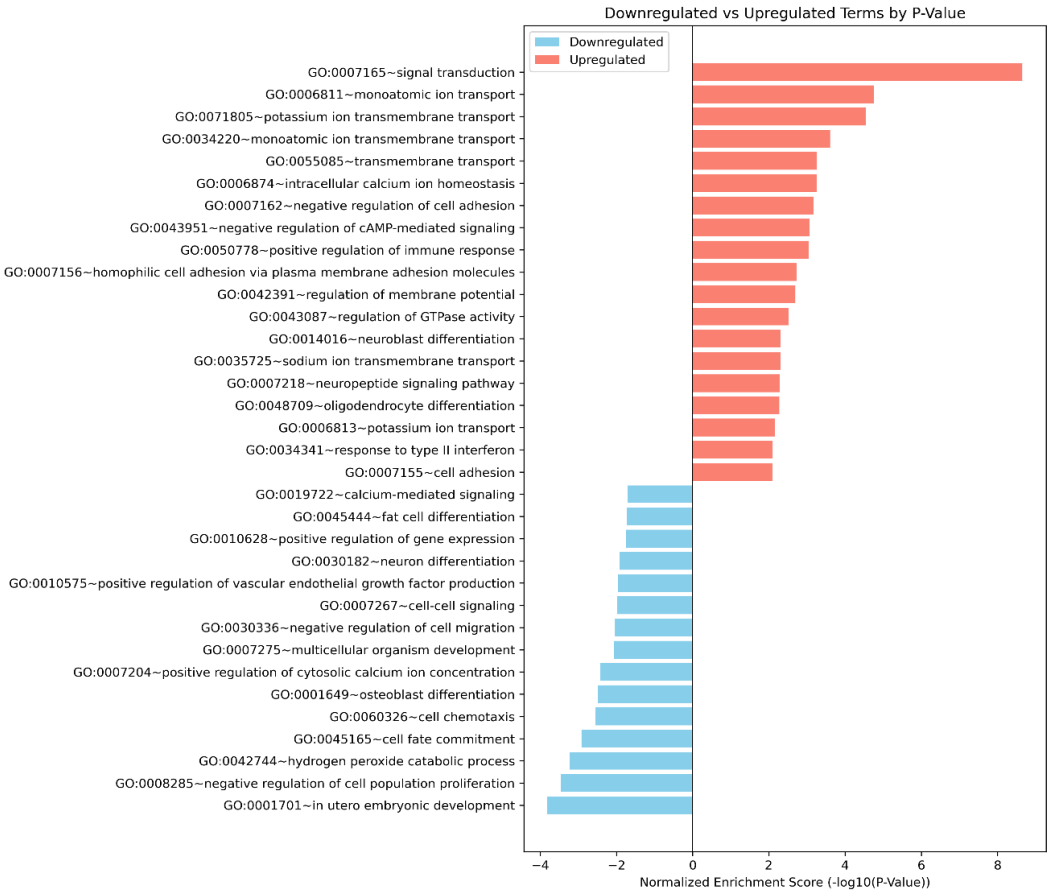

Figure 28. Enrichment Analysis of Gene Ontology (GO) Terms Between Oct4 and GFP Groups Using DAVID. The enrichment analysis highlights differences between the Oct4 and GFP groups (Oct4/GFP). GO analysis was performed with the following criteria: Fold Change (FC) $\geq \pm 1.2$, P-value < 0.05, FDR < 1.5, and Benjamini < 1.5, focusing on Biological Processes.

In the GO:0048709 (oligodendrocyte differentiation) category, the related gene list and P-values are presented in Table 5. Differential expression analysis was performed to identify significant changes, with DRD3, DLX2, and NLGN3 showing significant upregulation in the Oct4 group compared to control groups (P-value < 0.05, FDR-corrected). This upregulation is also visualized through the TPM values in the heatmap (Figure 29).

	Gene name	**Fold change (Oct4/Unt)**	***P-value***	**Fold change (Oct4/GFP)**	***P-value***
GO:0048709~ oligodendrocyte differentiation	DRD3	1.815	0.025	2.530	0.001
	DLX2	1.698	0.017	1.403	0.079
	NLGN3	1.579	0.000	1.357	0.008
	MTOR	1.459	0.000	1.220	0.093
	DLX1	1.386	0.227	1.553	0.104

Table 5. Upregulated genes in the oligodendrocyte differentiation pathway. The fold change values and FDR-corrected P-values for DRD3, DLX2, and NLGN3 are shown, highlighting their significant upregulation in the Oct4 group compared to control groups.

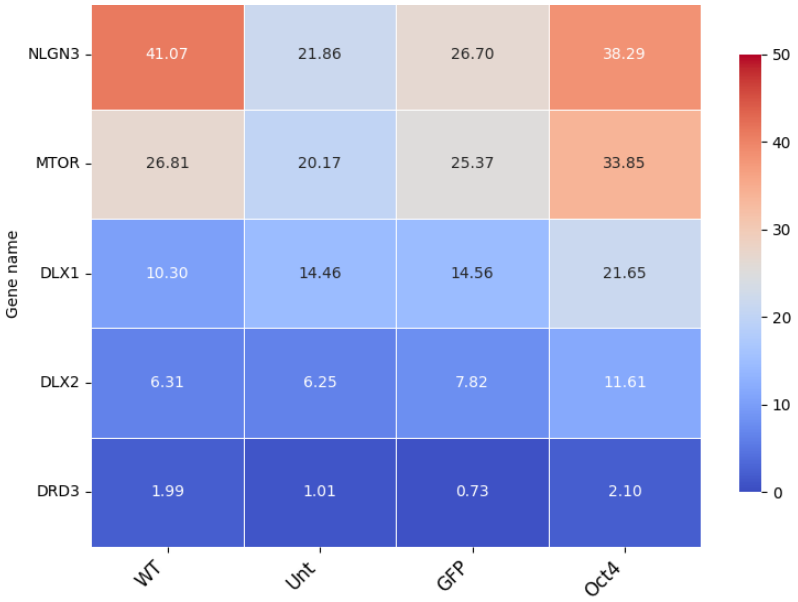

Figure 29. Heatmap of oligodendrocyte differentiation-related genes across experimental groups. The TPM values of oligodendrocyte differentiation-related genes, including DRD3, DLX2, and NLGN3, are displayed for comparison across the Untreated, GFP, and Oct4 groups.

Oct4 is well known for its role in maintaining pluripotency, which is closely associated with the regulation of cell division and the cell cycle. To determine whether Oct4 overexpression affects these processes, its impact on cell division and cell cycle dynamics was assessed. Although several cell cycle transcripts reached statistical significance ($P < 0.05$), their fold change values remained below the predefined threshold of $|\text{Fold Change}| \geq 1.2$. These differences are therefore considered negligible for functional significance, and Oct4 overexpression is interpreted as not inducing abnormal cell cycle re-entry (Table 6, Figure 30).

	Gene name	Oct4/Unt	*P-value*	Oct4/GFP	*P-value*
GO:0051301~	TNKS	1.813	0.000	1.391	0.021
Cell division	TTC28	1.517	0.002	1.573	0.001
	CDCA3	-1.512	0.015	1.299	0.346
	KIF11	-1.540	0.006	1.222	0.424
	ASPM	-1.582	0.005	1.458	0.236
	ANLN	-1.584	0.000	1.461	0.090
	CDK1	-1.686	0.031	1.256	0.492
	NUSAP1	-1.706	0.002	1.316	0.330
	MIS18BP1	-1.832	0.006	1.317	0.425
	ITGB3BP	-1.945	0.002	1.248	0.325
	CDC6	-1.965	0.011	1.280	0.383
KW-0131~	CDCA3	-1.512	0.015	1.299	0.346
Cell cycle	TNKS	1.813	0.000	1.391	0.021
	CKAP2	-1.813	0.018	1.253	0.500
	KIF11	-1.540	0.006	1.222	0.424
	CDC6	-1.965	0.011	1.280	0.383
	MLF1	-2.260	0.035	1.495	0.166
	TTC28	1.517	0.002	1.573	0.001
	ANLN	-1.584	0.000	1.461	0.090
	ASPM	-1.582	0.005	1.458	0.236
	RBL1	-1.669	0.000	1.271	0.103
	MIS18BP1	-1.832	0.006	1.317	0.425
	NUSAP1	-1.706	0.002	1.316	0.330
	CDK1	-1.686	0.031	1.256	0.492
	MCM3	-1.516	0.004	1.329	0.127
	ITGB3BP	-1.945	0.002	1.248	0.325

Table 6. Upregulated genes associated with cell division and cell cycle. The table lists upregulated genes associated with cell division and cell cycle, with their respective fold change values, P-values, and FDR corrections. Although some genes reached statistical significance ($P < 0.05$), fold change values remained below the threshold of $|FC| \geq 1.2$, indicating minimal biological significance.

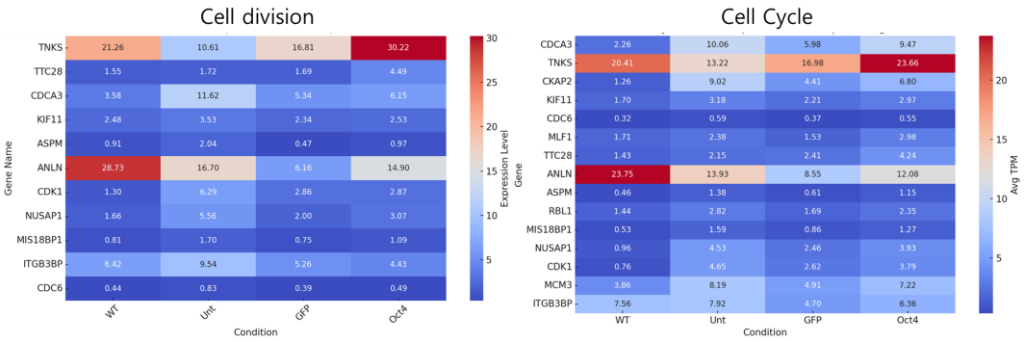

Figure 30. Heatmap of cell cycle and cell division-related genes across experimental groups. The TPM values of genes associated with cell cycle and cell division are displayed for comparison across the Untreated, GFP, and Oct4 groups.

To investigate the overall impact of Oct4 overexpression on mRNA expression patterns, we compared the Oct4 group with the GFP control group to identify differentially expressed genes (Tables 7-97). Gene Ontology analysis and functional characterization of individual genes revealed that Oct4 overexpression upregulated genes associated with oligodendrocyte differentiation, vascular and ion/metabolite transport, cell adhesion and migration, and signal transduction. In contrast, genes related to immune responses, inflammation, and apoptosis were downregulated, along with suppression of astrocyte differentiation and inhibition of the MAPK/STAT signaling pathway.

GO ID	GO Term	Gene Symbol	log2FC	*P-value*	Function Summary
GO:0010876	Lipid localization	Ecrg4	19.174	0.000	Probable hormone that may attenuate cell proliferation and induce senescence of oligodendrocyte and neural precursor cells in the central nervous system.
		Abca4	3.134	0.046	Flippase that catalyzes in an ATP-dependent manner the transport of retinal-phosphatidylethanolamine conjugates like the 11-cis and all-trans isomers of N-retinylidene-phosphatidylethanolamine from th.
		Drd3	2.530	0.001	GPCR dopamine receptor that couples to inhibitory G-proteins, dampening adenylyl cyclase signalling.
		Abca8a	2.094	0.012	Facilitates the transport of cholesterol and taurocholate out of cells.
		Slc22a8	1.924	0.002	Acts as an exchanger for organic anions and dicarboxylates, indirectly driven by the sodium gradient.
		Slco1a4	1.917	0.000	Enables sodium-independent transport of organic anions including taurocholate, cholate, conjugated steroids, prostaglandins, and cardiac glycosides.
		Lbp	1.911	0.001	Involved in host innate immunity by participating in pathogen recognition.
		Xkr6	1.827	0.004	Likely participates in apoptosis during development, aiding in apoptotic cell clearance and phosphatidylserine exposure.
		Atp10b	1.788	0.012	Catalytic integral element of a P4-ATPase flippase complex. It Functions as the catalytic subunit of P4-ATPase flippase, breaking down ATP to transport glucosylceramide across lysosomal membranes.
		Anxa1	1.758	0.018	Critical for innate immunity, participating in glucocorticoid signaling and controlling inflammation.
		Spp1	1.659	0.000	Catalyzes the dephosphorylation of sphingosine 1-phosphate and its analogs, including dihydro-S1P and phyto-S1P.

Atp10a	1.644	0.023	Enzyme subunit of the P4-ATPase flippase that hydrolyzes ATP to facilitate phosphatidylcholine translocation across the plasma membrane.
Gdf9	1.622	0.047	Required for ovarian folliculogenesis.
C3	1.607	0.009	Precursor of non-enzymatic components of the classical, alternative, lectin and GZMK complement pathways, which consist in a cascade of proteins that leads to phagocytosis and breakdown of pathogens a.
Nme4	1.597	0.041	Essential for the mitochondrial synthesis of nucleoside triphosphates distinct from ATP.
Acacb	1.562	0.018	Enzyme catalyzing acetyl-CoA carboxylation into malonyl-CoA, pivotal for fatty acid metabolism.
Wnk4	1.536	0.030	Kinase involved in the WNK4-SPAK/OSR1 pathway, crucial for regulating nephron ion transport and blood pressure.
Abcb1a	1.528	0.002	Acts as a transporter moving drugs and phospholipids through the cell membrane.

Table 7. Upregulated genes associated with lipid localization. The table lists upregulated genes associated with lipid localization, with their respective fold change values, P-values, and FDR corrections. Differential expression analysis was performed using a threshold of FC $\geq \pm 1.2$ and P-value < 0.05.

GO ID	GO Term	Gene Symbol	log_2FC	P-value	Function Summary
GO:0050886	Endocrine process	Ecrg4	19.174	0.000	Probable hormone that may attenuate cell proliferation and induce senescence of oligodendrocyte and neural precursor cells in the central nervous system.
		Aqp1	5.310	0.001	Creates water channels vital for water transport and maintaining tissue fluid balance.
		Oprm1	2.717	0.000	Serves as a binding site for natural opioids including beta-endorphin and endomorphin.
		Drd3	2.530	0.001	GPCR dopamine receptor that couples to inhibitory G-proteins, dampening adenylyl cyclase signalling.
		Edn3	2.123	0.004	Encodes an endothelin peptide, a potent vasoconstrictor produced by endothelial cells.
		Anpep	1.669	0.000	Aminopeptidase with broad substrate range, crucial for breaking down peptides after protein digestion by gastric and pancreatic enzymes.
		Spp1	1.659	0.000	Catalyzes the dephosphorylation of sphingosine 1-phosphate and its analogs, including dihydro-S1P and phyto-S1P.
		Gdf9	1.622	0.047	Required for ovarian folliculogenesis.
		Wnk4	1.536	0.030	Kinase involved in the WNK4-SPAK/OSR1 pathway, crucial for regulating nephron ion transport and blood pressure.

Table 8. Upregulated genes associated with endocrine process. The table lists upregulated genes associated with endocrine process, with their respective fold change values, P-values, and FDR corrections. Differential expression analysis was performed using a threshold of FC $\geq \pm 1.2$ and P-value < 0.05.

GO ID	GO Term	Gene Symbol	log2FC	P-value	Function Summary
GO:0006813	Potassium ion transport	Kcnj13	7.588	0.013	Potassium channel that favors inward K^+ flow over outward movement, contributing to membrane potential stabilization.
		Kcne2	5.345	0.049	Ancillary protein that functions as a regulatory subunit of the voltage-gated potassium channel complex composed of pore-forming and potassium-conducting alpha subunits and of regulatory beta sub.
		Aqp1	5.310	0.001	Creates water channels vital for water transport and maintaining tissue fluid balance.
		Slc24a5	5.077	0.009	Calcium, potassium:sodium antiporter that transports 1 Ca and 1 K to the melanosome in exchange for 4 cytoplasmic Na.
		Drd3	2.530	0.001	GPCR dopamine receptor that couples to inhibitory G-proteins, dampening adenylyl cyclase signalling.
		Kcna3	2.243	0.003	Controls voltage-gated potassium ion flow in excitable cell membranes.
		Kcnh5	2.129	0.000	Forms part of delayed rectifier K^+ channels, enabling outward K^+ currents that remain stable upon depolarization.
		Edn3	2.123	0.004	Encodes an endothelin peptide, a potent vasoconstrictor produced by endothelial cells.
		Kcnb2	1.846	0.027	Potassium channel facilitating K^+ movement across excitable membranes, especially in neurons and smooth muscle.
		Lrrc55	1.679	0.034	Accessory subunit supporting large-conductance voltage- and calcium-activated K^+ channels.
		Wnk4	1.536	0.030	Kinase involved in the WNK4-SPAK/OSR1 pathway, crucial for regulating nephron ion transport and blood pressure.
		Casq2	1.500	0.040	Functions as an intracellular calcium buffer in muscle, with high capacity and moderate affinity.

Table 9. Upregulated genes associated with potassium ion transport. The table lists upregulated genes associated with potassium ion transport, with their respective fold change values, P-values, and FDR corrections. Differential expression analysis was performed using a threshold of FC $\geq \pm 1.2$ and P-value < 0.05.

GO ID	GO Term	Gene Symbol	log2FC	P-value	Function Summary
GO:0006869	Lipid transport	Ecrg4	19.174	0.000	Probable hormone that may attenuate cell proliferation and induce senescence of oligodendrocyte and neural precursor cells in the central nervous system.
		Abca4	3.134	0.046	Flippase that catalyzes in an ATP-dependent manner the transport of retinal-phosphatidylethanolamine conjugates like the 11-cis and all-trans isomers of N-retinylidene-phosphatidylethanolamine.
		Drd3	2.530	0.001	GPCR dopamine receptor that couples to inhibitory G-proteins, dampening adenylyl cyclase signalling.
		Abca8a	2.094	0.012	Facilitates the transport of cholesterol and taurocholate out of cells.
		Slc22a8	1.924	0.002	Acts as an exchanger for organic anions and dicarboxylates, indirectly driven by the sodium gradient.
		Slco1a4	1.917	0.000	Enables sodium-independent transport of organic anions including taurocholate, cholate, conjugated steroids, prostaglandins, and cardiac glycosides.
		Lbp	1.911	0.001	Involved in host innate immunity by participating in pathogen recognition.
		Xkr6	1.827	0.004	Likely participates in apoptosis during development, aiding in apoptotic cell clearance and phosphatidylserine exposure.
		Atp10b	1.788	0.012	Catalytic integral element of a P4-ATPase flippase complex. It Functions as the catalytic subunit of P4-ATPase flippase, breaking down ATP to transport glucosylceramide across lysosomal membranes.
		Anxa1	1.758	0.018	Critical for innate immunity, participating in glucocorticoid signaling and controlling inflammation.
		Spp1	1.659	0.000	Catalyzes the dephosphorylation of sphingosine 1-phosphate and its analogs, including dihydro-S1P and phyto-S1P.
		Atp10a	1.644	0.023	Enzyme subunit of the P4-ATPase flippase that hydrolyzes ATP to facilitate phosphatidylcholine translocation across the plasma membrane.
		Gdf9	1.622	0.047	Required for ovarian folliculogenesis.
		Nme4	1.597	0.041	Essential for the mitochondrial synthesis of nucleoside triphosphates distinct from ATP.
		Wnk4	1.536	0.030	Kinase involved in the WNK4-SPAK/OSR1 pathway, crucial for regulating nephron ion transport and blood pressure.
		Abcb1a	1.528	0.002	Acts as a transporter moving drugs and phospholipids through the cell membrane.

Table 10. Upregulated genes associated with lipid transport. The table lists upregulated genes associated with lipid transport, with their respective fold change values, P-values, and FDR corrections. Differential expression analysis was performed using a threshold of FC $\geq \pm 1.2$ and P-value < 0.05.

GO ID	GO Term	Gene Symbol	log2FC	P-value	Function Summary
GO:0072337	Modified amino acid transport	Folr1	32.244	0.000	Facilitates cellular uptake of folate and its derivatives, moving 5-methyltetrahydrofolate and related compounds.
		Lrp2	1.941	0.003	Endocytic receptor capable of binding multiple ligands.
		Slc22a8	1.924	0.002	Acts as an exchanger for organic anions and dicarboxylates, indirectly driven by the sodium gradient.
		Folr2	1.897	0.045	Facilitates cellular uptake of folate and its derivatives, moving 5-methyltetrahydrofolate and related compounds.
		Slc46a1	1.506	0.011	Proton-coupled folate symporter that mediates folate absorption using an H gradient as a driving force.

Table 11. Upregulated genes associated with modified amino acid transport. The table lists upregulated genes associated with modified amino acid transport, with their respective fold change values, P-values, and FDR corrections. Differential expression analysis was performed using a threshold of FC $\geq \pm 1.2$ and P-value < 0.05.

GO ID	GO Term	Gene Symbol	log2FC	P-value	Function Summary
GO:0015711	Organic anion transport	Folr1	32.244	0.000	Facilitates cellular uptake of folate and its derivatives, moving 5-methyltetrahydrofolate and related compounds.
		Cldn2	20.675	0.001	Forms paracellular channels: polymerizes in tight junction strands with cation- and water-selective channels through the strands, conveying epithelial permeability in a process known as paracellular t.
		Drd3	2.530	0.001	GPCR dopamine receptor that couples to inhibitory G-proteins, dampening adenylyl cyclase signalling.
		Slc16a4	2.286	0.005	Mediates proton-coupled transport of monocarboxylates.
		Lrp2	1.941	0.003	Endocytic receptor capable of binding multiple ligands.
		Slc22a8	1.924	0.002	Acts as an exchanger for organic anions and dicarboxylates, indirectly driven by the sodium gradient.
		Slco1a4	1.917	0.000	Enables sodium-independent transport of organic anions including taurocholate, cholate, conjugated steroids, prostaglandins, and cardiac glycosides.
		Folr2	1.897	0.045	Facilitates cellular uptake of folate and its derivatives, moving 5-methyltetrahydrofolate and related compounds.
		Slc35d2	1.779	0.021	Nucleotide sugar antiporter transporting UDP-N-acetylglucosamine and UDP-glucose from the cytosol into the lumen of the Golgi in exchange of UMP.
		Anxa1	1.758	0.018	Critical for innate immunity, participating in glucocorticoid signaling and controlling inflammation.
		Slc38a6	1.606	0.000	Amino acid transporter with an apparent selectivity for L-glutamine and L-glutamate.
		Acacb	1.562	0.018	Enzyme catalyzing acetyl-CoA carboxylation into malonyl-CoA, pivotal for fatty acid metabolism.
		Slc37a2	1.540	0.000	Functions as a phosphate/glucose-6-phosphate exchanger across membranes.
		Abcb1a	1.528	0.002	Acts as a transporter moving drugs and phospholipids through the cell membrane.
		Slc46a1	1.506	0.011	Proton-coupled folate symporter that mediates folate absorption using an H gradient as a driving force.

Table 12. Upregulated genes associated with organic anion transport. The table lists upregulated genes associated with organic anion transport, with their respective fold change values, P-values, and FDR corrections. Differential expression analysis was performed using a threshold of FC $\geq \pm 1.2$ and P-value < 0.05.

GO ID	GO Term	Gene Symbol	log2FC	P-value	Function Summary
GO:0015698	Inorganic anion transport	Kcne2	5.345	0.049	Ancillary protein that functions as a regulatory subunit of the voltage-gated potassium channel complex composed of pore-forming and potassium-conducting alpha subunits and of regulatory beta sub.
		Oca2	4.089	0.002	Contributes to a melanosome-specific anion current that modulates melanosomal pH for optimal tyrosinase activity required for melanogenesis and the melanosome maturation.
		Best3	3.512	0.036	Ligand-gated anion channel that allows the movement of chloride monoatomic anions across cell membranes when activated by calcium.
		Clic6	1.937	0.008	In the soluble state, catalyzes glutaredoxin-like thiol disulfide exchange reactions with reduced glutathione as electron donor.
		Slc22a8	1.924	0.002	Acts as an exchanger for organic anions and dicarboxylates, indirectly driven by the sodium gradient.
		Gabra2	1.811	0.001	Alpha subunit of the heteropentameric ligand-gated chloride channel gated by gamma-aminobutyric acid, a major inhibitory neurotransmitter in the brain.
		Slc37a2	1.540	0.000	Functions as a phosphate/glucose-6-phosphate exchanger across membranes.
		Wnk4	1.536	0.030	Kinase involved in the WNK4-SPAK/OSR1 pathway, crucial for regulating nephron ion transport and blood pressure.
		Abcb1a	1.528	0.002	Acts as a transporter moving drugs and phospholipids through the cell membrane.

Table 13. Upregulated genes associated with inorganic anion transport. The table lists upregulated genes associated with inorganic anion transport, with their respective fold change values, P-values, and FDR corrections. Differential expression analysis was performed using a threshold of FC $\geq \pm 1.2$ and P-value < 0.05.

GO ID	GO Term	Gene Symbol	log2FC	P-value	Function Summary
GO:0046942	Carboxylic acid transport	Folr1	32.244	0.000	Facilitates cellular uptake of folate and its derivatives, moving 5-methyltetrahydrofolate and related compounds.
		Cldn2	20.675	0.001	Forms paracellular channels: polymerizes in tight junction strands with cation- and water-selective channels through the strands, conveying epithelial permeability in a process known as paracellular t.
		Drd3	2.530	0.001	GPCR dopamine receptor that couples to inhibitory G-proteins, dampening adenylyl cyclase signalling.
		Slc16a4	2.286	0.005	Mediates proton-coupled transport of monocarboxylates.
		Lrp2	1.941	0.003	Endocytic receptor capable of binding multiple ligands.
		Slc22a8	1.924	0.002	Acts as an exchanger for organic anions and dicarboxylates, indirectly driven by the sodium gradient.
		Slco1a4	1.917	0.000	Enables sodium-independent transport of organic anions including taurocholate, cholate, conjugated steroids, prostaglandins, and cardiac glycosides.
		Folr2	1.897	0.045	Facilitates cellular uptake of folate and its derivatives, moving 5-methyltetrahydrofolate and related compounds.
		Anxa1	1.758	0.018	Critical for innate immunity, participating in glucocorticoid signaling and controlling inflammation.
		Slc38a6	1.606	0.000	Amino acid transporter with an apparent selectivity for L-glutamine and L-glutamate.
		Acacb	1.562	0.018	Enzyme catalyzing acetyl-CoA carboxylation into malonyl-CoA, pivotal for fatty acid metabolism.
		Abcb1a	1.528	0.002	Acts as a transporter moving drugs and phospholipids through the cell membrane.
		Slc46a1	1.506	0.011	Proton-coupled folate symporter that mediates folate absorption using an H gradient as a driving force.

Table 14. Upregulated genes associated with carboxylic acid transport. The table lists upregulated genes associated with carboxylic acid transport, with their respective fold change values, P-values, and FDR corrections. Differential expression analysis was performed using a threshold of FC $\geq \pm 1.2$ and P-value < 0.05.

GO ID	GO Term	Gene Symbol	log2FC	P-value	Function Summary
GO:0015849	Organic acid transport	Folr1	32.244	0.000	Facilitates cellular uptake of folate and its derivatives, moving 5-methyltetrahydrofolate and related compounds.
		Cldn2	20.675	0.001	Forms paracellular channels: polymerizes in tight junction strands with cation- and water-selective channels through the strands, conveying epithelial permeability in a process known as paracellular t.
		Drd3	2.530	0.001	GPCR dopamine receptor that couples to inhibitory G-proteins, dampening adenylyl cyclase signalling.
		Slc16a4	2.286	0.005	Mediates proton-coupled transport of monocarboxylates.
		Lrp2	1.941	0.003	Endocytic receptor capable of binding multiple ligands.
		Slc22a8	1.924	0.002	Acts as an exchanger for organic anions and dicarboxylates, indirectly driven by the sodium gradient.
		Slco1a4	1.917	0.000	Enables sodium-independent transport of organic anions including taurocholate, cholate, conjugated steroids, prostaglandins, and cardiac glycosides.
		Folr2	1.897	0.045	Facilitates cellular uptake of folate and its derivatives, moving 5-methyltetrahydrofolate and related compounds.
		Anxa1	1.758	0.018	Critical for innate immunity, participating in glucocorticoid signaling and controlling inflammation.
		Slc38a6	1.606	0.000	Amino acid transporter with an apparent selectivity for L-glutamine and L-glutamate.
		Acacb	1.562	0.018	Enzyme catalyzing acetyl-CoA carboxylation into malonyl-CoA, pivotal for fatty acid metabolism.
		Abcb1a	1.528	0.002	Acts as a transporter moving drugs and phospholipids through the cell membrane.
		Slc46a1	1.506	0.011	Proton-coupled folate symporter that mediates folate absorption using an H gradient as a driving force.

Table 15. Upregulated genes associated with organic acid transport. The table lists upregulated genes associated with organic acid transport, with their respective fold change values, P-values, and FDR corrections. Differential expression analysis was performed using a threshold of FC $\geq \pm 1.2$ and P-value < 0.05.

GO ID	GO Term	Gene Symbol	log2FC	P-value	Function Summary
GO:0045766	Positive regulation of angiogenesis	Aqp1	5.310	0.001	Creates water channels vital for water transport and maintaining tissue fluid balance.
		Cxcr3	5.120	0.001	Chemokine receptor for CXCL9, CXCL10, and CXCL11, regulating mesangial cell proliferation and angiogenesis via G-protein signaling.
		Itgb8	1.901	0.000	Integrin αVβ8 receptor that binds fibronectin, mediating cell-matrix interactions.
		Ago2	1.627	0.002	Essential component of RISC complex, enabling RNA interference and gene silencing.
		Adam12	1.624	0.001	Plays a key role in muscle regeneration by promoting initial stages of myoblast fusion.
		C3	1.607	0.009	Precursor of non-enzymatic components of the classical, alternative, lectin and GZMK complement pathways, which consist in a cascade of proteins that leads to phagocytosis and breakdown of pathogens a.
		Cxcr4	1.590	0.004	Binds CXCL12/SDF-1 chemokine, triggering calcium influx and activation of MAPK pathways.
		Cela1	1.564	0.048	Serine protease targeting elastin and other extracellular matrix proteins.
		Hyal1	1.549	0.002	May have a role in promoting tumor progression.

Table 16. Upregulated genes associated with positive regulation of angiogenesis. The table lists upregulated genes associated with positive regulation of angiogenesis, with their respective fold change values, P-values, and FDR corrections. Differential expression analysis was performed using a threshold of FC ≥ ±1.2 and P-value < 0.05.

GO ID	GO Term	Gene Symbol	log2FC	P-value	Function Summary
GO:0098742	Cell-cell adhesion via plasma-membrane adhesion molecules	Cldn2	20.675	0.001	Forms paracellular channels: polymerizes in tight junction strandas with cation- and water-selective channels through the strands, conveying epithelial permeability in a process known as paracellular transportation.
		Hmcn1	2.667	0.000	Participates in TGF-beta-induced cytoskeletal changes in podocytes, altering actin fibers and podocyte morphology.
		Crb1	2.058	0.010	Facilitates retinal photoreceptor morphogenesis by guiding their structural maturation and stability.
		Cldn1	1.813	0.014	Integral tight junction protein regulating epithelial barrier permeability.
		Crb2	1.757	0.004	Apical polarity regulator vital for epithelial-mesenchymal transition during gastrulation.
		Itga4	1.675	0.045	Integrin α4 associates with β1 or β7 subunits, enabling adhesion to fibronectin.
		Lgals1	1.656	0.005	Beta-galactoside-binding lectin interacting with various complex carbohydrate structures.
		Itgal	1.600	0.004	The ITGAL–ITGB2 integrin heterodimer yields a receptor that recognises ICAM ligands.
		Pcdh20	1.596	0.020	Predicted to act as a calcium-dependent cell adhesion molecule.
		Pcdha4	1.551	0.022	Mediates calcium-dependent adhesion critical for cell recognition and discrimination.

Table 17. Upregulated genes associated with cell-cell adhesion via plasma-membrane adhesion molecules. The table lists upregulated genes associated with cell-cell adhesion via plasma-membrane adhesion molecules, with their respective fold change values, P-values, and FDR corrections. Differential expression analysis was performed using a threshold of FC ≥ ±1.2 and P-value < 0.05.

GO ID	GO Term	Gene Symbol	log2FC	P-value	Function Summary
GO:1904018	Positive regulation of vasculature development	Aqp1	5.310	0.001	Creates water channels vital for water transport and maintaining tissue fluid balance.
		Cxcr3	5.120	0.001	Chemokine receptor for CXCL9, CXCL10, and CXCL11, regulating mesangial cell proliferation and angiogenesis via G-protein signaling.
		Itgb8	1.901	0.000	Integrin αVβ8 receptor that binds fibronectin, mediating cell-matrix interactions.
		Ago2	1.627	0.002	Essential component of RISC complex, enabling RNA interference and gene silencing.
		Adam12	1.624	0.001	Plays a key role in muscle regeneration by promoting initial stages of myoblast fusion.
		C3	1.607	0.009	Precursor of non-enzymatic components of the classical, alternative, lectin and GZMK complement pathways, which consist in a cascade of proteins that leads to phagocytosis and breakdown of pathogens a.
		Cxcr4	1.590	0.004	Binds CXCL12/SDF-1 chemokine, triggering calcium influx and activation of MAPK pathways.
		Cela1	1.564	0.048	Serine protease targeting elastin and other extracellular matrix proteins.
		Hyal1	1.549	0.002	May have a role in promoting tumor progression.

Table 18. Upregulated genes associated with positive regulation of vasculature development. The table lists upregulated genes associated with positive regulation of vasculature development, with their respective fold change values, P-values, and FDR corrections. Differential expression analysis was performed using a threshold of FC ≥ ±1.2 and P-value < 0.05.

GO ID	GO Term	Gene Symbol	log2FC	P-value	Function Summary
GO:0015748	Organophosphate ester transport	Abca4	3.134	0.046	Flippase that catalyzes in an ATP-dependent manner the transport of retinal-phosphatidylethanolamine conjugates like the 11-cis and all-trans isomers of N-retinylidene-phosphatidylethanolamine from th.
		Xkr6	1.827	0.004	Likely participates in apoptosis during development, aiding in apoptotic cell clearance and phosphatidylserine exposure.
		Atp10b	1.788	0.012	Catalytic integral element of a P4-ATPase flippase complex. It Functions as the catalytic subunit of P4-ATPase flippase, breaking down ATP to transport glucosylceramide across lysosomal membranes.
		Slc35d2	1.779	0.021	Nucleotide sugar antiporter transporting UDP-N-acetylglucosamine and UDP-glucose from the cytosol into the lumen of the Golgi in exchange of UMP.
		Atp10a	1.644	0.023	Enzyme subunit of the P4-ATPase flippase that hydrolyzes ATP to facilitate phosphatidylcholine translocation across the plasma membrane.
		Gjb1	1.610	0.026	Forms gap junction channels (connexons) enabling small molecule diffusion between adjacent cells.
		Slc37a2	1.540	0.000	Functions as a phosphate/glucose-6-phosphate exchanger across membranes.
		Abcb1a	1.528	0.002	Acts as a transporter moving drugs and phospholipids through the cell membrane.

Table 19. Upregulated genes associated with organophosphate ester transport. The table lists upregulated genes associated with organophosphate ester transport, with their respective fold change values, P-values, and FDR corrections. Differential expression analysis was performed using a threshold of FC $\geq \pm 1.2$ and P-value < 0.05.

GO ID	GO Term	Gene Symbol	log2FC	P-value	Function Summary
GO:0045332	Phospholipid translocation	Abca4	3.134	0.046	Flippase that catalyzes in an ATP-dependent manner the transport of retinal-phosphatidylethanolamine conjugates like the 11-cis and all-trans isomers of N-retinylidene-phosphatidylethanolamine from th.
		Xkr6	1.827	0.004	Likely participates in apoptosis during development, aiding in apoptotic cell clearance and phosphatidylserine exposure.
		Atp10b	1.788	0.012	Catalytic integral element of a P4-ATPase flippase complex. It Functions as the catalytic subunit of P4-ATPase flippase, breaking down ATP to transport glucosylceramide across lysosomal membranes.
		Atp10a	1.644	0.023	Enzyme subunit of the P4-ATPase flippase that hydrolyzes ATP to facilitate phosphatidylcholine translocation across the plasma membrane.
		Abcb1a	1.528	0.002	Acts as a transporter moving drugs and phospholipids through the cell membrane.

Table 20. Upregulated genes associated with phospholipid translocation. The table lists upregulated genes associated with phospholipid translocation, with their respective fold change values, P-values, and FDR corrections. Differential expression analysis was performed using a threshold of FC $\geq \pm 1.2$ and P-value < 0.05.

GO ID	GO Term	Gene Symbol	log2FC	P-value	Function Summary
GO:0006820	Monoatomic anion transport	Kcne2	5.345	0.049	Ancillary protein that functions as a regulatory subunit of the voltage-gated potassium channel complex composed of pore-forming and potassium-conducting alpha subunits and of regulatory beta sub.
		Oca2	4.089	0.002	Contributes to a melanosome-specific anion current that modulates melanosomal pH for optimal tyrosinase activity required for melanogenesis and the melanosome maturation.
		Best3	3.512	0.036	Ligand-gated anion channel that allows the movement of chloride monoatomic anions across cell membranes when activated by calcium.
		Clic6	1.937	0.008	In the soluble state, catalyzes glutaredoxin-like thiol disulfide exchange reactions with reduced glutathione as electron donor.
		Slco1a4	1.917	0.000	Enables sodium-independent transport of organic anions including taurocholate, cholate, conjugated steroids, prostaglandins, and cardiac glycosides.
		Gabra2	1.811	0.001	Alpha subunit of the heteropentameric ligand-gated chloride channel gated by gamma-aminobutyric acid, a major inhibitory neurotransmitter in the brain.
		Wnk4	1.536	0.030	Kinase involved in the WNK4-SPAK/OSR1 pathway, crucial for regulating nephron ion transport and blood pressure.
		Abcb1a	1.528	0.002	Acts as a transporter moving drugs and phospholipids through the cell membrane.

Table 21. Upregulated genes associated with monoatomic anion transport. The table lists upregulated genes associated with monoatomic anion transport, with their respective fold change values, P-values, and FDR corrections. Differential expression analysis was performed using a threshold of FC $\geq \pm 1.2$ and P-value < 0.05.

GO ID	GO Term	Gene Symbol	log2FC	P-value	Function Summary
GO:0048713	Regulation of oligodendrocyte differentiation	Enpp2	4.227	0.008	Secreted lysophospholipase D that hydrolyzes lysophospholipids to produce the signaling molecule lysophosphatidic acid in extracellular fluids.
		Gsx2	3.531	0.001	Transcription factor that binds 5'-CNAATTAG-3' DNA sequence and regulates the expression of numerous genes including genes important for brain development.
		Drd3	2.530	0.001	GPCR dopamine receptor that couples to inhibitory G-proteins, dampening adenylyl cyclase signalling.
		Nkx2-2os	2.076	0.030	Acts upstream of or within positive regulation of gene expression and positive regulation of oligodendrocyte differentiation.
		Cxcr4	1.590	0.004	Binds CXCL12/SDF-1 chemokine, triggering calcium influx and activation of MAPK pathways.

Table 22. Upregulated genes associated with regulation of oligodendrocyte differentiation. The table lists upregulated genes associated with regulation of oligodendrocyte differentiation, with their respective fold change values, P-values, and FDR corrections. Differential expression analysis was performed using a threshold of FC $\geq \pm 1.2$ and P-value < 0.05.

GO ID	GO Term	Gene Symbol	log2FC	P-value	Function Summary
GO:0034204	Lipid translocation	Abca4	3.134	0.046	Flippase that catalyzes in an ATP-dependent manner the transport of retinal-phosphatidylethanolamine conjugates like the 11-cis and all-trans isomers of N-retinylidene-phosphatidylethanolamine from th.
		Xkr6	1.827	0.004	Likely participates in apoptosis during development, aiding in apoptotic cell clearance and phosphatidylserine exposure.
		Atp10b	1.788	0.012	Catalytic integral element of a P4-ATPase flippase complex. It Functions as the catalytic subunit of P4-ATPase flippase, breaking down ATP to transport glucosylceramide across lysosomal membranes.
		Atp10a	1.644	0.023	Enzyme subunit of the P4-ATPase flippase that hydrolyzes ATP to facilitate phosphatidylcholine translocation across the plasma membrane.
		Abcb1a	1.528	0.002	Acts as a transporter moving drugs and phospholipids through the cell membrane.

Table 23. Upregulated genes associated with lipid translocation. The table lists upregulated genes associated with lipid translocation, with their respective fold change values, P-values, and FDR corrections. Differential expression analysis was performed using a threshold of FC $\geq \pm 1.2$ and P-value < 0.05.

GO ID	GO Term	Gene Symbol	log2FC	P-value	Function Summary
GO:0030198	Extracellular matrix organization	Col8a2	5.178	0.017	Macromolecular integral element of the subendothelium.
		Col8a1	4.092	0.042	Macromolecular integral element of the subendothelium.
		Col4a3	3.007	0.005	Principal integral element of type IV collagen networks in glomerular basement membranes.
		Mia	2.800	0.005	Demonstrates in vitro anti-proliferative effects against melanoma cells and exerts growth-inhibitory influence on other neuroectodermal tumors like gliomas.
		Hmcn1	2.667	0.000	Participates in TGF-beta-induced cytoskeletal changes in podocytes, altering actin fibers and podocyte morphology.
		Adamtsl1	1.977	0.001	Predicted to have important functions in the extracellular matrix.
		Col4a4	1.938	0.003	Key structural element in basement membranes, forming type IV collagen networks.
		Col4a6	1.847	0.015	Contributes to basement membrane integrity via type IV collagen scaffold formation.
		Col9a3	1.775	0.003	Provides structural support in hyaline cartilage and vitreous humor.
		Mmp19	1.607	0.005	Matrix metalloproteinase degrading ECM proteins including aggrecan and cartilage oligomers.
		Has3	1.526	0.026	Enzyme responsible for elongating hyaluronan by adding GlcNAc and GlcUA.

Table 24. Upregulated genes associated with extracellular matrix organization. The table lists upregulated genes associated with extracellular matrix organization, with their respective fold change values, P-values, and FDR corrections. Differential expression analysis was performed using a threshold of FC $\geq \pm 1.2$ and P-value < 0.05.

GO ID	GO Term	Gene Symbol	log2FC	P-value	Function Summary
GO:0048714	Positive regulation of oligodendrocyte differentiation	Enpp2	4.227	0.008	Secreted lysophospholipase D that hydrolyzes lysophospholipids to produce the signaling molecule lysophosphatidic acid in extracellular fluids.
		Gsx2	3.531	0.001	Transcription factor that binds 5'-CNAATTAG-3' DNA sequence and regulates the expression of numerous genes including genes important for brain development.
		Nkx2-2os	2.076	0.030	Acts upstream of or within positive regulation of gene expression and positive regulation of oligodendrocyte differentiation.
		Cxcr4	1.590	0.004	Binds CXCL12/SDF-1 chemokine, triggering calcium influx and activation of MAPK pathways.

Table 25. Upregulated genes associated with positive regulation of oligodendrocyte differentiation. The table lists upregulated genes associated with positive regulation of oligodendrocyte differentiation, with their respective fold change values, P-values, and FDR corrections. Differential expression analysis was performed using a threshold of FC $\geq \pm 1.2$ and P-value < 0.05.

GO ID	GO Term	Gene Symbol	log2FC	P-value	Function Summary
GO:0097035	Regulation of membrane lipid distribution	Abca4	3.134	0.046	Flippase that catalyzes in an ATP-dependent manner the transport of retinal-phosphatidylethanolamine conjugates like the 11-cis and all-trans isomers of N-retinylidene-phosphatidylethanolamine from th.
		Xkr6	1.827	0.004	Likely participates in apoptosis during development, aiding in apoptotic cell clearance and phosphatidylserine exposure.
		Atp10b	1.788	0.012	Catalytic integral element of a P4-ATPase flippase complex. It Functions as the catalytic subunit of P4-ATPase flippase, breaking down ATP to transport glucosylceramide across lysosomal membranes.
		Atp10a	1.644	0.023	Enzyme subunit of the P4-ATPase flippase that hydrolyzes ATP to facilitate phosphatidylcholine translocation across the plasma membrane.
		Abcb1a	1.528	0.002	Acts as a transporter moving drugs and phospholipids through the cell membrane.

Table 26. Upregulated genes associated with regulation of membrane lipid distribution. The table lists upregulated genes associated with regulation of membrane lipid distribution, with their respective fold change values, P-values, and FDR corrections. Differential expression analysis was performed using a threshold of FC $\geq \pm 1.2$ and P-value < 0.05.

GO ID	GO Term	Gene Symbol	log2FC	P-value	Function Summary
GO:0042886	Amide transport	Folr1	32.244	0.000	Facilitates cellular uptake of folate and its derivatives, moving 5-methyltetrahydrofolate and related compounds.
		Ecrg4	19.174	0.000	Probable hormone that may attenuate cell proliferation and induce senescence of oligodendrocyte and neural precursor cells in the central nervous system.
		Aqp1	5.310	0.001	Creates water channels vital for water transport and maintaining tissue fluid balance.
		Glp1r	2.489	0.032	Functions as a glucagon-like peptide-1 responsive G-protein coupled receptor involved in signal transduction.
		Edn3	2.123	0.004	Encodes an endothelin peptide, a potent vasoconstrictor produced by endothelial cells.
		Lrp2	1.941	0.003	Endocytic receptor capable of binding multiple ligands.
		Slc22a8	1.924	0.002	Acts as an exchanger for organic anions and dicarboxylates, indirectly driven by the sodium gradient.
		Folr2	1.897	0.045	Facilitates cellular uptake of folate and its derivatives, moving 5-methyltetrahydrofolate and related compounds.
		Anxa1	1.758	0.018	Critical for innate immunity, participating in glucocorticoid signaling and controlling inflammation.
		Zbed6	1.641	0.006	Acts as a transcriptional suppressor by recognizing the 5′-GCTCGC-3′ motif, exerting tissue-dependent regulatory control.
		Abcb1a	1.528	0.002	Acts as a transporter moving drugs and phospholipids through the cell membrane.
		Slc46a1	1.506	0.011	Proton-coupled folate symporter that mediates folate absorption using an H gradient as a driving force.

Table 27. Upregulated genes associated with amide transport. The table lists upregulated genes associated with amide transport, with their respective fold change values, P-values, and FDR corrections. Differential expression analysis was performed using a threshold of FC ≥ ±1.2 and P-value < 0.05.

GO ID	GO Term	Gene Symbol	log2FC	P-value	Function Summary
GO:0030644	Intracellular chloride ion homeostasis	Spp1	1.659	0.000	Catalyzes the dephosphorylation of sphingosine 1-phosphate and its analogs, including dihydro-S1P and phyto-S1P.
		Tbxas1	1.597	0.005	Catalyzes the conversion of prostaglandin H2 to thromboxane A2, a potent inducer of blood vessel constriction and platelet aggregation.
		Wnk4	1.536	0.030	Kinase involved in the WNK4-SPAK/OSR1 pathway, crucial for regulating nephron ion transport and blood pressure.

Table 28. Upregulated genes associated with intracellular chloride ion homeostasis. The table lists upregulated genes associated with intracellular chloride ion homeostasis, with their respective fold change values, P-values, and FDR corrections. Differential expression analysis was performed using a threshold of FC $\geq \pm 1.2$ and P-value < 0.05.

GO ID	GO Term	Gene Symbol	log2FC	P-value	Function Summary
GO:0051785	Positive regulation of nuclear division	Ooep	3.902	0.007	Component of the subcortical maternal complex, a multiprotein complex that plays a key role in early embryonic development.
		Msx1	3.412	0.001	Acts as a transcriptional repressor.
		Cd28	2.586	0.027	Receptor that plays a role in T-cell activation, proliferation, survival and the maintenance of immune homeostasis.
		Drd3	2.530	0.001	GPCR dopamine receptor that couples to inhibitory G-proteins, dampening adenylyl cyclase signalling.
		Edn3	2.123	0.004	Endothelins are endothelium-derived vasoconstrictor peptides.

Table 29. Upregulated genes associated with positive regulation of nuclear division. The table lists upregulated genes associated with positive regulation of nuclear division, with their respective fold change values, P-values, and FDR corrections. Differential expression analysis was performed using a threshold of FC ≥ ±1.2 and P-value < 0.05.

GO ID	GO Term	Gene Symbol	log2FC	P-value	Function Summary
GO:0043266	Regulation of potassium ion transport	Kcne2	5.345	0.049	Ancillary protein that functions as a regulatory subunit of the voltage-gated potassium channel complex composed of pore-forming and potassium-conducting alpha subunits and of regulatory beta sub.
		Drd3	2.530	0.001	GPCR dopamine receptor that couples to inhibitory G-proteins, dampening adenylyl cyclase signalling.
		Edn3	2.123	0.004	Encodes an endothelin peptide, a potent vasoconstrictor produced by endothelial cells.
		Lrrc55	1.679	0.034	Accessory subunit supporting large-conductance voltage- and calcium-activated K^+ channels.
		Wnk4	1.536	0.030	Kinase involved in the WNK4-SPAK/OSR1 pathway, crucial for regulating nephron ion transport and blood pressure.
		Casq2	1.500	0.040	Functions as an intracellular calcium buffer in muscle, with high capacity and moderate affinity.

Table 30. Upregulated genes associated with regulation of potassium ion transport. The table lists upregulated genes associated with regulation of potassium ion transport, with their respective fold change values, P-values, and FDR corrections. Differential expression analysis was performed using a threshold of FC $\geq \pm 1.2$ and P-value < 0.05.

GO ID	GO Term	Gene Symbol	log2FC	P-value	Function Summary
GO:0030002	Intracellular monoatomic anion homeostasis	Spp1	1.659	0.000	Catalyzes the dephosphorylation of sphingosine 1-phosphate and its analogs, including dihydro-S1P and phyto-S1P.
		Tbxas1	1.597	0.005	Catalyzes the conversion of prostaglandin H2 to thromboxane A2, a potent inducer of blood vessel constriction and platelet aggregation.
		Wnk4	1.536	0.030	Kinase involved in the WNK4-SPAK/OSR1 pathway, crucial for regulating nephron ion transport and blood pressure.

Table 31. Upregulated genes associated with intracellular monoatomic anion homeostasis. The table lists upregulated genes associated with intracellular monoatomic anion homeostasis, with their respective fold change values, P-values, and FDR corrections. Differential expression analysis was performed using a threshold of FC $\geq \pm 1.2$ and P-value < 0.05.

GO ID	GO Term	Gene Symbol	log2FC	P-value	Function Summary
GO:0043277	Apoptotic cell clearance	Xkr6	1.827	0.004	Likely participates in apoptosis during development, aiding in apoptotic cell clearance and phosphatidylserine exposure.
		Anxa1	1.758	0.018	Critical for innate immunity, participating in glucocorticoid signaling and controlling inflammation.
		C2	1.675	0.017	Precursor of the catalytic component of the C3 and C5 convertase complexes, which are part of the complement pathway, a cascade of proteins that leads to phagocytosis and breakdown of pathogens and si.
		C3	1.607	0.009	Precursor of non-enzymatic components of the classical, alternative, lectin and GZMK complement pathways, which consist in a cascade of proteins that leads to phagocytosis and breakdown of pathogens a.
		Edn3	2.123	0.004	Encodes an endothelin peptide, a potent vasoconstrictor produced by endothelial cells.

Table 32. Upregulated genes associated with apoptotic cell clearance. The table lists upregulated genes associated with apoptotic cell clearance, with their respective fold change values, P-values, and FDR corrections. Differential expression analysis was performed using a threshold of FC $\geq \pm 1.2$ and P-value < 0.05.

GO ID	GO Term	Gene Symbol	log2FC	P-value	Function Summary
GO:0055074	Calcium ion homeostasis	Cxcr3	5.120	0.001	Chemokine receptor for CXCL9, CXCL10, and CXCL11, regulating mesangial cell proliferation and angiogenesis via G-protein signaling.
		Slc24a5	5.077	0.009	Calcium, potassium:sodium antiporter that transports 1 Ca and 1 K to the melanosome in exchange for 4 cytoplasmic Na.
		Kl	4.952	0.006	Displays low-level glycosidase activity against steroids bearing glucuronyl groups.
		Grid2ip	2.614	0.006	Serves as a postsynaptic scaffold in Purkinje neurons, anchoring GRID2 to the actin network and associated signalling complexes.
		Drd3	2.530	0.001	GPCR dopamine receptor that couples to inhibitory G-proteins, dampening adenylyl cyclase signalling.
		Glp1r	2.489	0.032	Functions as a glucagon-like peptide-1 responsive G-protein coupled receptor involved in signal transduction.
		Edn3	2.123	0.004	Encodes an endothelin peptide, a potent vasoconstrictor produced by endothelial cells.
		Spp1	1.659	0.000	Catalyzes the dephosphorylation of sphingosine 1-phosphate and its analogs, including dihydro-S1P and phyto-S1P.
		Atp7b	1.565	0.018	Copper ion transmembrane transporter playing a role in the export of copper out of the cells, such as the efflux of hepatic copper into the bile.
		Wnk4	1.536	0.030	Kinase involved in the WNK4-SPAK/OSR1 pathway, crucial for regulating nephron ion transport and blood pressure.
		Casq2	1.500	0.040	Functions as an intracellular calcium buffer in muscle, with high capacity and moderate affinity.

Table 33. Upregulated genes associated with calcium ion homeostasis. The table lists upregulated genes associated with calcium ion homeostasis, with their respective fold change values, P-values, and FDR corrections. Differential expression analysis was performed using a threshold of FC $\geq \pm 1.2$ and P-value < 0.05.

GO ID	GO Term	Gene Symbol	log2FC	P-value	Function Summary
GO:0015850	Organic hydroxy compound transport	Ecrg4	19.174	0.000	Probable hormone that may attenuate cell proliferation and induce senescence of oligodendrocyte and neural precursor cells in the central nervous system.
		Kcne2	5.345	0.049	Ancillary protein that functions as a regulatory subunit of the voltage-gated potassium channel complex composed of pore-forming and potassium-conducting alpha subunits and of regulatory beta sub.
		Aqp1	5.310	0.001	Creates water channels vital for water transport and maintaining tissue fluid balance.
		Slc6a3	3.715	0.021	Mediates sodium- and chloride-dependent transport of dopamine.
		Drd3	2.530	0.001	GPCR dopamine receptor that couples to inhibitory G-proteins, dampening adenylyl cyclase signalling.
		Abca8a	2.094	0.012	Facilitates the transport of cholesterol and taurocholate out of cells.
		Slco1a4	1.917	0.000	Enables sodium-independent transport of organic anions including taurocholate, cholate, conjugated steroids, prostaglandins, and cardiac glycosides.
		Spp1	1.659	0.000	Catalyzes the dephosphorylation of sphingosine 1-phosphate and its analogs, including dihydro-S1P and phyto-S1P.
		Acacb	1.562	0.018	Enzyme catalyzing acetyl-CoA carboxylation into malonyl-CoA, pivotal for fatty acid metabolism.
		Wnk4	1.536	0.030	Kinase involved in the WNK4-SPAK/OSR1 pathway, crucial for regulating nephron ion transport and blood pressure.

Table 34. Upregulated genes associated with organic hydroxy compound transport. The table lists upregulated genes associated with organic hydroxy compound transport, with their respective fold change values, P-values, and FDR corrections. Differential expression analysis was performed using a threshold of FC $\geq \pm 1.2$ and P-value < 0.05.

GO ID	GO Term	Gene Symbol	log2FC	P-value	Function Summary
GO:0031589	Cell-substrate adhesion	Enpp2	4.227	0.008	Secreted lysophospholipase D that hydrolyzes lysophospholipids to produce the signaling molecule lysophosphatidic acid in extracellular fluids.
		Col8a1	4.092	0.042	Macromolecular integral element of the subendothelium.
		Mia	2.800	0.005	Demonstrates in vitro anti-proliferative effects against melanoma cells and exerts growth-inhibitory influence on other neuroectodermal tumors like gliomas.
		Itgb7	2.006	0.012	Integrin ITGA4/ITGB7 is an adhesion molecule that mediates lymphocyte migration and homing to gut-associated lymphoid tissue.
		Itgb8	1.901	0.000	Integrin αVβ8 receptor that binds fibronectin, mediating cell-matrix interactions.
		Itga4	1.675	0.045	Integrin α4 associates with β1 or β7 subunits, enabling adhesion to fibronectin.
		Itgb4	1.668	0.044	Integrin alpha-6/beta-4 is a receptor for laminin.
		Spp1	1.659	0.000	Catalyzes the dephosphorylation of sphingosine 1-phosphate and its analogs, including dihydro-S1P and phyto-S1P.
		Lgals1	1.656	0.005	Beta-galactoside-binding lectin interacting with various complex carbohydrate structures.
		Itgal	1.600	0.004	The ITGAL–ITGB2 integrin heterodimer yields a receptor that recognises ICAM ligands.
		Rreb1	1.568	0.007	RREB1 is a transcription factor that selectively targets RAS-responsive promoter elements.

Table 35. Upregulated genes associated with cell-substrate adhesion. The table lists upregulated genes associated with cell-substrate adhesion, with their respective fold change values, P-values, and FDR corrections. Differential expression analysis was performed using a threshold of FC $\geq \pm 1.2$ and P-value < 0.05.

GO ID	GO Term	Gene Symbol	log2FC	P-value	Function Summary
GO:0045765	Regulation of angiogenesis	Aqp1	5.310	0.001	Creates water channels vital for water transport and maintaining tissue fluid balance.
		Cxcr3	5.120	0.001	Chemokine receptor for CXCL9, CXCL10, and CXCL11, regulating mesangial cell proliferation and angiogenesis via G-protein signaling.
		Col4a3	3.007	0.005	Principal integral element of type IV collagen networks in glomerular basement membranes.
		Itgb8	1.901	0.000	Integrin αVβ8 receptor that binds fibronectin, mediating cell-matrix interactions.
		Ago2	1.627	0.002	Essential component of RISC complex, enabling RNA interference and gene silencing.
		Adam12	1.624	0.001	Plays a key role in muscle regeneration by promoting initial stages of myoblast fusion.
		C3	1.607	0.009	Precursor of non-enzymatic components of the classical, alternative, lectin and GZMK complement pathways, which consist in a cascade of proteins that leads to phagocytosis and breakdown of pathogens a.
		Cxcr4	1.590	0.004	Binds CXCL12/SDF-1 chemokine, triggering calcium influx and activation of MAPK pathways.
		Cela1	1.564	0.048	Serine protease targeting elastin and other extracellular matrix proteins.
		Hyal1	1.549	0.002	May have a role in promoting tumor progression.

Table 36. Upregulated genes associated with regulation of angiogenesis. The table lists upregulated genes associated with regulation of angiogenesis, with their respective fold change values, P-values, and FDR corrections. Differential expression analysis was performed using a threshold of FC ≥ ±1.2 and P-value < 0.05.

GO ID	GO Term	Gene Symbol	log2FC	P-value	Function Summary
GO:0042908	Xenobiotic transport	Abca8a	2.094	0.012	Facilitates the transport of cholesterol and taurocholate out of cells.
		Slc22a8	1.924	0.002	Acts as an exchanger for organic anions and dicarboxylates, indirectly driven by the sodium gradient.
		Cldn1	1.813	0.014	Integral tight junction protein regulating epithelial barrier permeability.
		Abcb1a	1.528	0.002	Acts as a transporter moving drugs and phospholipids through the cell membrane.

Table 37. Upregulated genes associated with xenobiotic transport. The table lists upregulated genes associated with xenobiotic transport, with their respective fold change values, P-values, and FDR corrections. Differential expression analysis was performed using a threshold of FC $\geq \pm 1.2$ and P-value < 0.05.

GO ID	GO Term	Gene Symbol	log2FC	P-value	Function Summary
GO:0032623	Interleukin-2 production	Gpr174	2.731	0.027	G-protein-coupled receptor of lysophosphatidylserine that plays different roles in immune response.
		Cd247	2.658	0.003	Component of the T-cell receptor–CD3 complex on T lymphocytes, vital for adaptive immune signalling.
		Cd28	2.586	0.027	Receptor that plays a role in T-cell activation, proliferation, survival and the maintenance of immune homeostasis.
		Card11	2.167	0.028	Adapter polypeptide, which is essential for adaptive immune response by transducing the activation of NF-kappa-B downstream of T-cell receptor and B-cell receptor engagement.
		Anxa1	1.758	0.018	Critical for innate immunity, participating in glucocorticoid signaling and controlling inflammation.

Table 38. Upregulated genes associated with interleukin-2 production. The table lists upregulated genes associated with interleukin-2 production, with their respective fold change values, P-values, and FDR corrections. Differential expression analysis was performed using a threshold of FC $\geq \pm 1.2$ and P-value < 0.05.

GO ID	GO Term	Gene Symbol	log2FC	P-value	Function Summary
GO:1901342	Regulation of vasculature development	Aqp1	5.310	0.001	Creates water channels vital for water transport and maintaining tissue fluid balance.
		Cxcr3	5.120	0.001	Chemokine receptor for CXCL9, CXCL10, and CXCL11, regulating mesangial cell proliferation and angiogenesis via G-protein signaling.
		Col4a3	3.007	0.005	Principal integral element of type IV collagen networks in glomerular basement membranes.
		Itgb8	1.901	0.000	Integrin αVβ8 receptor that binds fibronectin, mediating cell-matrix interactions.
		Ago2	1.627	0.002	Essential component of RISC complex, enabling RNA interference and gene silencing.
		Adam12	1.624	0.001	Plays a key role in muscle regeneration by promoting initial stages of myoblast fusion.
		C3	1.607	0.009	Precursor of non-enzymatic components of the classical, alternative, lectin and GZMK complement pathways, which consist in a cascade of proteins that leads to phagocytosis and breakdown of pathogens a.
		Cxcr4	1.590	0.004	Binds CXCL12/SDF-1 chemokine, triggering calcium influx and activation of MAPK pathways.
		Cela1	1.564	0.048	Serine protease targeting elastin and other extracellular matrix proteins.
		Hyal1	1.549	0.002	May have a role in promoting tumor progression.

Table 39. Upregulated genes associated with regulation of vasculature development. The table lists upregulated genes associated with regulation of vasculature development, with their respective fold change values, P-values, and FDR corrections. Differential expression analysis was performed using a threshold of FC ≥ ±1.2 and P-value < 0.05.

GO ID	GO Term	Gene Symbol	log2FC	P-value	Function Summary
GO:0090092	Regulation of transmembrane receptor protein serine/threonine kinase signaling pathway	Folr1	32.244	0.000	Facilitates cellular uptake of folate and its derivatives, moving 5-methyltetrahydrofolate and related compounds.
		Wfikkn2	7.812	0.021	Multidomain protein acting as a broad-spectrum protease inhibitor with several discrete inhibitory modules.
		Sostdc1	4.259	0.002	May be playing a role in the onset of endometrial receptivity for implantation/sensitization for the decidual cell reaction.
		Msx1	3.412	0.001	Acts as a transcriptional repressor.
		Lrp2	1.941	0.003	Endocytic receptor capable of binding multiple ligands.
		Lefty1	1.938	0.012	Key modulator of LEFTY2 and NODAL pathways, indispensable for establishing the left-right body axis.
		Bmp5	1.901	0.030	TGF-β superfamily growth factor contributing to cartilage and bone formation as well as neurogenesis.
		Crb2	1.757	0.004	Apical polarity regulator vital for epithelial-mesenchymal transition during gastrulation.
		Notch2	1.584	0.000	Transmembrane receptor that binds Jagged-1/2 and Delta-1 ligands to orchestrate cell-fate decisions.

Table 40. Upregulated genes associated with regulation of transmembrane receptor protein serine/threonine kinase signaling pathway. The table lists upregulated genes associated with regulation of transmembrane receptor protein serine/threonine kinase signaling pathway, with their respective fold change values, P-values, and FDR corrections. Differential expression analysis was performed using a threshold of FC $\geq \pm 1.2$ and P-value < 0.05.

GO ID	GO Term	Gene Symbol	log2FC	P-value	Function Summary
GO:0046651	Lymphocyte proliferation	Il7r	2.684	0.000	Receptor for interleukin-7.
		Cd28	2.586	0.027	Receptor that plays a role in T-cell activation, proliferation, survival and the maintenance of immune homeostasis.
		Card11	2.167	0.028	Adapter polypeptide, which is essential for adaptive immune response by transducing the activation of NF-kappa-B downstream of T-cell receptor and B-cell receptor engagement.
		Tnfsf13	2.099	0.044	Secreted signalling molecule, which binds to TNFRSF13B/TACI and to TNFRSF17/BCMA.
		Gpnmb	1.806	0.000	Could be a melanogenic enzyme.
		Anxa1	1.758	0.018	Critical for innate immunity, participating in glucocorticoid signaling and controlling inflammation.
		Dock2	1.604	0.002	Participates in cytoskeletal rearrangements required for lymphocyte migration in response of chemokines.
		Itgal	1.600	0.004	The ITGAL–ITGB2 integrin heterodimer yields a receptor that recognises ICAM ligands.
		Cxcr4	1.590	0.004	Binds CXCL12/SDF-1 chemokine, triggering calcium influx and activation of MAPK pathways.
		Igfbp2	1.506	0.038	Multifunctional protein that plays a critical role in regulating the availability of IGFs such as IGF1 and IGF2 to their receptors and thereby regulates IGF-mediated cellular processes including proli.

Table 41. Upregulated genes associated with lymphocyte proliferation. The table lists upregulated genes associated with lymphocyte proliferation, with their respective fold change values, P-values, and FDR corrections. Differential expression analysis was performed using a threshold of FC $\geq \pm 1.2$ and P-value < 0.05.

GO ID	GO Term	Gene Symbol	log2FC	P-value	Function Summary
GO:1901379	Regulation of potassium ion transmembrane transport	Kcne2	5.345	0.049	Ancillary protein that functions as a regulatory subunit of the voltage-gated potassium channel complex composed of pore-forming and potassium-conducting alpha subunits and of regulatory beta sub.
		Edn3	2.123	0.004	Encodes an endothelin peptide, a potent vasoconstrictor produced by endothelial cells.
		Lrrc55	1.679	0.034	Accessory subunit supporting large-conductance voltage- and calcium-activated K^+ channels.
		Wnk4	1.536	0.030	Kinase involved in the WNK4-SPAK/OSR1 pathway, crucial for regulating nephron ion transport and blood pressure.
		Casq2	1.500	0.040	Functions as an intracellular calcium buffer in muscle, with high capacity and moderate affinity.

Table 42. Upregulated genes associated with regulation of potassium ion transmembrane transport. The table lists upregulated genes associated with regulation of potassium ion transmembrane transport, with their respective fold change values, P-values, and FDR corrections. Differential expression analysis was performed using a threshold of FC $\geq \pm 1.2$ and P-value < 0.05.

GO ID	GO Term	Gene Symbol	log2FC	P-value	Function Summary
GO:0035088	Establishment or maintenance of apical/basal cell polarity	Ooep	3.902	0.007	Component of the subcortical maternal complex, a multiprotein complex that plays a key role in early embryonic development.
		Crb3	2.437	0.022	Participates in the establishment of cell polarity in mammalian epithelial cells.
		Crb1	2.058	0.010	Facilitates retinal photoreceptor morphogenesis by guiding their structural maturation and stability.
		Crb2	1.757	0.004	Apical polarity regulator vital for epithelial-mesenchymal transition during gastrulation.

Table 43. Upregulated genes associated with establishment or maintenance of apical/basal cell polarity. The table lists upregulated genes associated with establishment or maintenance of apical/basal cell polarity, with their respective fold change values, P-values, and FDR corrections. Differential expression analysis was performed using a threshold of FC $\geq \pm 1.2$ and P-value < 0.05.

GO ID	GO Term	Gene Symbol	log2FC	P-value	Function Summary
GO:0043114	Regulation of vascular permeability	Cldn5	-1.607	0.001	Tight-junction protein crucial for sealing intercellular gaps via calcium-independent adhesion.
		Adm	-1.810	0.002	Adrenomedullin/ADM and proadrenomedullin N-20 terminal peptide/PAMP are peptide hormones that act as potent hypotensive and vasodilatator agents.
		Cdh5	-1.825	0.015	Calcium-dependent cadherin mediating homotypic adhesion between endothelial cells.
		Akap12	-1.990	0.002	Scaffolding protein that spatially organises PKA and PKC signalling domains.
		C2cd4b	-2.489	0.014	Involved in positive regulation of acute inflammatory response; regulation of cell adhesion; and regulation of vascular permeability involved in acute inflammatory response.

Table 44. Downregulated genes associated with regulation of vascular permeability. The table lists downregulated genes associated with regulation of vascular permeability, with their respective fold change values, P-values, and FDR corrections. Differential expression analysis was performed using a threshold of FC $\geq \pm 1.2$ and P-value < 0.05.

GO ID	GO Term	Gene Symbol	log2FC	P-value	Function Summary
GO:0050727	Regulation of inflammatory response	Nfkbia	-1.520	0.013	Restrains the activity of dimeric NF-kappa-B/REL complexes by trapping REL dimers in the cytoplasm by masking their nuclear localization signals.
		Serpine1	-1.635	0.004	Broad-spectrum inhibitor that targets serine proteases.
		Sphk1	-1.662	0.005	Drives the phosphorylation of sphingosine to form sphingosine 1-phosphate, a lipid mediator with both intra- and extracellular functions.
		Clcf1	-1.738	0.001	Forms a neurotrophic heterodimer with CRLF1, essential for neuronal development.
		Cdh5	-1.825	0.015	Calcium-dependent cadherin mediating homotypic adhesion between endothelial cells.
		Socs3	-1.844	0.000	SOCS family polypeptides form part of a classical negative feedback system, which regulates cytokine signal transduction.
		Zfp36	-2.008	0.004	Zinc-finger protein promoting decay of AU-rich mRNAs by accelerating deadenylation.
		Ier3	-2.036	0.000	Regulator maintaining ERK activity by blocking PP2A-PPP2R5C-driven dephosphorylation.
		C2cd4b	-2.489	0.014	Involved in positive regulation of acute inflammatory response; regulation of cell adhesion; and regulation of vascular permeability involved in acute inflammatory response.
		Ctla2a	-4.071	0.005	Not known, expressed in activated T-cell.

Table 45. Upregulated genes associated with regulation of inflammatory response. The table lists upregulated genes associated with regulation of inflammatory response, with their respective fold change values, P-values, and FDR corrections. Differential expression analysis was performed using a threshold of FC $\geq \pm 1.2$ and P-value < 0.05.

GO ID	GO Term	Gene Symbol	log2FC	P-value	Function Summary
GO:0045765	Regulation of angiogenesis	Cldn5	-1.607	0.001	Tight-junction protein crucial for sealing intercellular gaps via calcium-independent adhesion.
		Serpine1	-1.635	0.004	Broad-spectrum inhibitor that targets serine proteases.
		Sphk1	-1.662	0.005	Drives the phosphorylation of sphingosine to form sphingosine 1-phosphate, a lipid mediator with both intra- and extracellular functions.
		Lif	-1.676	0.002	Leukemia inhibitory factor drives the terminal differentiation of leukemic cells.
		Adm	-1.810	0.002	Adrenomedullin/ADM and proadrenomedullin N-20 terminal peptide/PAMP are peptide hormones that act as potent hypotensive and vasodilatator agents.
		Cdh5	-1.825	0.015	Calcium-dependent cadherin mediating homotypic adhesion between endothelial cells.
		Adamts1	-1.866	0.000	Metalloprotease which cleaves aggrecan, a cartilage proteoglycan, at the '1691-Glu-|-Leu-1692' site, and may be involved in its turnover.
		Adamts9	-1.867	0.004	ADAMTS family metalloprotease implicated in proteoglycan cleavage, organ morphogenesis and anti-angiogenic control.
		Angpt2	-2.299	0.011	Antagonises ANGPT1 by binding TEK/TIE2 receptors, thereby reshaping endothelial angiopoietin signalling.

Table 46. Upregulated genes associated with regulation of angiogenesis. The table lists upregulated genes associated with regulation of angiogenesis, with their respective fold change values, P-values, and FDR corrections. Differential expression analysis was performed using a threshold of FC $\geq \pm 1.2$ and P-value < 0.05.

GO ID	GO Term	Gene Symbol	log2FC	P-value	Function Summary
GO:1901342	Regulation of vasculature development	Cldn5	-1.607	0.001	Tight-junction protein crucial for sealing intercellular gaps via calcium-independent adhesion.
		Serpine1	-1.635	0.004	Broad-spectrum inhibitor that targets serine proteases.
		Sphk1	-1.662	0.005	Drives the phosphorylation of sphingosine to form sphingosine 1-phosphate, a lipid mediator with both intra- and extracellular functions.
		Lif	-1.676	0.002	Leukemia inhibitory factor drives the terminal differentiation of leukemic cells.
		Adm	-1.810	0.002	Adrenomedullin/ADM and proadrenomedullin N-20 terminal peptide/PAMP are peptide hormones that act as potent hypotensive and vasodilatator agents.
		Cdh5	-1.825	0.015	Calcium-dependent cadherin mediating homotypic adhesion between endothelial cells.
		Adamts1	-1.866	0.000	Metalloprotease which cleaves aggrecan, a cartilage proteoglycan, at the '1691-Glu-|-Leu-1692' site, and may be involved in its turnover.
		Adamts9	-1.867	0.004	ADAMTS family metalloprotease implicated in proteoglycan cleavage, organ morphogenesis and anti-angiogenic control.
		Angpt2	-2.299	0.011	Antagonises ANGPT1 by binding TEK/TIE2 receptors, thereby reshaping endothelial angiopoietin signalling.

Table 47. Upregulated genes associated with regulation of vasculature development. The table lists upregulated genes associated with regulation of vasculature development, with their respective fold change values, P-values, and FDR corrections. Differential expression analysis was performed using a threshold of FC $\geq \pm 1.2$ and P-value < 0.05.

GO ID	GO Term	Gene Symbol	log2FC	P-value	Function Summary
GO:0016525	Negative regulation of angiogenesis	Cldn5	-1.607	0.001	Tight-junction protein crucial for sealing intercellular gaps via calcium-independent adhesion.
		Serpine1	-1.635	0.004	Broad-spectrum inhibitor that targets serine proteases.
		Lif	-1.676	0.002	Leukemia inhibitory factor drives the terminal differentiation of leukemic cells.
		Adamts1	-1.866	0.000	Metalloprotease which cleaves aggrecan, a cartilage proteoglycan, at the '1691-Glu-|-Leu-1692' site, and may be involved in its turnover.
		Adamts9	-1.867	0.004	ADAMTS family metalloprotease implicated in proteoglycan cleavage, organ morphogenesis and anti-angiogenic control.
		Angpt2	-2.299	0.011	Antagonises ANGPT1 by binding TEK/TIE2 receptors, thereby reshaping endothelial angiopoietin signalling.

Table 48. Upregulated genes associated with negative regulation of angiogenesis. The table lists upregulated genes associated with negative regulation of angiogenesis, with their respective fold change values, P-values, and FDR corrections. Differential expression analysis was performed using a threshold of FC $\geq \pm 1.2$ and P-value < 0.05.

GO ID	GO Term	Gene Symbol	log2FC	P-value	Function Summary
GO:2000181	Negative regulation of blood vessel morphogenesis	Cldn5	-1.607	0.001	Tight-junction protein crucial for sealing intercellular gaps via calcium-independent adhesion.
		Serpine1	-1.635	0.004	Broad-spectrum inhibitor that targets serine proteases.
		Lif	-1.676	0.002	Leukemia inhibitory factor drives the terminal differentiation of leukemic cells.
		Adamts1	-1.866	0.000	Metalloprotease which cleaves aggrecan, a cartilage proteoglycan, at the '1691-Glu-|-Leu-1692' site, and may be involved in its turnover.
		Adamts9	-1.867	0.004	ADAMTS family metalloprotease implicated in proteoglycan cleavage, organ morphogenesis and anti-angiogenic control.
		Angpt2	-2.299	0.011	Antagonises ANGPT1 by binding TEK/TIE2 receptors, thereby reshaping endothelial angiopoietin signalling.

Table 49. Upregulated genes associated with negative regulation of blood vessel morphogenesis. The table lists upregulated genes associated with negative regulation of blood vessel morphogenesis, with their respective fold change values, P-values, and FDR corrections. Differential expression analysis was performed using a threshold of FC ≥ ±1.2 and P-value < 0.05.

GO ID	GO Term	Gene Symbol	log2FC	P-value	Function Summary
GO:1901343	Negative regulation of vasculature development	Cldn5	-1.607	0.001	Tight-junction protein crucial for sealing intercellular gaps via calcium-independent adhesion.
		Serpine1	-1.635	0.004	Broad-spectrum inhibitor that targets serine proteases.
		Lif	-1.676	0.002	Leukemia inhibitory factor drives the terminal differentiation of leukemic cells.
		Adamts1	-1.866	0.000	Metalloprotease which cleaves aggrecan, a cartilage proteoglycan, at the '1691-Glu-|-Leu-1692' site, and may be involved in its turnover.
		Adamts9	-1.867	0.004	ADAMTS family metalloprotease implicated in proteoglycan cleavage, organ morphogenesis and anti-angiogenic control.
		Angpt2	-2.299	0.011	Antagonises ANGPT1 by binding TEK/TIE2 receptors, thereby reshaping endothelial angiopoietin signalling.

Table 50. Upregulated genes associated with negative regulation of vasculature development. The table lists upregulated genes associated with negative regulation of vasculature development, with their respective fold change values, P-values, and FDR corrections. Differential expression analysis was performed using a threshold of FC ≥ ±1.2 and P-value < 0.05.

GO ID	GO Term	Gene Symbol	log2FC	P-value	Function Summary
GO:2000352	Negative regulation of endothelial cell apoptotic process	Icam1	-1.506	0.007	Adhesion molecule that engages integrin LFA-1, enabling leukocyte–endothelium interactions.
		Serpine1	-1.635	0.004	Broad-spectrum inhibitor that targets serine proteases.
		Cdh5	-1.825	0.015	Calcium-dependent cadherin mediating homotypic adhesion between endothelial cells.
		Angptl4	-2.337	0.001	Secreted modulator that deactivates lipoprotein lipase, thereby regulating serum triglyceride clearance.

Table 51. Upregulated genes associated with negative regulation of endothelial cell apoptotic process. The table lists upregulated genes associated with negative regulation of endothelial cell apoptotic process, with their respective fold change values, P-values, and FDR corrections. Differential expression analysis was performed using a threshold of FC ≥ ±1.2 and P-value < 0.05.

GO ID	GO Term	Gene Symbol	log2FC	P-value	Function Summary
GO:0030198	Extracellular matrix organization	Has1	-1.533	0.045	Enzyme responsible for elongating hyaluronan by adding GlcNAc and GlcUA.
		Crispld2	-1.746	0.022	Promotes matrix assembly.
		Adamts1	-1.866	0.000	Metalloprotease which cleaves aggrecan, a cartilage proteoglycan, at the '1691-Glu-|-Leu-1692' site, and may be involved in its turnover.
		Adamts9	-1.867	0.004	ADAMTS family metalloprotease implicated in proteoglycan cleavage, organ morphogenesis and anti-angiogenic control.
		Col6a4	-1.921	0.042	Collagen VI subunit functioning as a cellular adhesion scaffold.
		Bcl3	-1.963	0.005	Transcriptional co-factor influencing NF-κB-driven gene expression.
		Impg2	-2.119	0.008	Matrix proteoglycan binding chondroitin sulfate and hyaluronan, supporting photoreceptor maturation and maintenance.
		Has2	-2.312	0.000	Enzyme responsible for elongating hyaluronan by adding GlcNAc and GlcUA.

Table 52. Upregulated genes associated with extracellular matrix organization. The table lists upregulated genes associated with extracellular matrix organization, with their respective fold change values, P-values, and FDR corrections. Differential expression analysis was performed using a threshold of FC ≥ ±1.2 and P-value < 0.05.

GO ID	GO Term	Gene Symbol	log2FC	P-value	Function Summary
GO:0043062	Extracellular structure organization	Has1	-1.533	0.045	Enzyme responsible for elongating hyaluronan by adding GlcNAc and GlcUA.
		Crispld2	-1.746	0.022	Promotes matrix assembly.
		Adamts1	-1.866	0.000	Metalloprotease which cleaves aggrecan, a cartilage proteoglycan, at the '1691-Glu-|-Leu-1692' site, and may be involved in its turnover.
		Adamts9	-1.867	0.004	ADAMTS family metalloprotease implicated in proteoglycan cleavage, organ morphogenesis and anti-angiogenic control.
		Col6a4	-1.921	0.042	Collagen VI subunit functioning as a cellular adhesion scaffold.
		Bcl3	-1.963	0.005	Transcriptional co-factor influencing NF-κB-driven gene expression.
		Impg2	-2.119	0.008	Matrix proteoglycan binding chondroitin sulfate and hyaluronan, supporting photoreceptor maturation and maintenance.
		Has2	-2.312	0.000	Enzyme responsible for elongating hyaluronan by adding GlcNAc and GlcUA.

Table 53. Upregulated genes associated with extracellular structure organization. The table lists upregulated genes associated with extracellular structure organization, with their respective fold change values, P-values, and FDR corrections. Differential expression analysis was performed using a threshold of FC ≥ ±1.2 and P-value < 0.05.

GO ID	GO Term	Gene Symbol	log2FC	P-value	Function Summary
GO:0030856	Regulation of epithelial cell differentiation	Cldn5	-1.607	0.001	Tight-junction protein crucial for sealing intercellular gaps via calcium-independent adhesion.
		Maff	-1.627	0.003	Small Maf protein that forms homodimers acting as transcriptional repressors due to absence of an activation domain.
		Serpine1	-1.635	0.004	Broad-spectrum inhibitor that targets serine proteases.
		Lif	-1.676	0.002	Leukemia inhibitory factor drives the terminal differentiation of leukemic cells.
		Cdh5	-1.825	0.015	Calcium-dependent cadherin mediating homotypic adhesion between endothelial cells.
		Zfp36	-2.008	0.004	Zinc-finger protein promoting decay of AU-rich mRNAs by accelerating deadenylation.

Table 54. Downregulated genes associated with regulation of epithelial cell differentiation. The table lists downregulated genes associated with regulation of epithelial cell differentiation, with their respective fold change values, P-values, and FDR corrections. Differential expression analysis was performed using a threshold of FC ≥ ±1.2 and P-value < 0.05.

GO ID	GO Term	Gene Symbol	log2FC	P-value	Function Summary
GO:0070371	ERK1 and ERK2 cascade	Icam1	-1.506	0.007	Adhesion molecule that engages integrin LFA-1, enabling leukocyte–endothelium interactions.
		Myc	-1.578	0.000	Broad-acting transcription factor that recognises the 5′-CAC(G/A)TG-3′ motif to modulate gene expression.
		Thpo	-1.580	0.002	Lineage-restricted cytokine that drives megakaryocyte proliferation and maturation.
		Lif	-1.676	0.002	Leukemia inhibitory factor drives the terminal differentiation of leukemic cells.
		Clcf1	-1.738	0.001	Forms a neurotrophic heterodimer with CRLF1, essential for neuronal development.
		Akap12	-1.990	0.002	Scaffolding protein that spatially organises PKA and PKC signalling domains.
		Acta2	-2.120	0.009	Alpha-smooth muscle actin contributing to diverse actin-based motility processes.
		Ccl19	-2.210	0.003	Chemokine that potently attracts naïve $CD4^+$ and $CD8^+$ T cells and modestly recruits resting B cells.

Table 55. Downregulated genes associated with ERK1 and ERK2 cascade. The table lists downregulated genes associated with ERK1 and ERK2 cascade, with their respective fold change values, P-values, and FDR corrections. Differential expression analysis was performed using a threshold of FC ≥ ±1.2 and P-value < 0.05.

GO ID	GO Term	Gene Symbol	log2FC	P-value	Function Summary
GO:2000351	Regulation of endothelial cell apoptotic process	Icam1	-1.506	0.007	Adhesion molecule that engages integrin LFA-1, enabling leukocyte–endothelium interactions.
		Serpine1	-1.635	0.004	Broad-spectrum inhibitor that targets serine proteases.
		Cdh5	-1.825	0.015	Calcium-dependent cadherin mediating homotypic adhesion between endothelial cells.
		Angptl4	-2.337	0.001	Secreted modulator that deactivates lipoprotein lipase, thereby regulating serum triglyceride clearance.

Table 56. Downregulated genes associated with regulation of endothelial cell apoptotic process. The table lists downregulated genes associated with regulation of endothelial cell apoptotic process, with their respective fold change values, P-values, and FDR corrections. Differential expression analysis was performed using a threshold of FC ≥ ±1.2 and P-value < 0.05.

GO ID	GO Term	Gene Symbol	log2FC	P-value	Function Summary
GO:0043116	Negative regulation of vascular permeability	Cldn5	-1.607	0.001	Tight-junction protein crucial for sealing intercellular gaps via calcium-independent adhesion.
		Adm	-1.810	0.002	Adrenomedullin/ADM and proadrenomedullin N-20 terminal peptide/PAMP are peptide hormones that act as potent hypotensive and vasodilatator agents.
		Akap12	-1.990	0.002	Scaffolding protein that spatially organises PKA and PKC signalling domains.

Table 57. Downregulated genes associated with negative regulation of vascular permeability. The table lists downregulated genes associated with negative regulation of vascular permeability, with their respective fold change values, P-values, and FDR corrections. Differential expression analysis was performed using a threshold of FC ≥ ±1.2 and P-value < 0.05.

GO ID	GO Term	Gene Symbol	log2FC	P-value	Function Summary
GO:0038066	p38MAPK cascade	Gadd45b	-1.565	0.005	Involved in the regulation of growth and apoptosis.
		Sphk1	-1.662	0.005	Drives the phosphorylation of sphingosine to form sphingosine 1-phosphate, a lipid mediator with both intra- and extracellular functions.
		Map3k6	-1.711	0.011	Component of a protein kinase signal transduction cascade.
		Zfp36	-2.008	0.004	Zinc-finger protein promoting decay of AU-rich mRNAs by accelerating deadenylation.

Table 58. Downregulated genes associated with p38MAPK cascade. The table lists downregulated genes associated with p38MAPK cascade, with their respective fold change values, P-values, and FDR corrections. Differential expression analysis was performed using a threshold of FC $\geq \pm 1.2$ and P-value < 0.05.

GO ID	GO Term	Gene Symbol	log2FC	P-value	Function Summary
GO:0072577	Endothelial cell apoptotic process	Icam1	-1.506	0.007	Adhesion molecule that engages integrin LFA-1, enabling leukocyte–endothelium interactions.
		Serpine1	-1.635	0.004	Broad-spectrum inhibitor that targets serine proteases.
		Cdh5	-1.825	0.015	Calcium-dependent cadherin mediating homotypic adhesion between endothelial cells.
		Angptl4	-2.337	0.001	Secreted modulator that deactivates lipoprotein lipase, thereby regulating serum triglyceride clearance.

Table 59. Downregulated genes associated with endothelial cell apoptotic process. The table lists downregulated genes associated with endothelial cell apoptotic process, with their respective fold change values, P-values, and FDR corrections. Differential expression analysis was performed using a threshold of FC $\geq \pm 1.2$ and P-value < 0.05.

GO ID	GO Term	Gene Symbol	log2FC	P-value	Function Summary
GO:0048145	Regulation of fibroblast proliferation	Myc	-1.578	0.000	Broad-acting transcription factor that recognises the 5′-CAC(G/A)TG-3′ motif to modulate gene expression.
		Pmaip1	-1.583	0.008	Pro-apoptotic factor that activates caspases by neutralising anti-apoptotic Bcl-2 proteins.
		Serpine1	-1.635	0.004	Broad-spectrum inhibitor that targets serine proteases.
		Sphk1	-1.662	0.005	Drives the phosphorylation of sphingosine to form sphingosine 1-phosphate, a lipid mediator with both intra- and extracellular functions.
		Lif	-1.676	0.002	Leukemia inhibitory factor drives the terminal differentiation of leukemic cells.

Table 60. Downregulated genes associated with regulation of fibroblast proliferation. The table lists downregulated genes associated with regulation of fibroblast proliferation, with their respective fold change values, P-values, and FDR corrections. Differential expression analysis was performed using a threshold of FC $\geq \pm 1.2$ and P-value < 0.05.

GO ID	GO Term	Gene Symbol	log2FC	P-value	Function Summary
GO:0071356	Cellular response to tumor necrosis factor	Nfkbia	-1.520	0.013	Restrains the activity of dimeric NF-kappa-B/REL complexes by trapping REL dimers in the cytoplasm by masking their nuclear localization signals.
		Sphk1	-1.662	0.005	Drives the phosphorylation of sphingosine to form sphingosine 1-phosphate, a lipid mediator with both intra- and extracellular functions.
		Akap12	-1.990	0.002	Scaffolding protein that spatially organises PKA and PKC signalling domains.
		Zfp36	-2.008	0.004	Zinc-finger protein promoting decay of AU-rich mRNAs by accelerating deadenylation.
		Naip1	-2.079	0.027	Anti-apoptotic protein that suppresses caspase-3, -7 and -9 activities.
		Has2	-2.312	0.000	Enzyme responsible for elongating hyaluronan by adding GlcNAc and GlcUA.

Table 61. Downregulated genes associated with cellular response to tumor necrosis factor. The table lists downregulated genes associated with cellular response to tumor necrosis factor, with their respective fold change values, P-values, and FDR corrections. Differential expression analysis was performed using a threshold of FC $\geq \pm 1.2$ and P-value < 0.05.

GO ID	GO Term	Gene Symbol	log2FC	P-value	Function Summary
GO:1903317	Regulation of protein maturation	Plaur	-1.514	0.025	Cell-surface receptor for urokinase plasminogen activator, mediating localized proteolysis.
		Tfr2	-1.517	0.040	Transferrin receptor facilitating iron uptake independently of intracellular iron levels.
		Serpine1	-1.635	0.004	Broad-spectrum inhibitor that targets serine proteases.
		Ctla2a	-4.071	0.005	Not known, expressed in activated T-cell.

Table 62. Downregulated genes associated with regulation of protein maturation. The table lists downregulated genes associated with regulation of protein maturation, with their respective fold change values, P-values, and FDR corrections. Differential expression analysis was performed using a threshold of FC $\geq \pm 1.2$ and P-value < 0.05.

GO ID	GO Term	Gene Symbol	log2FC	P-value	Function Summary
GO:0070098	Chemokine-mediated signaling pathway	Ccl25	-1.563	0.028	Potentially involved in T-cell development.
		Thpo	-1.580	0.002	Lineage-restricted cytokine that drives megakaryocyte proliferation and maturation.
		Ccl19	-2.210	0.003	Chemokine that potently attracts naïve $CD4^+$ and $CD8^+$ T cells and modestly recruits resting B cells.
		Ackr1	-2.323	0.003	Transferrin receptor facilitating iron uptake independently of intracellular iron levels.

Table 63. Downregulated genes associated with chemokine-mediated signaling pathway. The table lists downregulated genes associated with chemokine-mediated signaling pathway, with their respective fold change values, P-values, and FDR corrections. Differential expression analysis was performed using a threshold of FC $\geq \pm 1.2$ and P-value < 0.05.

GO ID	GO Term	Gene Symbol	log2FC	P-value	Function Summary
GO:0032102	Negative regulation of response to external stimulus	Plaur	-1.514	0.025	Cell-surface receptor for urokinase plasminogen activator, mediating localized proteolysis.
		Serpine1	-1.635	0.004	Broad-spectrum inhibitor that targets serine proteases.
		Cdh5	-1.825	0.015	Calcium-dependent cadherin mediating homotypic adhesion between endothelial cells.
		Socs3	-1.844	0.000	SOCS family polypeptides form part of a classical negative feedback system, which regulates cytokine signal transduction.
		Zfp36	-2.008	0.004	Zinc-finger protein promoting decay of AU-rich mRNAs by accelerating deadenylation.
		Ier3	-2.036	0.000	Regulator maintaining ERK activity by blocking PP2A-PPP2R5C-driven dephosphorylation.
		Angpt2	-2.299	0.011	Antagonises ANGPT1 by binding TEK/TIE2 receptors, thereby reshaping endothelial angiopoietin signalling.
		Ctla2a	-4.071	0.005	Not known, expressed in activated T-cell.

Table 64. Downregulated genes associated with negative regulation of response to external stimulus. The table lists downregulated genes associated with negative regulation of response to external stimulus, with their respective fold change values, P-values, and FDR corrections. Differential expression analysis was performed using a threshold of FC $\geq \pm 1.2$ and P-value < 0.05.

GO ID	GO Term	Gene Symbol	log2FC	P-value	Function Summary
GO:0048146	Positive regulation of fibroblast proliferation	Myc	-1.578	0.000	Broad-acting transcription factor that recognises the 5′-CAC(G/A)TG-3′ motif to modulate gene expression.
		Serpine1	-1.635	0.004	Broad-spectrum inhibitor that targets serine proteases.
		Sphk1	-1.662	0.005	Drives the phosphorylation of sphingosine to form sphingosine 1-phosphate, a lipid mediator with both intra- and extracellular functions.
		Lif	-1.676	0.002	Leukemia inhibitory factor drives the terminal differentiation of leukemic cells.

Table 65. Downregulated genes associated with positive regulation of fibroblast proliferation. The table lists downregulated genes associated with positive regulation of fibroblast proliferation, with their respective fold change values, P-values, and FDR corrections. Differential expression analysis was performed using a threshold of FC ≥ ±1.2 and P-value < 0.05.

GO ID	GO Term	Gene Symbol	log2FC	P-value	Function Summary
GO:0034612	Response to tumor necrosis factor	Nfkbia	-1.520	0.013	Restrains the activity of dimeric NF-kappa-B/REL complexes by trapping REL dimers in the cytoplasm by masking their nuclear localization signals.
		Sphk1	-1.662	0.005	Drives the phosphorylation of sphingosine to form sphingosine 1-phosphate, a lipid mediator with both intra- and extracellular functions.
		Akap12	-1.990	0.002	Scaffolding protein that spatially organises PKA and PKC signalling domains.
		Zfp36	-2.008	0.004	Zinc-finger protein promoting decay of AU-rich mRNAs by accelerating deadenylation.
		Naip1	-2.079	0.027	Anti-apoptotic protein that suppresses caspase-3, -7 and -9 activities.
		Has2	-2.312	0.000	Enzyme responsible for elongating hyaluronan by adding GlcNAc and GlcUA.

Table 66. Downregulated genes associated with response to tumor necrosis factor. The table lists downregulated genes associated with response to tumor necrosis factor, with their respective fold change values, P-values, and FDR corrections. Differential expression analysis was performed using a threshold of FC $\geq \pm 1.2$ and P-value < 0.05.

GO ID	GO Term	Gene Symbol	log2FC	P-value	Function Summary
GO:0070372	Regulation of ERK1 and ERK2 cascade	Icam1	-1.506	0.007	Adhesion molecule that engages integrin LFA-1, enabling leukocyte–endothelium interactions.
		Thpo	-1.580	0.002	Lineage-restricted cytokine that drives megakaryocyte proliferation and maturation.
		Lif	-1.676	0.002	Leukemia inhibitory factor drives the terminal differentiation of leukemic cells.
		Clcf1	-1.738	0.001	Forms a neurotrophic heterodimer with CRLF1, essential for neuronal development.
		Akap12	-1.990	0.002	Scaffolding protein that spatially organises PKA and PKC signalling domains.
		Acta2	-2.120	0.009	Alpha-smooth muscle actin contributing to diverse actin-based motility processes.
		Ccl19	-2.210	0.003	Chemokine that potently attracts naïve $CD4^+$ and $CD8^+$ T cells and modestly recruits resting B cells.

Table 67. Downregulated genes associated with regulation of ERK1 and ERK2 cascade. The table lists downregulated genes associated with regulation of ERK1 and ERK2 cascade, with their respective fold change values, P-values, and FDR corrections. Differential expression analysis was performed using a threshold of FC ≥ ±1.2 and P-value < 0.05.

GO ID	GO Term	Gene Symbol	log2FC	P-value	Function Summary
GO:0071347	Cellular response to interleukin-1	Nfkbia	-1.520	0.013	Restrains the activity of dimeric NF-kappa-B/REL complexes by trapping REL dimers in the cytoplasm by masking their nuclear localization signals.
		Serpine1	-1.635	0.004	Broad-spectrum inhibitor that targets serine proteases.
		Akap12	-1.990	0.002	Scaffolding protein that spatially organises PKA and PKC signalling domains.
		Has2	-2.312	0.000	Enzyme responsible for elongating hyaluronan by adding GlcNAc and GlcUA.

Table 68. Downregulated genes associated with cellular response to interleukin-1. The table lists downregulated genes associated with cellular response to interleukin-1, with their respective fold change values, P-values, and FDR corrections. Differential expression analysis was performed using a threshold of FC $\geq \pm 1.2$ and P-value < 0.05.

GO ID	GO Term	Gene Symbol	log2FC	P-value	Function Summary
GO:0048144	Fibroblast proliferation	Myc	-1.578	0.000	Broad-acting transcription factor that recognises the 5′-CAC(G/A)TG-3′ motif to modulate gene expression.
		Pmaip1	-1.583	0.008	Pro-apoptotic factor that activates caspases by neutralising anti-apoptotic Bcl-2 proteins.
		Serpine1	-1.635	0.004	Broad-spectrum inhibitor that targets serine proteases.
		Sphk1	-1.662	0.005	Drives the phosphorylation of sphingosine to form sphingosine 1-phosphate, a lipid mediator with both intra- and extracellular functions.
		Lif	-1.676	0.002	Leukemia inhibitory factor drives the terminal differentiation of leukemic cells.

Table 69. Downregulated genes associated with fibroblast proliferation. The table lists downregulated genes associated with fibroblast proliferation, with their respective fold change values, P-values, and FDR corrections. Differential expression analysis was performed using a threshold of FC $\geq \pm 1.2$ and P-value < 0.05.

GO ID	GO Term	Gene Symbol	log2FC	P-value	Function Summary
GO:0008625	Extrinsic apoptotic signaling pathway via death domain receptors	Icam1	-1.506	0.007	Adhesion molecule that engages integrin LFA-1, enabling leukocyte–endothelium interactions.
		Tnfrsf10b	-1.582	0.025	Death-domain receptor that binds the cytotoxic ligand TRAIL (TNFSF10) to initiate extrinsic apoptosis.
		Pmaip1	-1.583	0.008	Pro-apoptotic factor that activates caspases by neutralising anti-apoptotic Bcl-2 proteins.
		Serpine1	-1.635	0.004	Broad-spectrum inhibitor that targets serine proteases.

Table 70. Downregulated genes associated with extrinsic apoptotic signaling pathway via death domain receptors. The table lists downregulated genes associated with extrinsic apoptotic signaling pathway via death domain receptors, with their respective fold change values, P-values, and FDR corrections. Differential expression analysis was performed using a threshold of FC $\geq \pm 1.2$ and P-value < 0.05.

GO ID	GO Term	Gene Symbol	log2FC	P-value	Function Summary
GO:1990868	Response to chemokine	Ccl25	-1.563	0.028	Potentially involved in T-cell development.
		Thpo	-1.580	0.002	Lineage-restricted cytokine that drives megakaryocyte proliferation and maturation.
		Ccl19	-2.210	0.003	Chemokine that potently attracts naïve $CD4^+$ and $CD8^+$ T cells and modestly recruits resting B cells.
		Ackr1	-2.323	0.003	Transferrin receptor facilitating iron uptake independently of intracellular iron levels.

Table 71. Downregulated genes associated with response to chemokine. The table lists downregulated genes associated with response to chemokine, with their respective fold change values, P-values, and FDR corrections. Differential expression analysis was performed using a threshold of FC $\geq \pm 1.2$ and P-value < 0.05.

GO ID	GO Term	Gene Symbol	log2FC	P-value	Function Summary
GO:0001570	Vasculogenesis	Rasip1	-1.713	0.000	Required for the proper formation of vascular structures that develop via both vasculogenesis and angiogenesis.
		Adm	-1.810	0.002	Adrenomedullin/ADM and proadrenomedullin N-20 terminal peptide/PAMP are peptide hormones that act as potent hypotensive and vasodilatator agents.
		Has2	-2.312	0.000	Enzyme responsible for elongating hyaluronan by adding GlcNAc and GlcUA.
		Asb4	-2.834	0.001	Substrate-recognition subunit of an ECS-type SCF E3 ligase, directing ubiquitination and proteasomal turnover of target proteins.

Table 72. Downregulated genes associated with vasculogenesis. The table lists downregulated genes associated with vasculogenesis, with their respective fold change values, P-values, and FDR corrections. Differential expression analysis was performed using a threshold of FC ≥ ±1.2 and P-value < 0.05.

GO ID	GO Term	Gene Symbol	log2FC	P-value	Function Summary
GO:0050728	Negative regulation of inflammatory response	Cdh5	-1.825	0.015	Calcium-dependent cadherin mediating homotypic adhesion between endothelial cells.
		Socs3	-1.844	0.000	SOCS family polypeptides form part of a classical negative feedback system, which regulates cytokine signal transduction.
		Zfp36	-2.008	0.004	Zinc-finger protein promoting decay of AU-rich mRNAs by accelerating deadenylation.
		Ier3	-2.036	0.000	Regulator maintaining ERK activity by blocking PP2A-PPP2R5C-driven dephosphorylation.
		Ctla2a	-4.071	0.005	Not known, expressed in activated T-cell.

Table 73. Downregulated genes associated with negative regulation of inflammatory response. The table lists downregulated genes associated with negative regulation of inflammatory response, with their respective fold change values, P-values, and FDR corrections. Differential expression analysis was performed using a threshold of FC ≥ ±1.2 and P-value < 0.05.

GO ID	GO Term	Gene Symbol	log2FC	P-value	Function Summary
GO:0070555	Response to interleukin-1	Nfkbia	-1.520	0.013	Restrains the activity of dimeric NF-kappa-B/REL complexes by trapping REL dimers in the cytoplasm by masking their nuclear localization signals.
		Serpine1	-1.635	0.004	Broad-spectrum inhibitor that targets serine proteases.
		Akap12	-1.990	0.002	Scaffolding protein that spatially organises PKA and PKC signalling domains.
		Has2	-2.312	0.000	Enzyme responsible for elongating hyaluronan by adding GlcNAc and GlcUA.

Table 74. Downregulated genes associated with response to interleukin-1. The table lists downregulated genes associated with response to interleukin-1, with their respective fold change values, P-values, and FDR corrections. Differential expression analysis was performed using a threshold of FC $\geq \pm 1.2$ and P-value < 0.05.

GO ID	GO Term	Gene Symbol	log2FC	P-value	Function Summary
GO:0045766	Positive regulation of angiogenesis	Serpine1	-1.635	0.004	Broad-spectrum inhibitor that targets serine proteases.
		Sphk1	-1.662	0.005	Drives the phosphorylation of sphingosine to form sphingosine 1-phosphate, a lipid mediator with both intra- and extracellular functions.
		Adm	-1.810	0.002	Adrenomedullin/ADM and proadrenomedullin N-20 terminal peptide/PAMP are peptide hormones that act as potent hypotensive and vasodilatator agents.
		Cdh5	-1.825	0.015	Calcium-dependent cadherin mediating homotypic adhesion between endothelial cells.
		Angpt2	-2.299	0.011	Antagonises ANGPT1 by binding TEK/TIE2 receptors, thereby reshaping endothelial angiopoietin signalling.

Table 75. Downregulated genes associated with positive regulation of angiogenesis. The table lists downregulated genes associated with positive regulation of angiogenesis, with their respective fold change values, P-values, and FDR corrections. Differential expression analysis was performed using a threshold of FC $\geq \pm 1.2$ and P-value < 0.05.

GO ID	GO Term	Gene Symbol	log2FC	P-value	Function Summary
GO:1904018	Positive regulation of vasculature development	Serpine1	-1.635	0.004	Broad-spectrum inhibitor that targets serine proteases.
		Sphk1	-1.662	0.005	Drives the phosphorylation of sphingosine to form sphingosine 1-phosphate, a lipid mediator with both intra- and extracellular functions.
		Adm	-1.810	0.002	Adrenomedullin/ADM and proadrenomedullin N-20 terminal peptide/PAMP are peptide hormones that act as potent hypotensive and vasodilatator agents.
		Cdh5	-1.825	0.015	Calcium-dependent cadherin mediating homotypic adhesion between endothelial cells.
		Angpt2	-2.299	0.011	Antagonises ANGPT1 by binding TEK/TIE2 receptors, thereby reshaping endothelial angiopoietin signalling.

Table 76. Downregulated genes associated with positive regulation of vasculature development. The table lists downregulated genes associated with positive regulation of vasculature development, with their respective fold change values, P-values, and FDR corrections. Differential expression analysis was performed using a threshold of FC $\geq \pm 1.2$ and P-value < 0.05.

GO ID	GO Term	Gene Symbol	log2FC	P-value	Function Summary
GO:2001214	Positive regulation of vasculogenesis	Adm	-1.810	0.002	Adrenomedullin/ADM and proadrenomedullin N-20 terminal peptide/PAMP are peptide hormones that act as potent hypotensive and vasodilatator agents.
		Asb4	-2.834	0.001	Substrate-recognition subunit of an ECS-type SCF E3 ligase, directing ubiquitination and proteasomal turnover of target proteins.

Table 77. Downregulated genes associated with positive regulation of vasculogenesis. The table lists downregulated genes associated with positive regulation of vasculogenesis, with their respective fold change values, P-values, and FDR corrections. Differential expression analysis was performed using a threshold of FC $\geq \pm 1.2$ and P-value < 0.05.

GO ID	GO Term	Gene Symbol	log2FC	P-value	Function Summary
GO:0097696	Cell surface receptor signaling pathway via STAT	Thpo	-1.580	0.002	Lineage-restricted cytokine that drives megakaryocyte proliferation and maturation.
		Lif	-1.676	0.002	Leukemia inhibitory factor drives the terminal differentiation of leukemic cells.
		Clcf1	-1.738	0.001	Forms a neurotrophic heterodimer with CRLF1, essential for neuronal development.
		Socs3	-1.844	0.000	SOCS family polypeptides form part of a classical negative feedback system, which regulates cytokine signal transduction.
		Bcl3	-1.963	0.005	Transcriptional co-factor influencing NF-κB-driven gene expression.

Table 78. Downregulated genes associated with cell surface receptor signaling pathway via STAT. The table lists downregulated genes associated with cell surface receptor signaling pathway via STAT, with their respective fold change values, P-values, and FDR corrections. Differential expression analysis was performed using a threshold of FC $\geq \pm 1.2$ and P-value < 0.05.

GO ID	GO Term	Gene Symbol	log2FC	P-value	Function Summary
GO:1902041	Regulation of extrinsic apoptotic signaling pathway via death domain receptors	Icam1	-1.506	0.007	Adhesion molecule that engages integrin LFA-1, enabling leukocyte–endothelium interactions.
		Pmaip1	-1.583	0.008	Pro-apoptotic factor that activates caspases by neutralising anti-apoptotic Bcl-2 proteins.
		Serpine1	-1.635	0.004	Broad-spectrum inhibitor that targets serine proteases.

Table 79. Downregulated genes associated with regulation of extrinsic apoptotic signaling pathway via death domain receptors. The table lists downregulated genes associated with regulation of extrinsic apoptotic signaling pathway via death domain receptors, with their respective fold change values, P-values, and FDR corrections. Differential expression analysis was performed using a threshold of FC $\geq \pm 1.2$ and P-value < 0.05.

GO ID	GO Term	Gene Symbol	log2FC	P-value	Function Summary
GO:0008630	Intrinsic apoptotic signaling pathway in response to DNA damage	Myc	-1.578	0.000	Broad-acting transcription factor that recognises the 5′-CAC(G/A)TG-3′ motif to modulate gene expression.
		Pmaip1	-1.583	0.008	Pro-apoptotic factor that activates caspases by neutralising anti-apoptotic Bcl-2 proteins.
		Bcl3	-1.963	0.005	Transcriptional co-factor influencing NF-κB-driven gene expression.
		Ier3	-2.036	0.000	Regulator maintaining ERK activity by blocking PP2A-PPP2R5C-driven dephosphorylation.

Table 80. Downregulated genes associated with intrinsic apoptotic signaling pathway in response to DNA damage. The table lists downregulated genes associated with intrinsic apoptotic signaling pathway in response to DNA damage, with their respective fold change values, P-values, and FDR corrections. Differential expression analysis was performed using a threshold of FC ≥ ±1.2 and P-value < 0.05.

GO ID	GO Term	Gene Symbol	log2FC	P-value	Function Summary
GO:0010762	Regulation of fibroblast migration	Has1	-1.533	0.045	Enzyme responsible for elongating hyaluronan by adding GlcNAc and GlcUA.
		Akap12	-1.990	0.002	Scaffolding protein that spatially organises PKA and PKC signalling domains.
		Acta2	-2.120	0.009	Alpha-smooth muscle actin contributing to diverse actin-based motility processes.

Table 81. Downregulated genes associated with regulation of fibroblast migration. The table lists downregulated genes associated with regulation of fibroblast migration, with their respective fold change values, P-values, and FDR corrections. Differential expression analysis was performed using a threshold of FC $\geq \pm 1.2$ and P-value < 0.05.

GO ID	GO Term	Gene Symbol	log2FC	P-value	Function Summary
GO:0042092	Type 2 immune response	Rsad2	-1.686	0.005	Interferon-stimulated antiviral protein pivotal for establishing robust cellular defense against viruses.
		Clcf1	-1.738	0.001	Forms a neurotrophic heterodimer with CRLF1, essential for neuronal development.
		Bcl3	-1.963	0.005	Transcriptional co-factor influencing NF-κB-driven gene expression.

Table 82. Downregulated genes associated with type 2 immune response. The table lists downregulated genes associated with type 2 immune response, with their respective fold change values, P-values, and FDR corrections. Differential expression analysis was performed using a threshold of FC ≥ ±1.2 and P-value < 0.05.

GO ID	GO Term	Gene Symbol	log2FC	P-value	Function Summary
GO:0038061	Non-canonical NF-kappaB signal transduction	Nfkbia	-1.520	0.013	Restrains the activity of dimeric NF-kappa-B/REL complexes by trapping REL dimers in the cytoplasm by masking their nuclear localization signals.
		Sphk1	-1.662	0.005	Drives the phosphorylation of sphingosine to form sphingosine 1-phosphate, a lipid mediator with both intra- and extracellular functions.
		Bcl3	-1.963	0.005	Transcriptional co-factor influencing NF-κB-driven gene expression.
		Ccl19	-2.210	0.003	Chemokine that potently attracts naïve $CD4^+$ and $CD8^+$ T cells and modestly recruits resting B cells.

Table 83. Downregulated genes associated with non-canonical NF-kappaB signal transduction. The table lists downregulated genes associated with non-canonical NF-kappaB signal transduction, with their respective fold change values, P-values, and FDR corrections. Differential expression analysis was performed using a threshold of FC ≥ ±1.2 and P-value < 0.05.

GO ID	GO Term	Gene Symbol	log2FC	P-value	Function Summary
GO:0003376	Sphingosine-1-phosphate receptor signaling pathway	Sphk1	-1.662	0.005	Drives the phosphorylation of sphingosine to form sphingosine 1-phosphate, a lipid mediator with both intra- and extracellular functions.
		Mfsd2b	-2.062	0.038	Membrane transporter that exports sphingosine-1-phosphate from erythrocytes and platelets.

Table 84. Downregulated genes associated with sphingosine-1-phosphate receptor signaling pathway. The table lists downregulated genes associated with sphingosine-1-phosphate receptor signaling pathway, with their respective fold change values, P-values, and FDR corrections. Differential expression analysis was performed using a threshold of FC ≥ ±1.2 and P-value < 0.05.

GO ID	GO Term	Gene Symbol	log2FC	P-value	Function Summary
GO:0048711	Positive regulation of astrocyte differentiation	Lif	-1.676	0.002	Leukemia inhibitory factor drives the terminal differentiation of leukemic cells.
		Clcf1	-1.738	0.001	Forms a neurotrophic heterodimer with CRLF1, essential for neuronal development.

Table 85. Downregulated genes associated with positive regulation of astrocyte differentiation. The table lists downregulated genes associated with positive regulation of astrocyte differentiation, with their respective fold change values, P-values, and FDR corrections. Differential expression analysis was performed using a threshold of FC ≥ ±1.2 and P-value < 0.05.

GO ID	GO Term	Gene Symbol	log2FC	P-value	Function Summary
GO:0030336	Negative regulation of cell migration	Has1	-1.533	0.045	Enzyme responsible for elongating hyaluronan by adding GlcNAc and GlcUA.
		Ccl25	-1.563	0.028	Potentially involved in T-cell development.
		Cldn5	-1.607	0.001	Tight-junction protein crucial for sealing intercellular gaps via calcium-independent adhesion.
		Serpine1	-1.635	0.004	Broad-spectrum inhibitor that targets serine proteases.
		Adamts9	-1.867	0.004	ADAMTS family metalloprotease implicated in proteoglycan cleavage, organ morphogenesis and anti-angiogenic control.
		Angpt2	-2.299	0.011	Antagonises ANGPT1 by binding TEK/TIE2 receptors, thereby reshaping endothelial angiopoietin signalling.

Table 86. Downregulated genes associated with negative regulation of cell migration. The table lists downregulated genes associated with negative regulation of cell migration, with their respective fold change values, P-values, and FDR corrections. Differential expression analysis was performed using a threshold of FC $\geq \pm 1.2$ and P-value < 0.05.

GO ID	GO Term	Gene Symbol	log2FC	P-value	Function Summary
GO:2001212	Regulation of vasculogenesis	Adm	-1.810	0.002	Adrenomedullin/ADM and proadrenomedullin N-20 terminal peptide/PAMP are peptide hormones that act as potent hypotensive and vasodilatator agents.
		Asb4	-2.834	0.001	Substrate-recognition subunit of an ECS-type SCF E3 ligase, directing ubiquitination and proteasomal turnover of target proteins.

Table 87. Downregulated genes associated with regulation of vasculogenesis. The table lists downregulated genes associated with regulation of vasculogenesis, with their respective fold change values, P-values, and FDR corrections. Differential expression analysis was performed using a threshold of FC $\geq \pm 1.2$ and P-value < 0.05.

GO ID	GO Term	Gene Symbol	log2FC	P-value	Function Summary
GO:0022409	Positive regulation of cell-cell adhesion	Icam1	-1.506	0.007	Adhesion molecule that engages integrin LFA-1, enabling leukocyte–endothelium interactions.
		Plaur	-1.514	0.025	Cell-surface receptor for urokinase plasminogen activator, mediating localized proteolysis.
		Mfsd2b	-2.062	0.038	Membrane transporter that exports sphingosine-1-phosphate from erythrocytes and platelets.
		Ccl19	-2.210	0.003	Chemokine that potently attracts naïve $CD4^+$ and $CD8^+$ T cells and modestly recruits resting B cells.
		Has2	-2.312	0.000	Enzyme responsible for elongating hyaluronan by adding GlcNAc and GlcUA.
		Tnfsf9	-2.570	0.004	Cytokine that binds to TNFRSF9.

Table 88. Downregulated genes associated with positive regulation of cell-cell adhesion. The table lists downregulated genes associated with positive regulation of cell-cell adhesion, with their respective fold change values, P-values, and FDR corrections. Differential expression analysis was performed using a threshold of FC $\geq \pm 1.2$ and P-value < 0.05.

GO ID	GO Term	Gene Symbol	log2FC	P-value	Function Summary
GO:0070374	Positive regulation of ERK1 and ERK2 cascade	Icam1	-1.506	0.007	Adhesion molecule that engages integrin LFA-1, enabling leukocyte–endothelium interactions.
		Thpo	-1.580	0.002	Lineage-restricted cytokine that drives megakaryocyte proliferation and maturation.
		Akap12	-1.990	0.002	Scaffolding protein that spatially organises PKA and PKC signalling domains.
		Acta2	-2.120	0.009	Alpha-smooth muscle actin contributing to diverse actin-based motility processes.
		Ccl19	-2.210	0.003	Chemokine that potently attracts naïve $CD4^+$ and $CD8^+$ T cells and modestly recruits resting B cells.

Table 89. Downregulated genes associated with positive regulation of ERK1 and ERK2 cascade. The table lists downregulated genes associated with positive regulation of ERK1 and ERK2 cascade, with their respective fold change values, P-values, and FDR corrections. Differential expression analysis was performed using a threshold of FC $\geq \pm 1.2$ and P-value < 0.05.

GO ID	GO Term	Gene Symbol	log2FC	P-value	Function Summary
GO:0097193	Intrinsic apoptotic signaling pathway	Plaur	-1.514	0.025	Cell-surface receptor for urokinase plasminogen activator, mediating localized proteolysis.
		Myc	-1.578	0.000	Broad-acting transcription factor that recognises the 5′-CAC(G/A)TG-3′ motif to modulate gene expression.
		Tnfrsf10b	-1.582	0.025	Death-domain receptor that binds the cytotoxic ligand TRAIL (TNFSF10) to initiate extrinsic apoptosis.
		Pmaip1	-1.583	0.008	Pro-apoptotic factor that activates caspases by neutralising anti-apoptotic Bcl-2 proteins.
		Bcl3	-1.963	0.005	Transcriptional co-factor influencing NF-κB-driven gene expression.
		Ier3	-2.036	0.000	Regulator maintaining ERK activity by blocking PP2A-PPP2R5C-driven dephosphorylation.

Table 90. Downregulated genes associated with intrinsic apoptotic signaling pathway. The table lists downregulated genes associated with intrinsic apoptotic signaling pathway, with their respective fold change values, P-values, and FDR corrections. Differential expression analysis was performed using a threshold of FC ≥ ±1.2 and P-value < 0.05.

GO ID	GO Term	Gene Symbol	log2FC	P-value	Function Summary
GO:0042509	Regulation of tyrosine phosphorylation of STAT protein	Lif	-1.676	0.002	Leukemia inhibitory factor drives the terminal differentiation of leukemic cells.
		Clcf1	-1.738	0.001	Forms a neurotrophic heterodimer with CRLF1, essential for neuronal development.
		Socs3	-1.844	0.000	SOCS family polypeptides form part of a classical negative feedback system, which regulates cytokine signal transduction.

Table 91. Downregulated genes associated with regulation of tyrosine phosphorylation of STAT protein. The table lists downregulated genes associated with regulation of tyrosine phosphorylation of STAT protein, with their respective fold change values, P-values, and FDR corrections. Differential expression analysis was performed using a threshold of FC ≥ ±1.2 and P-value < 0.05.

GO ID	GO Term	Gene Symbol	log2FC	P-value	Function Summary
GO:0051445	Regulation of meiotic cell cycle	Lif	-1.676	0.002	Leukemia inhibitory factor drives the terminal differentiation of leukemic cells.
		Nanos2	-1.774	0.012	RNA-binding factor steering germ cells toward the male pathway while suppressing female differentiation.
		Piwil2	-1.882	0.037	Piwi-like endoribonuclease essential for spermatogenesis through transposon silencing.

Table 92. Downregulated genes associated with regulation of meiotic cell cycle. The table lists downregulated genes associated with regulation of meiotic cell cycle, with their respective fold change values, P-values, and FDR corrections. Differential expression analysis was performed using a threshold of FC $\geq \pm 1.2$ and P-value < 0.05.

GO ID	GO Term	Gene Symbol	log2FC	P-value	Function Summary
GO:0045637	Regulation of myeloid cell differentiation	Nfkbia	-1.520	0.013	Restrains the activity of dimeric NF-kappa-B/REL complexes by trapping REL dimers in the cytoplasm by masking their nuclear localization signals.
		Myc	-1.578	0.000	Broad-acting transcription factor that recognises the 5′-CAC(G/A)TG-3′ motif to modulate gene expression.
		Thpo	-1.580	0.002	Lineage-restricted cytokine that drives megakaryocyte proliferation and maturation.
		Lif	-1.676	0.002	Leukemia inhibitory factor drives the terminal differentiation of leukemic cells.
		Zfp36	-2.008	0.004	Zinc-finger protein promoting decay of AU-rich mRNAs by accelerating deadenylation.
		Ier3	-2.036	0.000	Regulator maintaining ERK activity by blocking PP2A-PPP2R5C-driven dephosphorylation.

Table 93. Downregulated genes associated with regulation of myeloid cell differentiation. The table lists downregulated genes associated with regulation of myeloid cell differentiation, with their respective fold change values, P-values, and FDR corrections. Differential expression analysis was performed using a threshold of FC ≥ ±1.2 and P-value < 0.05.

GO ID	GO Term	Gene Symbol	log2FC	P-value	Function Summary
GO:0030217	T cell differentiation	Rsad2	-1.686	0.005	Interferon-stimulated antiviral protein pivotal for establishing robust cellular defense against viruses.
		Cyp26b1	-1.776	0.001	Cytochrome P450 enzyme that catabolises retinoic acid, tuning vitamin-A-dependent signalling.
		Bcl3	-1.963	0.005	Transcriptional co-factor influencing NF-κB-driven gene expression.
		Ccl19	-2.210	0.003	Chemokine that potently attracts naïve $CD4^+$ and $CD8^+$ T cells and modestly recruits resting B cells.
		Tnfsf9	-2.570	0.004	Cytokine that binds to TNFRSF9.
		Ctla2a	-4.071	0.005	Not known, expressed in activated T-cell.

Table 94. Downregulated genes associated with T cell differentiation. The table lists downregulated genes associated with T cell differentiation, with their respective fold change values, P-values, and FDR corrections. Differential expression analysis was performed using a threshold of FC $\geq \pm 1.2$ and P-value < 0.05.

GO ID	GO Term	Gene Symbol	log2FC	P-value	Function Summary
GO:0002830	Positive regulation of type 2 immune response	Rsad2	-1.686	0.005	Interferon-stimulated antiviral protein pivotal for establishing robust cellular defense against viruses.
		Clcf1	-1.738	0.001	Forms a neurotrophic heterodimer with CRLF1, essential for neuronal development.

Table 95. Downregulated genes associated with positive regulation of type 2 immune response. The table lists downregulated genes associated with positive regulation of type 2 immune response, with their respective fold change values, P-values, and FDR corrections. Differential expression analysis was performed using a threshold of FC ≥ ±1.2 and P-value < 0.05.

GO ID	GO Term	Gene Symbol	log2FC	P-value	Function Summary
GO:0090520	Sphingolipid mediated signaling pathway	Sphk1	-1.662	0.005	Drives the phosphorylation of sphingosine to form sphingosine 1-phosphate, a lipid mediator with both intra- and extracellular functions.
		Mfsd2b	-2.062	0.038	Membrane transporter that exports sphingosine-1-phosphate from erythrocytes and platelets.

Table 96. Downregulated genes associated with sphingolipid mediated signaling pathway. The table lists downregulated genes associated with sphingolipid mediated signaling pathway, with their respective fold change values, P-values, and FDR corrections. Differential expression analysis was performed using a threshold of FC ≥ ±1.2 and P-value < 0.05.

GO ID	GO Term	Gene Symbol	log2FC	P-value	Function Summary
GO:0030098	Lymphocyte differentiation	Rsad2	-1.686	0.005	Interferon-stimulated antiviral protein pivotal for establishing robust cellular defense against viruses.
		Clcf1	-1.738	0.001	Forms a neurotrophic heterodimer with CRLF1, essential for neuronal development.
		Cyp26b1	-1.776	0.001	Cytochrome P450 enzyme that catabolises retinoic acid, tuning vitamin-A-dependent signalling.
		Bcl3	-1.963	0.005	Transcriptional co-factor influencing NF-κB-driven gene expression.
		Ccl19	-2.210	0.003	Chemokine that potently attracts naïve $CD4^+$ and $CD8^+$ T cells and modestly recruits resting B cells.
		Tnfsf9	-2.570	0.004	Cytokine that binds to TNFRSF9.
		Ctla2a	-4.071	0.005	Not known, expressed in activated T-cell.

Table 97. Downregulated genes associated with lymphocyte differentiation. The table lists downregulated genes associated with lymphocyte differentiation, with their respective fold change values, P-values, and FDR corrections. Differential expression analysis was performed using a threshold of FC $\geq \pm 1.2$ and P-value < 0.05.

GO ID	GO Term	Gene Symbol	log2FC	P-value	Function Summary
GO:0070613	Regulation of protein processing	Plaur	-1.514	0.025	Cell-surface receptor for urokinase plasminogen activator, mediating localized proteolysis.
		Serpine1	-1.635	0.004	Broad-spectrum inhibitor that targets serine proteases.
		Ctla2a	-4.071	0.005	Not known, expressed in activated T-cell.

Table 98. Downregulated genes associated with regulation of protein processing. The table lists downregulated genes associated with regulation of protein processing, with their respective fold change values, P-values, and FDR corrections. Differential expression analysis was performed using a threshold of FC $\geq \pm 1.2$ and P-value < 0.05.

4. Discussion

Krabbe disease remains a devastating leukodystrophy with limited therapeutic options beyond early hematopoietic stem cell transplantation[26]. In this study, we demonstrate that intracerebroventricular delivery of AAV9-Oct4 at P1 preserved motor function and white matter integrity in twitcher mice without affecting overall somatic growth. Importantly, improvements in rotarod and hanging wire performance were mirrored by higher fractional anisotropy on diffusion tensor imaging and sustained levels of myelin basic protein and myelin density, indicating true structure-function rescue, consistent with previous reports linking white matter integrity to functional outcomes in leukodystrophies[27,28].

Neither galactocerebrosidase (Galc) mRNA levels nor enzymatic activity differed between groups, confirming that behavioral recovery did not arise from replacement of the missing lysosomal enzyme[1,2]. This finding distinguishes our approach from conventional enzyme replacement therapy or gene therapy strategies that directly target GALC deficiency[7,29]. Instead, Oct4 overexpression increased the pool of $Olig2^{+}$ lineage cells and nestin-positive progenitors while reducing reactive astrocytosis, supporting the concept that reprogramming approaches can compensate for enzymatic deficiencies by enhancing endogenous repair mechanisms[30,31].

To further explore the molecular mechanisms underlying these phenotypic improvements, we performed transcriptomic profiling of the striatum to assess the global impact of Oct4 expression on mRNA signatures. Differential expression analysis between the Oct4 and control (GFP) groups identified a robust set of genes. Gene Ontology (GO) enrichment analysis and functional annotation revealed that Oct4 overexpression significantly upregulated genes associated with oligodendrocyte differentiation (GO:0048709), vascular and ion/metabolite transport, cell adhesion and migration, and intracellular signaling pathways. Notably, key oligodendrocyte-related transcripts such as DRD3, DLX2, and NLGN3 were prominently increased, supporting the hypothesis that Oct4 re-primes neural precursors toward the oligodendrocyte lineage and facilitates endogenous remyelination. These findings align with previous studies demonstrating Oct4's capacity to induce oligodendrocyte differentiation from various cell types both in vitro and in vivo[23,24].

Conversely, genes involved in immune responses, inflammatory pathways, and apoptosis were markedly downregulated. This included suppression of pro-inflammatory mediators and regulators of reactive gliosis, as well as reduced activity of pathways such as MAPK/STAT signaling. These transcriptomic changes suggest that Oct4 not only enhances oligodendrocyte lineage commitment but also attenuates detrimental neuroinflammatory processes, potentially creating a more permissive environment for repair. This dual mechanism is particularly relevant given the prominent role of neuroinflammation in Krabbe disease pathogenesis[12,13].

Although several cell division transcripts reached nominal statistical significance, their fold changes were below our predefined biological relevance cutoff ($|\text{Fold Change}| < 1.2$). We therefore conclude that Oct4 did not measurably alter global proliferative activity, reducing the concern for uncontrolled cell growth often associated with pluripotency factors. This is particularly important

given previous safety concerns regarding Oct4's oncogenic potential[32,33]. Consistent with these findings, hematoxylin and eosin (H&E) staining revealed no evidence of morphological abnormalities or dysplasia across experimental groups, further supporting the absence of pathological proliferation.

Together, these results extend prior reports where Oct4 converted fibroblasts or astrocytes into oligodendrocyte-like cells in vitro and in demyelinating lesions[23,24,30]. The present in vivo approach is notable in that it uses a single-factor vector and a one-time neonatal injection, simplifying regulatory translation compared to multi-factor reprogramming protocols[34,35]. Compared with enzyme replacement or HSCT, Oct4 gene transfer acts upstream by rebuilding the myelinating cell population while simultaneously suppressing inflammatory barriers to repair, rather than merely supplementing lysosomal activity[5,36].

Nevertheless, our study has important limitations. The follow-up period, limited to postnatal day 38, precludes assessment of long-term efficacy and potential adverse effects, such as tumorigenicity. Long-term safety studies are crucial for reprogramming factor-based therapies, as demonstrated in other contexts[37,38]. Additionally, we did not assess regional Oct4 protein distribution, leaving open questions about the completeness and uniformity of remyelination. The heterogeneous nature of myelin repair in leukodystrophies necessitates comprehensive regional analysis[27,39]. Lastly, the modest lifespan extension observed suggests that early CNS rescue alone may not suffice to prevent peripheral neuropathy or systemic metabolic complications, consistent with the multi-organ nature of Krabbe disease[39,40]. Future work combining Oct4 with GALC enzyme replacement, or employing lineage-restricted reprogramming factors, may provide synergistic benefits and enhance translational potential[41,42].

5. Conclusion

In conclusion, this study demonstrates that overexpression of Oct4 in twitcher mice, a model of Krabbe disease, confers significant protective effects on motor function and white matter integrity. Behavioral assessments consistently indicated preserved motor function and neuromuscular strength in the Oct4 group. Furthermore, MRI and DTI analyses revealed improved white matter structural integrity in the corpus callosum, while immunofluorescence analyses confirmed enhanced myelin density and preservation of myelin basic protein. RNA sequencing revealed the upregulation of oligodendrocyte differentiation-related genes, particularly DRD3, DLX2, and NLGN3, highlighting Oct4's role in promoting oligodendrocyte lineage commitment and facilitating endogenous remyelination. Importantly, Oct4 overexpression led to a reduction in inflammatory response and apoptosis-related genes, suggesting its dual mechanism of enhancing repair while suppressing detrimental neuroinflammatory processes. Notably, no significant changes in cell division or cell cycle pathways were observed, indicating that Oct4's therapeutic effects are specific to differentiation and neuroprotection without inducing abnormal proliferation. Collectively, these findings underscore the therapeutic potential of Oct4-mediated reprogramming in addressing the neurological deficits associated with Krabbe disease, offering insights into novel regenerative approaches that bypass enzymatic deficiencies through enhanced endogenous repair mechanisms.

References

1. Graziano ACE, Cardile V. History, genetic, and recent advances on Krabbe disease. Gene 2015;555:2-13.

2. Suzuki K, Suzuki Y. Globoid cell leucodystrophy (Krabbe's disease): deficiency of galactocerebroside beta-galactosidase. Proc Natl Acad Sci U S A 1970;66:302-9.

3. Ferreira CR, Gahl WA. Lysosomal storage diseases. Transl Sci Rare Dis 2017;2:1-71.

4. Duffner PK, Barczykowski A, Jalal K, Yan L, Kay DM, Carter RL. Early infantile Krabbe disease: results of the world-wide Krabbe registry. Pediatr Neurol 2011;45:141-8.

5. Escolar ML, Poe MD, Provenzale JM, Richards KC, Allison J, Wood S, et al. Transplantation of umbilical-cord blood in babies with infantile Krabbe's disease. N Engl J Med 2005;352:2069-81.

6. Galbiati F, Givogri M, Cantuti L, Lopez Rosas A, Cao H, Van Breemen R, et al. Combined hematopoietic and lentiviral gene-transfer therapies in newborn Twitcher mice reveal contemporaneous neurodegeneration and demyelination in Krabbe disease. J Neurosci Res 2009;87:1748-59.

7. Reddy AS, Kim JH, Hawkins-Salsbury JA, Macauley SL, Tracy ET, Vogler CA, et al. Bone marrow transplantation augments the effect of brain-and spinal cord-directed adeno-associated virus 2/5 gene therapy by altering inflammation in the murine model of globoid-cell leukodystrophy. J Neurosci 2011;31:9945-57.

8. Pan X, Sands SA, Yue Y, Zhang K, LeVine SM, Duan D. An engineered galactosylceramidase construct improves AAV gene therapy for krabbe disease in twitcher mice. Hum Gene Ther 2019;30:1039-51.

9. Cleland W, Kennedy EP. The enzymatic synthesis of psychosine. J Biol Chem 1960;235:45-51.

10. Lin YN, Radin NS. Alternate pathways of cerebroside catabolism. Lipids 1973;8:732-6.

11. Li Y, Xu Y, Benitez BA, Nagree MS, Dearborn JT, Jiang X, et al. Genetic ablation of acid ceramidase in Krabbe disease confirms the psychosine hypothesis and identifies a new therapeutic target. Proc Natl Acad Sci U S A 2019;116:20097-103.

12. Pasqui A, Di Renzo M, Auteri A, Federico G, Puccetti L. Increased TNF-α production by peripheral blood mononuclear cells in patients with Krabbe's disease: effect of psychosine. Eur J Clin Invest 2007;37:742-5.

13. O'Sullivan C, Dev KK. Galactosylsphingosine (psychosine)-induced demyelination is attenuated by sphingosine 1-phosphate signalling. J Cell Sci 2015;128:3878-87.

14. Won JS, Kim J, Paintlia MK, Singh I, Singh AK. Role of endogenous psychosine accumulation in oligodendrocyte differentiation and survival: implication for Krabbe disease. Brain Res 2013;1508:44-52.

15. Giri S, Khan M, Rattan R, Singh I, Singh A. Krabbe disease: psychosine-mediated activation of phospholipase A2 in oligodendrocyte cell death. J Lipid Res 2006;47:1478-92.

16. Castelvetri LC, Givogri MI, Hebert A, Smith B, Song Y, Kaminska A, et al. The sphingolipid psychosine inhibits fast axonal transport in Krabbe disease by activation of GSK3β and deregulation of molecular motors. J Neurosci 2013;33:10048-56.

17. D'Auria L, Reiter C, Ward E, Moyano AL, Marshall MS, Nguyen D, et al. Psychosine enhances the shedding of membrane microvesicles: Implications in demyelination in Krabbe's disease. PLoS One 2017;12:e0178103.

18. Hawkins-Salsbury JA, Parameswar AR, Jiang X, Schlesinger PH, Bongarzone E, Ory DS, et al. Psychosine, the cytotoxic sphingolipid that accumulates in globoid cell leukodystrophy, alters membrane architecture. J Lipid Res 2013;54:3303-11.

19. White AB, Givogri MI, Lopez-Rosas A, Cao H, van Breemen R, Thinakaran G, et al. Psychosine accumulates in membrane microdomains in the brain of krabbe patients, disrupting the raft architecture. J Neurosci 2009;29:6068-77.

20. Pan GJ, Chang ZY, Schöler HR, Pei D. Stem cell pluripotency and transcription factor Oct4. Cell Res 2002;12:321-9.

21. Kim JB, Sebastiano V, Wu G, Araúzo-Bravo MJ, Sasse P, Gentile L, et al. Oct4-induced pluripotency in adult neural stem cells. Cell 2009;136:411-9.

22. Shi G, Jin Y. Role of Oct4 in maintaining and regaining stem cell pluripotency. Stem Cell Res Ther 2010;1:1-9.

23. Kim JB, Lee H, Araúzo-Bravo MJ, Hwang K, Nam D, Park MR, et al. Oct4-induced oligodendrocyte progenitor cells enhance functional recovery in spinal cord injury model. EMBO J 2015;34:2971-83.

24. Yun W, Choi KA, Hwang I, Zheng J, Park M, Hong W, et al. OCT4-induced oligodendrocyte progenitor cells promote remyelination and ameliorate disease. NPJ Regen Med 2022;7:4.

25. Dehghan S, Hesaraki M, Soleimani M, Mirnajafi-Zadeh J, Fathollahi Y, Javan M. Oct4 transcription factor in conjunction with valproic acid accelerates myelin repair in demyelinated optic chiasm in mice. Neuroscience 2016;318:178-89.

26. Allewelt H, Taskindoust M, Troy J, Page K, Wood S, Lehman L, et al. Long-term functional outcomes after hematopoietic stem cell transplantation for Krabbe disease. Blood 2016;128:2607-17.

27. Bonkowsky JL, Wilkes J, Bardsley T, Morava-Kozicz E, McDonald M, Srivastava R, et al. The burden of inherited leukodystrophies in children. Neurology 2010;75:718-25.

28. Franklin RJ, Ffrench-Constant C. Regenerating CNS myelin - from mechanisms to experimental medicines. Nat Rev Neurosci 2017;18:753-69.

29. Rafi MA, Rao HZ, Luzi P, Curtis MT, Vanier MT, Wenger DA. Extended normal life after AAVrh10-mediated gene therapy in the mouse model of Krabbe disease. Mol Ther 2012;20:2031-42.

30. Najm FJ, Lager AM, Zaremba A, Wyatt K, Hillyer EV, Watanabe M, et al. Transcription factor-mediated reprogramming of fibroblasts to expandable, myelinogenic oligodendrocyte progenitor cells. Nat Biotechnol 2013;31:426-33.

31. Wang S, Bates J, Li X, Schanz S, Chandler-Militello D, Levine C, et al. Human iPSC-derived oligodendrocyte progenitor cells can myelinate and rescue a mouse model of congenital hypomyelination. Cell Stem Cell 2013;12:252-64.

32. Hochedlinger K, Yamada Y, Beard C, Jaenisch R. Ectopic expression of Oct-4 blocks progenitor-cell differentiation and causes dysplasia in epithelial tissues. Cell 2005;121:465-77.

33. Okita K, Ichisaka T, Yamanaka S. Generation of germline-competent induced pluripotent stem cells. Nature 2007;448:313-7.

34. Takahashi K, Yamanaka S. Induction of pluripotent stem cells from mouse embryonic and adult fibroblast cultures by defined factors. Cell 2006;126:663-76.

35. Yu J, Vodyanik MA, Smuga-Otto K, Antosiewicz-Bourget J, Frane JL, Tian S, et al. Induced pluripotent stem cell lines derived from human somatic cells. Science 2007;318:1917-20.

36. Krivit W, Shapiro EG, Peters C, Wagner JE, Cornu G, Kurtzberg J, et al. Hematopoietic stem-cell transplantation in globoid-cell leukodystrophy. N Engl J Med 1998;338:1119-26.

37. Abad M, Mosteiro L, Pantoja C, Cañamero M, Rayon T, Ors I, et al. Reprogramming in vivo produces teratomas and iPS cells with totipotency features. Nature 2013;502:340-5.

38. Ohnishi K, Semi K, Yamamoto T, Shimizu M, Tanaka A, Mitsunaga K, et al. Premature termination of reprogramming in vivo leads to cancer development through altered epigenetic regulation. Cell 2014;156:663-77.

39. Wenger DA, Rafi MA, Luzi P, Datto J, Costantino-Ceccarini E. Krabbe disease: genetic aspects and progress toward therapy. Mol Genet Metab 2016;119:18-30.

40. Spada M, Pagliardini S, Yasuda M, Tukel T, Thiagarajan G, Sakuraba H, et al. High incidence of later-onset krabbe disease in a defined population. Am J Hum Genet 2006;79:739-44.

41. Cartier N, Hacein-Bey-Abina S, Bartholomae CC, Veres G, Schmidt M, Kutschera I, et al. Hematopoietic stem cell gene therapy with a lentiviral vector in X-linked

adrenoleukodystrophy. Science 2009;326:818-23.

42. Gentner B, Visigalli I, Hiramatsu H, Lechman E, Ungari S, Giustacchini A, et al. Identification of hematopoietic stem cell-specific miRNAs enables gene therapy of globoid cell leukodystrophy. Sci Transl Med 2010;2:58ra84.

Abstract in Korean

크라베 병에서 생체 내 리프로그래밍 인자 Oct4의 재수초화 유도 효과

본 논문은 크라베병에서 생체 내 리프로그래밍 인자 Oct4의 재수초화 유도 효과를 확인했다. 크라베병은 갈락토세레브로시다제(Galactocerebrosidase) 효소 결핍으로 인한 치명적인 탈수초성 질환으로, 전체 환자의 약 85-90%가 영아기에 발병하며 90% 이상이 2세 이내에 사망한다. 현재 조혈모세포 이식이 유일한 치료법이나 근본적인 해결책은 아니다. Galc 결핍으로 인해 갈락토실세라마이드와 사이코신이 축적되어 세포 독성을 일으키고, 희소돌기아교세포 분화를 억제하며 염증을 증가시킨다.

Oct4는 배아줄기세포의 다능성 유지에 핵심적인 전사인자로, 리프로그래밍을 통해 다양한 세포를 신경줄기세포나 희소돌기아교세포로 분화시킬 수 있다. 본 연구는 크라베병 동물모델인 twitcher 마우스에서 Oct4의 재수초화 효과를 검증하였다.

생후 1일 이내에 AAV9-Oct4를 뇌실 내 주입하고, 생후 21일, 28일, 35일차에 행동 실험을 실시하였다. Oct4군은 대조군 대비 rotarod (4 rpm, 4-40 rpm)에서 평균 47% ($P < 0.01$), hanging wire test 에서 39% ($P = 0.02$) 향상된 운동 수행력을 보여 운동 기능 저하가 유의하게 완화되었다.

영상학적 분석에서 MRI-DTI를 통해 뇌량 및 대뇌백질의 fractional anisotropy가 0.32에서 0.38로 18% 증가하였고 ($P < 0.01$), T2-가중 영상에서는 부종 신호가 감소하였다. Luxol fast blue 와 MBP 염색 분석 결과 탈수초 면적이 42% 감소하여 수초 보존 효과를 확인하였다.

세포학적 분석에서 뇌량의 $Olig2^+$ 희소돌기세포 계열 세포와 $nestin^+$ 전구세포가 각각 2.6배, 1.9배 증가한 반면, $GFAP^+$ 반응성 성상세포는 31% 감소하였다. BrdU 이중 표지 실험을 통해 신생 세포의 62%가 $Olig2^+$로 분화됨을 확인하여 Oct4가 신경 전구세포의 희소돌기아교세포 분화를 촉진함을 입증하였다.

분자학적 기전 분석을 위해 Oct4군과 GFP 대조군의 선조체에서 RNA-seq 을 실시한 결과, 총 427개의 차등 발현 유전자가 검출되었다. Gene Ontology 분석에서 oligodendrocyte differentiation 및 myelination 경로가 유의하게 상향 조절되었으며, 특히 DRD3, DLX2, NLGN3 등 핵심 희소돌기아교세포 분화 관련 유전자들이 현저히 증가하였다. 또한 혈관 및 이온/대사체 수송, 세포 부착 및 이동, 신호 전달 관련 유전자들도 광범위하게 증가하였다.

반면 면역 반응, 염증 및 apoptosis 관련 유전자들은 전반적으로 억제되었고, astrocyte 분화 및 MAPK/STAT 신호전달 경로가 하향 조절되었다. 이는 Oct4가 희소돌기아교세포 분화 촉진과 동시에 염증성 환경을 완화하여 재생에 유리한 미세환경을 조성하는 이중 기전을 갖고 있음을 시사한다.

중요하게도, 세포 분열 및 세포 주기 관련 유전자들은 통계적 유의성에도 불구하고 생물학적 유의성 기준(|Fold Change| ≥ 1.2) 미만의 변화만을 보여, Oct4 과발현이 비정상적인 세포 증식을 유도하지 않음을 확인하였다. H&E 염색에서도 형태학적 이상이나 이형성증의 증거는 관찰되지 않았다.

본 연구는 신생아기 AAV9-Oct4 단회 주입을 통해 Galc 효소 결핍을 직접 교정하지 않고도 내재성 신경 전구세포의 희소돌기아교세포 계열 전환을 촉진하여 재수초화와 운동 기능 보존을 달성할 수 있음을 증명하였다. 이는 효소 대체 요법이나 유전자 교정과는 다른 새로운 접근법으로, 생체 내 리프로그래밍이 크라베병과 같은 탈수초성 질환에 대한 혁신적인 치료 전략이 될 수 있음을 시사한다.

핵심되는 말: 크라베 병, 갈락토세레브로시다제, 생체 내 리프로그래밍, Oct4, 희소돌기아교세포, 수초화